CANADIAN CENTRE for ISOTOPIC MICROANALYSIS

METHODS AND REFERENCE MATERIALS FOR SIMS DIAMOND C- AND N-ISOTOPE ANALYSIS

CCIM RESEARCH REPORT 14-01

Stern, R.A[1], Palot, M. [1], Howell, D.[2], Stachel, T. [1], Pearson, D.G. [1], Cartigny, P. [3], Oh, A[1].

[1]Canadian Centre for Isotopic Microanalysis, Department of Earth and Atmospheric Sciences, University of Alberta, Canada

[2]ARC Center of Excellence for Core to Crust Fluid Systems (CCFS) and GEMOC, Department of Earth and Planetary Sciences, Macquarie University, Sydney, Australia

[3]Laboratoire de Géochimie des Isotopes Stables, IPGP, Sorbonne Paris Cité, Université Paris Diderot, France

Recommended citation:

Stern, R.A, Palot, M. , Howell, D., Stachel, T. , Pearson, D.G. , Cartigny, P. , Oh, A. (2014). Methods and reference materials for SIMS diamond C- and N-isotope analysis. Canadian Centre for Isotopic Microanalysis, Research Report 14-01. University of Alberta, Education and Research Archive. http://hdl.handle.net/10402/era.38738

CONTENTS

SUMMARY

This report describes the methods and samples utilized (to 2014) within the Canadian Centre for Isotopic Microanalysis (CCIM), University of Alberta, for routine analysis of $\delta^{13}C_{VPDB}$, $\delta^{15}N_{AIR}$, and N abundances of diamonds by secondary ion mass spectrometry (Cameca IMS 1280). Analyses by conventional and SIMS methods are described and evaluated to arrive at calibration values for new diamond reference materials S0270 and S0280.

1. DEFINITIONS AND TERMINOLOGY

Terminology for stable isotopes follows guidelines of Coplen (2011).

$\alpha\,^{13}C_{P/Q}$, $\alpha^{15}N_{P/Q}$: isotopic fractionation factor for C and N, respectively, between two materials P and Q. Q may be a reference material (RM) or other reference value.

$$\alpha\,^{13}C_{P/Q} = (^{13}C/^{12}C)_P/(^{13}C/^{12}C)_Q$$
$$\alpha\,^{15}N_{P/Q} = (^{15}N/^{14}N)_P/(^{15}N/^{14}N)_Q$$

at. ppm: atomic fraction, expressed in parts per million; in this report, all ppm values are atomic unless stated otherwise

$^{13}C/^{12}C_{VPDB} = 0.01118$

CL: cathodoluminescence (by scanning electron microscopy)

CGSMS: combustion–gas-source mass spectrometry

$\delta^{13}C_{P,Q}$, $\delta^{15}N_{P,Q}$: relative difference in C- and N-isotopic ratios (= isotope delta), where P and Q are the identities of the two materials or values. Q is typically a reference value, namely VPDB or AIR, respectively, but may take on any value as required.

$$\delta^{13}C_{P,Q} = (^{13}C/^{12}C)_P/(^{13}C/^{12}C)_Q - 1 = \alpha\,^{13}C_{P/Q} - 1$$

where $(^{13}C/^{12}C)_P$ is the ratio in sample P and $(^{13}C/^{12}C)_Q$ is the ratio in sample Q or a reference value (e.g., VPDB); the quantity has no units implied, but is commonly expressed in ‰. The subscripts P (sample) and/or Q (reference) are used when clarity is necessary.

$$\delta^{15}N_{P,Q} = (^{15}N/^{14}N)_P/(^{15}N/^{14}N)_Q - 1 = \alpha\,^{15}N_{P/Q} - 1$$

where $(^{15}N/^{14}N)_P$ is the ratio in sample P and $(^{15}N/^{14}N)_Q$ is the ratio in sample Q or a reference value (e.g., AIR); the quantity has no units implied, but is commonly expressed in ‰. The subscripts P (sample) and/or Q (reference) are used when clarity is necessary.

Examples:

$\delta^{13}C_{S0270,VPDB}$ is the relative difference in C-isotope ratios between sample S0270 and VPDB
$\delta^{15}N^{SIMS}_{S0270, S0280}$ is the relative difference in N-isotope ratios between samples S0270 and S0280 measured by SIMS
$\delta^{13}C$ is the relative difference in C-isotopes of a pair of ratios whose identities must be determined in the context of presentation, it should not be assumed the reference is VPDB

IMF: instrumental mass fractionation, a quantity describing the relationship between a measured isotope ratio and the true ratio in the sample, typically calculated as the ratio of a measured isotope ratio and the true ratio (similar to the α definition).

MSWD: mean square of weighted deviates. Equivalent to the reduced χ^2 function, where x_i is an individual value, σ_i is its uncertainty (absolute), x_{wm} is the weighted mean of all values, and N is the total number of values. The probability (P) of obtaining the resulting value or greater may also be reported, with P >0.05 considered significant.

$$MSWD = \left\{\sum_{i=1}^{N} \frac{(x_i - x_{wm})^2}{\sigma_i^2}\right\}/(N-1)$$

m/z: mass/charge ratio

[N]: nitrogen concentration (if unspecified, values are atomic fraction • 10^6 for diamond)

$^{15}N/^{14}N_{AIR} = 1/272$

ppm: parts per million; atomic proportions for [N], and weight proportions for other elements

R: mass resolution, m/Δm at 10% peak height, where m = mass/charge

RM: reference material (i.e., 'standard')

SEM: scanning electron microscope

1σ: 68% confidence interval; 2σ = 95%

SIMS: secondary ion mass spectrometry

STD/1STD: standard deviation

2. SAMPLES

At the start of this research program to develop SIMS methods of stable isotope ($\delta^{13}C$, $\delta^{15}N$, [N]) analysis of diamond, no well-characterized microbeam reference materials (RMs) of any type existed. Consequently, methods development and material evaluation

and characterization have taken place in parallel, and a variety of samples (natural and synthetic diamond and other types of synthetic carbon) of varying utility have been employed at different stages. Here, only those samples that have immediate relevance to the CCIM diamond stable isotope program are described:

a. SIMS primary RMs, now used routinely for the purpose of calibration;

b. SIMS secondary RMs, now used routinely in conjunction with primary RMs to aid calibration or assessing accuracy;

c. Comparative materials used during SIMs methods development to help constrain working values of primary and secondary RMs.

d. Discontinued RMs.

The samples are described in the following section in order of their sample numbers. For simplicity and uniformity in data handling, all samples within CCIM are assigned sequential 'S' numbers, with reference materials ('standards') given special recognition as S0### (e.g., S0270). Further aliquots or sub-portions of the sample (termed sub-samples) are assigned a letter suffix, e.g. S0270B. Other associated sample names (aliases) are also mentioned here for consistency with other reports.

2.1 S0011 SYNTHETIC DIAMOND (DISCONTINUED REFERENCE MATERIAL)

Prior to mid-2013, the primary RMs for C-isotope calibration were selected portions of a single (5.5 mm diameter x 3 mm thick), cube-form, green-yellow-coloured, synthetic diamond supplied by Dr. David Fisher, De Beers Technology UK (formerly Diamond Trading Company, Maidenhead, U.K.) in 2008. This diamond, called SYN365-1808/16L-2 and subsequently assigned CCIM sample number S0011, was manufactured by Element Six (www.e6.com) using the high pressure–high temperature method. It was supplied to CCIM as two ~0.7 mm thick, doubly-polished {001} plates that were subsequently laser cut into smaller subsamples.

The first plate (designated as '2i' by DTC) came from the outermost part of the original crystal, and the second ('2ii') came from the middle part of the crystal. For plate 2i, two cuts were made down the center of the plate spaced ~1 mm apart, creating a 0.9 x 5 mm sliver, which was then further cut into sub-samples each ~0.9 x 0.9 x 0.7 mm. A UV image of the plate is shown in Figure 1 with locations of the laser cuts, and three labelled sub-samples (S0011A, B, C). Two of these sub-samples (S0011B, C) were used extensively for SIMS calibration, and a third of similar size (unlabelled) was combusted

for isotopic analyses (see below). In some cases, it is necessary to distinguish the two {001} opposite faces of S0011B and C as follows: relative to the growth medium, the outermost {001} face is considered 'upwards,' and designated with a small letter 'u' (e.g., S0011Bu); the corresponding innermost or 'downwards' face is designated with the letter 'd', e.g., S0011Bd. Another sub-sample of significance, S0011A, was residual from cutting out the aforementioned sliver, having length ~5 mm and width ~ 2.5 mm (Fig. 1). S0011A was used in some experiments to investigate isotopic variations across the (001) surface and also normal to it by examining the side face. Figure 2 shows a CL image of S0011A in cross-section, illustrating the zonation from lighter to darker CL towards the 'upwards' face. Also shown in Figure 2 are the downwards (001) face of S0011Bd with its bright CL, and the very dark CL upwards face of S0011Cu. Figure 3 shows a magnified CL image of the central part of S0011A in cross-section, showing the diamond to be comprised of discrete, thin (5 – 10 μm) growth layers which exhibit subtle contrasts in CL intensity, but overall the CL intensity decreases towards the outer (upwards) growth direction. The decrease in CL corresponds with decreasing N concentrations (see below).

A fourth sub-sample, S0011G, was cut from plate 2ii, and is a ~1/4 pie-shaped piece (~ 5 x 5 mm) that was used in some cases for calibration of diamond N contents, but is now discontinued.

2.2 S0203 (BAK) NATURAL DIAMOND (COMPARATIVE MATERIAL)

This sample of natural diamond from the Bakwanga district (Mbuji-Mayi), DRC, is a doubly-polished plate measuring 10.0 x 12.0 x 1.8 mm. The plate exposes a clear, colourless center region, mantled by a ~2 mm-thick fibrous rim comprising turbid, grey diamond (Figure 4). The fibrous rim was cut out in six areas using a laser beam contained within a water jet to avoid heating the sample, and the resulting sub-samples were labeled S0203A, B, etc. (Fig. 5). Sample S0203A was ultimately fragmented for the purpose of combustion analysis. Figure 6 shows in CL the finely-laminated growth structure of the fibrous diamond from S0203B used in SIMS evaluation. Diamond samples from this district were previously studied by Boyd et al. (1987).

2.3 S0233A SYNTHETIC VITREOUS CARBON (REFERENCE MATERIAL)

The vitreous (glassy) carbon samples discussed here are the Sigradur G type, manufactured by HTW (Hochtemperatur-Werkstoffe) GmbH, Germany, obtained commercially from distributors in Canada (Canemco, Inc.) and USA (SPI

Supplies/Structure Probe, Inc.). A chemical analysis supplied with the material indicated <100 ppm (wt.) cation impurities, but our SIMS analysis indicates variable nitrogen impurities reaching >10,000 ppm in some samples. The material is supplied as mirror-finished square plates and disks ranging from 1 mm to 6 mm thick, and these were tested for C- and N-isotopic composition and N abundances by SIMS. All showed systematic heterogeneities through the plate thickness, but many had remarkable homogeneity across the original plate surface. The sample selected for routine diamond analysis is product SPI 4390GCP-AB, a square plate 25 x 25 x 6 mm, labelled S0233. Through SIMS evaluation of slices through the plate it was determined that a 1.5 mm middle horizon was sufficiently isotopically homogeneous in three dimensions. A sub-sample S0233A was isolated by slow speed saw and further subdivided into several ~1 mm cubes, each assigned a number, e.g., S0233A1, 2, 3, etc. Each S0233A# sub-sample has been epoxy mounted within brass tubing for ease of handling (Fig. 7).

2.4 S0270 (S1163, MC08) NATURAL DIAMOND (PRIMARY REFERENCE MATERIAL)

This diamond was purchased commercially as a 0.6 mm-thick doubly-polished plate (9.5 x 8.5 mm) by one of the authors (DH) as part of a study of mixed-habit diamonds (Howell et al., 2013a). Mixed-habit diamonds exhibit two coincident growth mechanisms, octahedral growth forming {111} sectors, and cuboid growth forming {100} sectors. These types of diamonds are sometimes referred to as star or cross diamonds due to the appearance of their visible sector zonation. The provenance of the diamond is unknown, but has distinct similarities with mixed-habit diamonds reported from Zimbabwe (Rakovan et al., 2014). The diamond, having sub-rounded morphology, was first labeled MC08 by Howell et al. (2013a), and assigned the CCIM sample number S1163 for internal CCIM purposes during the initial study. Subsequently, the diamond was renamed S0270 to indicate its status as a CCIM reference material; the designations MC08 and S1163 are discontinued for current CCIM purposes except where needed for clarity.

A plane light image of the original plate is shown in Figure 8, where the darker cuboid sectors form a cross pattern, which is the result of light scattering from graphitized disk-crack-like defects (see Howell et al., 2013a). The infrared absorption spectral data of Howell et al. (2013a) showed the diamond to be characterized by high N concentrations that exhibited low levels of N aggregation and small platelet intensities, while large H-related absorption bands (measured at 3107 cm^{-1}) were only found within the cuboid

sectors. Overall, Howell et al. (2013a) suggest that this diamond and others from the suite, with their high N concentrations and mixed habits, formed under very stable geological conditions, within a diamond mantle source region comprising unknown mantle host rocks (e.g., peridotite, eclogite).

Figures 9 and 10 show CL images of the original plate surfaces. The cuboid sectors show a brighter (and in fact, different coloured) CL than the octahedral sectors, despite there being more nitrogen in the octahedral sectors. The brighter (and green) CL response from the cuboid sectors is dominated by nickel defects (Howell et al., 2013b), whereas the weaker (and blue) CL response from the octahedral sectors is due to a small amount of N3 defects due to the low levels of nitrogen aggregation and requires strong electron beam currents to make it visible. The core of diamond S0270 is dominated by cuboid growth that exhibits an ovoid zoning, but as the diamond becomes more truly mixed-habit due to the appearance of octahedral sectors, the growth stratigraphy becomes hummocky, which is more characteristics of this type of growth. The growth stratigraphy in the octahedral sectors is much straighter and can be seen to be continuous across the sector boundaries (e.g., Fig. 11).

The diamond plate S0270 (MC08) was segmented into several 0.5 − 1 mm sub-samples with an ex-industry Nd-YAG laser cutter (Macquarie University) as indicated in the outlined regions in Figure 9. Twelve sub-samples available to CCIM were labeled S0270B, C, through M (Figs. 9, 12). Most of the sub-samples are from the inner parts of cuboid sectors. Several contain varying proportions of both cuboid and octahedral growth. CL imaging allows these components to be easily differentiated, with the octahedral components having darker CL (e.g., Figure 11). CL images of mostly homogeneous octahedral sub-sample S0270B and cuboid sub-sample S0270C (Figs. 13, 14, respectively) reveal weakly developed growth zoning. The entirely cuboid sub-samples S0270D, I, and J were fragmented and combusted for CGSMS analysis of C- and N-isotopes (see below), although only J resulted in usable data. Figure 15 shows a CL image of S0270J. To prevent the edges of the sub-samples from chipping during frequent insertion and extraction from SIMS indium mounts, the sub-samples were cast with epoxy into small (2 – 3 mm width) square brass tubes, as shown in Figure 16.

2.5 S0280 (MC13) NATURAL DIAMOND (REFERENCE MATERIAL)

This diamond is another plate (6.0 x 7.5mm x 0.6 mm thick) from the study of Howell et al. (2013a) discussed previously. In that study it was labeled MC13, and as above it was

first assigned S1166 and then S0280. A plane light image of the original plate is shown in Figure 17, where the extensive dark cuboid sectors are evident. The CL of the diamond is shown in Figure 18, illustrating once again the brighter CL for the cuboid sectors. In this case there is no obvious CL stratigraphy within either sector, implying compositional homogeneity, making it a good candidate for a N-abundance reference material. Selected portions of the innermost cuboid sectors of the diamond were laser cut into ~1 mm square sub-samples, and labeled S0280B, C, D, E. S0280D contains a small octahedral segment at one edge.

2.6 S0289 AND S0290 NATURAL DIAMOND (COMPARATIVE MATERIAL)

Two individual diamond crystals, each ~ 2 mm diameter and partially sectioned, were provided from the laboratory of P. Cartigny for comparison with CCIM materials. These samples (including a third, S0288 not discussed here) were lightly ground and polished at CCIM to improve surface flatness and expose more material. The sample S0289 is diamond NAM-027 from the study of Cartigny et al. (2004), and has faint, planar CL zoning, overprinted by cross-hatched features indicative of plastic deformation (Fig. 19). Sample S0290 (Cartigny sample N198) comprises a generally featureless interior region and an outer rim zone with brighter CL (Fig. 20). Other fragments of these diamonds had previously been analyzed for C- and N-isotopes by CGSMS (see below), although the exact location of the analyzed material relative to the observed CL structure is undocumented.

3. SIMS METHODS

SIMS analysis of diamonds at CCIM has evolved since startup of operations (2010), with improvement to methods and RMs. This description is of the current best practice (2014), and may deviate slightly from previous reports.

3.1 MOUNTS

The mounts utilized within CCIM for diamond analysis usually comprise brass receptacles containing indium, into which various forms of the diamond and carbon samples are pressed close together (< 15 mm diameter preferred, up to 20 mm) in the center region (Figure 21). The samples include free diamonds, those contained with small epoxy sub-assemblies, or those in brass-jackets (e.g., Figs. 7, 16) to ease handling and ensure good edge contacts on irregular samples. For example, only one of the pressed samples in Figure 21 is a free diamond (S0270B). The diamonds and

epoxy/brass assemblies are cleaned with alkaline lab soap and de-ionized water before pressing, and with de-ionized water prior to coating. Following pressing, mounts are coated with ~5 nm of Au, using either a sputter or evaporative coater, which sufficiently prevents charging during SEM characterization and mapping of the mounts. All nitrogen-containing diamonds reveal informative growth structures from the CL images. Following the SEM imaging, a further ~25 nm (total ~30 nm) of Au coat is added to the mount, and then placed within the ion probe mount storage chamber for a minimum of 12 hr before analysis to degas under high vacuum.

3.2 INSTRUMENTATION AND OVERALL SETTINGS

The CCIM instrument is a Cameca IMS 1280 multicollector ion microprobe (serial #314), installed in 2009. Only technical aspects relevant to diamond analysis are mentioned here. In particular, all three possible measurements (C-isotopes, N abundances, N-isotopes) are carried out within separate sessions using slightly different analytical setup, usually in that order (Table 1). An alternate N abundance measurement, however, can be extracted from the N-isotope determination, so in some cases the middle step may not be done. Both C- and N-isotope measurements are made from fresh spot locations (adjacent to one another), whereas N abundances may occupy existing spots.

The Cs^+ source utilized is operated at 10 kV accelerating voltage, and the primary ions tuned for a Gaussian (projected) beam density distribution to give maximum primary (and secondary) current. The typical probe conditions for diamond analysis result in a sampled area of ~15 μm diameter. Rastering of the probe (5 x 5 μm) during C-isotope analysis assists in stabilizing ratios during sputtering. For N-isotope analysis, raster acquisition is specifically avoided in order to prevent analysis of blank N towards the edges of the sputtered region. In all cases, the probe is also rastered for 30 – 60 s prior to data collection to clean the surface and implant Cs in a 25 x 25 μm region around the analysis site. In the case of [N] and N-isotope analysis, the probe used for spot conditioning is boosted in intensity by 1.5 – 2 x the normal run conditions in order to accentuate the cleaning.

The stage mechanism allows for the analysis of one 25 mm diameter mount at a time, with up to 5 others available for manual exchange from a linked vacuum storage chamber. Accordingly, RMs for isotopic analysis are placed with unknowns within a single mount, whereas for [N] analyses the RM is normally contained on a separate RM mount, as the calibration requirements are less stringent. The sample mount is held at -10

kV, inducing a total 20 keV impact energy on the $^{133}Cs^{+}$ primary ions arriving at an incidence angle of ~21º with respect to the normal to the mount surface. The stage position is repeatable to better than 2 μm, which allows for sequences of spot positions to be recorded and run unattended with excellent positioning accuracy.

Negative secondary ions are extracted into the transfer section of the instrument through a differential potential of 10 kV to ground. For diamonds, so far there has seldom been a sample for which the normal incidence electron gun (NEG) was required, which greatly simplifies the analytical protocol. It also has the added benefit that potential surface contaminants (water, hydrocarbons, etc.) surrounding the analyzed spot are not subject to electron beam ionization, thus avoiding unnecessary increases in hydrides or contaminant N. The transfer slits (entrance slit, field aperture) settings vary slightly depending on the type of analysis (Table 1), but all utilize 100x image magnification at the field aperture, which is a moderate setting that works well for many types of stable isotope analyses. Following spot conditioning with Cs^{+}, the negative secondary ions are automatically centered within the entrance and field aperture slits.

The energy slit is utilized in either full transmission mode (C-isotopes) or high-energy-ion-rejection ([N], N-isotopes), the latter to slightly improve peak shape. All analyses involve dual simultaneous ion detection utilizing the L'2 (Faraday cup) in the multicollector array in combination with detectors in the axial ('mono') system, either the FC2 (Faraday cup) or the ETP® discrete-dynode electron multiplier ('EM'; model AF133H). The FC2 is configured with a 10^{11} Ω resistor circuit, and the L'2 with either 10^{10} Ω (C-isotopes, [N]) or 10^{11} Ω (N-isotopes). For C-isotopes and [N], baseline noise or drift are insignificant, and it is sufficient to take one Faraday cup baseline measurement over 30 – 60 s at the start of the day. For N-isotopes, baselines are measured in L'2 for every spot (see below). The EM gain is set about 50 V above the knee in a scan of HV vs. signal. There is typically no significant ageing of the EM during the sessions involving detection of N-isotopes, presumably due to the relatively low count rates. Any such drift is tracked and accounted for during data reduction with repeated analysis of the RM. EM background (typically <0.02 cps) is measured as dark noise (beam off), and constitutes an insignificant factor for the analyses. EM deadtime is fixed electronically with the nominal value 44 ns. Deadtime was measured with N-isotope ratio experiments (session IP13032) of high-N S0233A vitreous carbon by varying the count rates, indicating that the deadtime is actually 40 ± 1 ns, which is the value now utilized for count rate correction of the EM signals.

Careful consideration was given to potential biases arising from low count rates of $^{26}[^{12}C^{14}N]^-$ detected in L'2 (10^{11} Ω) during N-isotope measurements. An EM is typically not used in this position for most diamonds, as the count rates are too high for typical diamonds, but there are also diamonds with low [N] where an EM would be preferable. There are several technical and practical reasons (not discussed) why an EM is currently not used in this position, although future developments may resolve the problems. As count rates of $^{26}[^{12}C^{14}N]^-$ decrease, the influence of Faraday cup baseline noise and drift become more significant for accurate count rate determination. Using similar protocols as above for determining the EM deadtime, whereby count rates were varied on N-rich RM, it was determined (session IP13032) that the lowermost count rate in Faraday cup L'2 for reliable isotopic analysis was 2.5×10^5 cps. For example, for a particular high-N RM, the ratio $^{27}[^{12}C^{15}N]^-/^{26}[^{12}C^{14}N]^-$ when normalized to $^{15}N/^{14}N_{AIR}$ gave $\delta^{27/26}N_{AIR}$ = +54.02 ±0.24 ‰ (2σ) when $^{26}[^{12}C^{14}N]^-$ ~ 1×10^7 cps. At a much lower $^{26}[^{12}C^{14}N]^-$ count rate of $2.6 – 5.5 \times 10^5$ cps, $\delta^{27/26}N_{AIR}$ = +53.90 ± 0.74 ‰ (2σ), essentially equivalent. Current protocol is for the baseline count rate for L'2 to be measured before each analysis during the 30 − 60 second beam sputter-conditioning period, which aids in accounting for any baseline drift variability over the course of the ~10 min analysis, as well as any statistical variability in the actual baseline mean value utilized. For a typical Cs^+ beam current of 3 nA, this lower count rate limit for L'2 is encountered with a diamond having [N] ~ 50 ppm. In case of [N] determination using the ratio method with $^{26}[^{12}C^{14}N]^-$ in FC2, the lower limit can be extended to ~1×10^5 cps and tracking baseline drift for each analysis is not required, as the precision and accuracy required is lower.

3.3 DATA PROCESSING

As is practice at CCIM, the total data set for RM analyses over the course of the session is used to determine a single IMF value for the session, after data have been time corrected for any drift back to the start of the session. Session drift in IMF occurs due to various instrument stability factors (such as temperature changes, EM gain, etc.), and occurs over periods of an hour or more, but is readily characterized with the regular, repeated analysis of an appropriate RM. Overall drift is minor, typically <1.0 ‰ for both C-isotopes and N-isotopes over periods of up to 12 hrs, and can be modelled by linear or quadratic functions. It is occasionally necessary to break a long session into sub-sessions if there is an observed step change in IMF, in which case data may be discarded during the period of rapid change. The CCIM approach emphasizes tracking and modelling long-term IMF drift, rather than short-term (<1 hr) fluctuations. Any shorter-term

fluctuations are revealed in the final (drift-corrected) data as excess scatter (as discussed below). This practice follows identical and well-accepted practice used for U-Pb analysis, and differs from the 'bracketing' approach, whereby a group of unknowns are processed using only analyses of the RMs immediately before and after this group of unknowns. The preference at CCIM is for session-based processing rather than the bracketing method, as the former is well-suited and statistically robust for analytical conditions that are stable over long periods of time. Further discussion of this topic can be found in Ickert and Stern (2013).

The analytical uncertainties of C- and N-isotopes per datum at CCIM include:

1. within-spot uncertainty, which is calculated as the standard error of the raw ratios of the particular spot measurement, whether RM or unknown. The analysis is arbitrarily subdivided in equal-time intervals ('cycles'), typically resulting in 10 to 20 ratios that are used in statistical calculations. Currently, these ratios are not time-corrected for any within-spot time-correlated variations, but may be in the future.

2. between-spot uncertainty, determined from repeated analysis of a RM (one or more pieces), a value which is the average 'excess' uncertainty required to explain the observed scatter, i.e., if observed standard deviation > average within-spot error, there will be an excess error component. The standard deviation of the primary RM data is determined after any correction for session drift back to a common time (typically, but not necessarily, the start of the session). The form of the within-session drift is typically a first- or second order polynomial function fit by least-squares, but may be higher if warranted. The between-spot uncertainty is added as a blanket error to all unknowns. For C-isotopes, a minimum excess component of ±0.05‰ (1σ) is propagated, even if the observed excess is zero.

3. between-session uncertainty, which is calculated from the 1σ uncertainty of the mean value of the repeated analysis of the RM within the session. This is typically a minor component, as there are usually many analyses of the RM. All else being equal, this is the last of three components required for comparing CCIM data sets with other CCIM data sets, and for general reporting of uncertainties in tables of data.

4. RM composition uncertainty. There is uncertainty relating to the accuracy of the composition of the RM analyzed during the SIMS session. This uncertainty arises from analytical factors and sample-related factors, the latter including the possible existence of heterogeneity within the RM used for SIMS calibration. The value of the uncertainty should be mentioned in the technique description. The RM uncertainty should normally not be propagated on an individual datum basis to the between-session uncertainty, as doing so may unnecessarily mask variations that do not depend on accuracy, such as plotting profiles and generating probability density diagrams. This uncertainty should be added arithmetically to the individual between-session uncertainty (type 3), or to uncertainties arising from calculations of means of subsets of such data, when it is required to compare SIMS-determined values with those of other labs or techniques. This component is propagated in answer to questions such as: is my result from CCIM distinct from the canonical mantle value? It should not be

propagated in considering questions such as: is there a measurable difference in the values between samples A and B within my suite?

3.4 C-ISOTOPES

Specific instrument conditions for carbon isotopes in diamond are summarized in Table 1. The only potentially significant isobaric interference for this measurement is between $^{13}C^-$ and $^{12}CH^-$, requiring R = 2900 for separation. The abundance of the hydride is typically <0.01 of $^{13}C^-$, and consequently at the typical operating resolution, R ~2900, hydride interference is eliminated (Figs. 22, 23). Mounts are normally constructed to contain both the primary RM (S0270) and a secondary RM, typically vitreous carbon (S0233A). S0233A is used for setting up the instrument and for initial performance tests, typically 10 replicate analyses, such that if the standard deviation of raw $^{13}C^-/^{12}C^-$ is < 0.05‰, the session proceeds. For a large number of analyses (e.g., > 100 analyses), S0233A will be measured once after every 4 unknowns, and S0270 once after every eight unknowns. In this way, S0233A is used solely for the purpose of tracking and correcting for session drift in IMF (see above). This method reduces the usage on the primary (diamond) RM, which is then used primarily for calculating and making the IMF correction for the session. For a small number of analyses, only S0270 is required using the 4:1 sequence. Currently we do not routinely incorporate the analysis of a secondary *diamond* RM for the purpose of assessing the accuracy of IMF-corrected $\delta^{13}C$ values, but as further diamond RMs become characterized, this will eventually be incorporated into the procedure. The use of vitreous carbon (e.g., S0233A) for primary or secondary IMF corrections has been evaluated, but is currently not implemented due to several factors, including the differential behaviour of this matrix relative to diamond when instrument conditions are slightly varied. Nevertheless, in certain circumstances, such as the unavailability of an abundant primary diamond RM, a carefully-selected and characterized vitreous carbon sample that has been (and can continue to be) inter-calibrated with a diamond RM by SIMS, could be employed as a routine primary RM if done with care. Typical uncertainties in final $\delta^{13}C_{VPDB}$ values are ± 0.15‰ (2σ), not including the uncertainty in the absolute composition of the reference material (type 4 uncertainty, Section 3.3), which would add a further ± 0.1‰ (see Section 5.1).

3.5 N-ISOTOPES

Specific instrument conditions are summarized in Table 1. As is well known, analysis of N-isotopes requires measurement of the CN^- molecular species ($^{27}[^{12}C^{15}N]^-/^{26}[^{12}C^{14}N]^-$)

due to the lack of sufficient secondary ionization of the atomic species. A mass resolution of 7150 is required for complete separation of the isobar $^{13}C^{13}C^-$ at higher m/z from $^{26}[^{12}C^{14}N]^-$. A mass resolution of ~6700 is achievable with the current (fixed) minimum L'2 exit slit of 150 µm, which is still sufficient to eliminate the isobar. Figures 24 and 25 show mass scans of m/z = 26 for a high [N] diamond (~2150 ppm, S0270). Figure 25 includes depiction of the high mass edge of the exit slit in the case where $^{26}[^{12}C^{14}N]^-$ is centred (position 1) and offset (position 2) within the slit window. The projected low-mass edge of $^{13}C^{13}C^-$ does not to extend across the slit edge in either case, showing that it will not affect accurate determination of $^{26}[^{12}C^{14}N]^-$, but for added separation, the peak offset position can be used to increase the effective mass resolution if required. The potential for tailing of $^{13}C^{13}C^-$ was examined with ultra-low N diamond (~1.5 ppm), the latter being much lower than currently analyzed for N-isotopes. Figures 26 and 27 show linear and log mass scans, respectively, for m/z = 26, and again there is no evidence from the scans of significant tailing into $^{26}[^{12}C^{14}N]^-$. The maximum tail contribution from $^{13}C^{13}C^-$ is estimated at ~10 cps at typical conditions, which even for the ultra-low N diamonds would trivially affect the count rate (<0.2‰). It should be noted that if isobaric contributions from $^{13}C^{13}C^-$ are important, they should result in $\delta^{15}N$ to be biased too low for low-N diamonds relative to related higher-N diamonds, as this isobar is a matrix element and has constant intensity for all points. No such systematic relationship has been observed.

For $^{27}[^{12}C^{15}N]^-$, the nearest isobar (at higher m/z) is $^{27}[^{13}C^{14}N]^-$, requiring R ~ 4300 for separation. The typical operating R ~ 7000 is more than adequate for separation (Figures 28, 29). Also, as this isobar is a CN^- species, the ratio $^{27}[^{12}C^{15}N]^-/^{27}[^{13}C^{14}N]^-$ is essentially fixed (~3.0) regardless of N concentration (compare Figures 28 and 29 for high and ultra-low diamond, respectively).

The $\delta^{15}N$ session commences with instrument setup and validation of performance using a dedicated mount containing various RMs, not the mount with the unknowns. Vitreous carbon, which contains very high [N], is used to verify instrument stability through repeat analyses. Then, several analyses are made of the N-abundance RM (S0280) to calibrate the yield of $^{26}[^{12}C^{14}N]^-$, i.e. cps/nA, from which the sensitivity factor for [N] can be calculated. This ('N-yield') method of determining [N] has the advantage that it is done on the same volume of material as for the N-isotopic measurement. The uncertainties in the N-yield method of determining [N] are estimated by repeat analysis of the reference diamond (S0280). For example, for session IP14019, the relative standard deviation of replicate analyses (N=16) of [N] by the yield method was 0.34%. Thus, a blanket

uncertainty of ±1% (2σ) is recommended as an estimate of the combined within-spot and between spot analytical uncertainties for the N-yield method for diamonds of widely varying [N]. This uncertainty should be used to compare data within the session. A further blanket uncertainty of (±5%) can be propagated to account for the uncertainties in the true [N] of the RM, for general reporting of data for publication.

The unknown mount is then inserted into the analysis chamber, and the $\delta^{15}N$ session proceeds with 5 analyses of the primary RM (S0270) to verify performance, and then once after every 3 unknowns. Special precautions are taken when analyzing low [N] diamond (i.e., <100 ppm), as there can be a significant surface blank contribution from residues of sample preparation if not dealt with, particularly if the diamond surface is rough. For such diamonds, extra time is spent (up to 120 s) in raster pre-conditioning the spot area. Furthermore, for all N-isotope work, extra care is spent with focusing the Cs probe geometry, and the probe is never rastered during data acquisition, all to minimize any possible contributions from surface N contamination. Data are processed in a similar way as for C-isotopes. The uncertainties for $\delta^{15}N$ values are predominantly governed by counting statistics (type 1 error, Section 3.3), and typically would range from ±0.5‰ − ±4.0‰ (2σ) over the [N] concentration range 2500 − 50 ppm, respectively. As is well accepted, aggregating several spots from the same zone is a valid way to improve precision for interpretative purposes.

3.6 NITROGEN ABUNDANCES

There are in fact two methods of determining [N]. The N-yield method is an outcome of $\delta^{15}N$ analysis (see Section 3.5). The other approach is the N-ratio method (i.e. CN^-/C_2^-) which is used principally when complete coverage (regardless of N-content) is required directly from spots previously analyzed for C-isotopes, or when N-isotopes are not to be measured. Although the ratio method is analytically more robust and versatile, both methods produce essentially equivalent results in terms of precision and accuracy. The instrument conditions for the ratio method are summarized in Table 1. There are no interferences near the matrix molecular ion $^{24}[^{12}C^{12}C]^-$ used for normalization. For $^{26}[^{12}C^{14}N]^-$, the mass resolution can be adjusted as required due to its detection in the axial position with a variable-width slit, but a resolution similar to that used for N-isotopes is adequate as discussed previously. Note that it would be possible to reduce the mass resolution to include the $^{13}C^{13}C^-$ isobar in the measurement, as this is also a matrix molecular species, but its inclusion would not benefit the [N] determination method.

The molecular ratio $^{26}[^{12}C^{14}N]^-/^{24}[^{12}C^{12}C]^-$ is directly proportional to [N], and consequently a sensitivity factor (= calibration constant, *k*) can be determined using RM (S0280) diamond with independently calibrated concentration ($[N]_{RM}$, Section 4.4), i.e.,

$$[N]_{RM} = k \bullet \{^{26}[^{12}C^{14}N]^-/^{24}[^{12}C^{12}C]^-\}_{RM}.$$

This measurement is accomplished using a special mount containing S0280 and conducting several analyses to determine *k*, and assess repeatability. The natural variation in [N] within diamonds requires the use of either FC2 (Faraday cup) or the EM for $^{26}[^{12}C^{14}N]^-$. The *k* value is determined first with S0280 using FC2 at normal beam currents, and then on the same spots with much lower beam current using the EM to inter-calibrate the FC2 and EM. The FC2 detector can be utilized with count rates as low as ~ 1 x 10^5 cps, and the EM for lower count rates. The unknown mount is then inserted to commence the session. Several analyses are initially made upon either the diamond N-isotope RM (closely-spaced spots, as it is not homogeneous in concentration over wide areas) or vitreous carbon S0233A, and then periodically analyzed (after every 10 unknowns) to check for drift or other analytical problems. For ultra-low N diamonds (e.g., <25 ppm), it may be necessary to conduct replicate analyses within the same pits to verify there was no contribution from blank surface N.

The uncertainties in the N-ratio method include the basic within-spot and between-spot components, the latter assessed by replicate [N] analyses of RMs, which give standard deviations <1%. As above, a blanket ±5% uncertainty can be propagated to the final values to reflect uncertainty in the reference material composition (type 4 uncertainty, Section 3.3).

4. CGSMS AND SIMS CHARACTERIZATION OF DIAMOND REFERENCE MATERIALS

Table 2 summarizes new (this study) and published combustion (CGSMS) $\delta^{13}C_{VPDB}$ and $\delta^{15}N_{AIR}$ determinations of diamond and other materials obtained from the Laboratoire de Géochimie des Isotopes Stables, Institut de Physique du Globe, Paris (IPGP). The CGSMS methods at IPGP follow those of Boyd et al. (1995). Diamonds were burned in an oxygen atmosphere at 1100°C, with resulting purified CO_2 and N_2 analyzed with dual inlet and triple-collector mass spectrometers, respectively. Analyses of IAEA-N-1 and N-2 ammonium sulfate RMs (Table 2) accompanying the new data suggest ±0.5‰ (2σ) accuracy of the CGSMS N-isotope data. The new CGSMS data include two $\delta^{13}C$ analyses of an in-house calcite (Renne II) deviating by only -0.06‰ from the reference

value calibrated to NBS 19 calcite (Table 2). Consequently, accuracy of the C-isotopes is consistent with the IPGP long-term value of ±0.1‰ (2σ).

Table 3 summarizes relative C-isotope ratios by CGSMS and SIMS of important RMs, and Table 4 summarizes the relative N-isotope ratios. Note the distinction between octahedral and cuboid sectors of the diamond samples, although in the following descriptions the assumption is that the cuboid sector is discussed unless explicitly indicated otherwise.

The *isotopic fractionation factor*, α, is a fundamental unit that is used to describe the fractional relationship between any pair of isotope ratios. Due to the fact that the values for α are close to unity for this work, we make customary use of the derived value, *relative isotopic difference* (= *isotope delta*, δ; see Section 1). It is important to note that δ is used here in a variety of ways, in addition to the necessary reporting of $\delta^{13}C_{VPDB}$ and $\delta^{15}N_{AIR}$ values. The definition of δ allows any pair of ratios to be compared, i.e., $\delta^{13}C_{P,Q}$ and $\delta^{15}N_{P,Q}$, where P is a sample value, and Q a reference value such as VPDB, another sample value, or an arbitrary value. For example, we frequently use δ values to illustrate small (‰) isotopic variations within samples by referencing the ratios to the mean of all the values measured. In a further example, in the case of comparing secondary RMs to the primary RM (S0270), the $\delta^{13}C_{S0xxx,\ S0270}$ value a convenient, precise, and accurate way to report their relative isotopic differences. Superscripts may be used to indicate the analytical method (i.e., CGSMS or SIMS), e.g., $\delta^{13}C^{CGSMS}{}_{S0xxx,\ S0270}$.

4.1 S0011 DIAMOND (DISCONTINUED REFERENCE MATERIAL)

The homogeneity of C-isotopes across the polished {001} faces of S0011 diamond sub-samples was initially confirmed by SIMS (i.e., STD <0.2‰). Based upon this finding, it was assumed that these diamond sub-samples were internally homogeneous in C-isotopes. Accordingly, one such sub-sample (unnamed), cut from the same slice and assumed compositionally equivalent to S0011B and S0011C (see Figs. 1, 2), was analyzed for C-isotopes by CGSMS, yielding $\delta^{13}C_{VPDB}$ = -22.58‰ ±0.02 (see Table 2). The reference value -22.58‰ was used for several projects during the initial phases of the CCIM diamond isotope program.

More extensive SIMS evaluation of S0011 sub-samples, however, revealed systematic variations in C-isotopes (and N-isotopes and N concentration, see below) normal to the {001} faces used for calibration. The experiments (ion probe session IP12088, mount M0142) involved co-mounting of the subsamples of S0011 (including B and C) in

various orientations (see Figs. 2, 3), such that both the outermost {001} face (or 'upwards' towards the growth medium, as indicated by the revised sample name S0011Bu), innermost {001} face (or 'downwards' growth, e.g., S0011Cd), and also the direction normal to {001} were exposed. Figure 3 shows a CL image of the central part of S0011A in cross section (the side face, normal to {001}), where the growth direction is towards the bottom of the image (towards darker CL). S0011A is large piece, almost one-half of the original plate, and was mounted on its edge. The image shows discrete, thin (5 – 10 μm) growth layers with subtle contrasts in CL intensity, but overall the CL intensity decreases towards the outer (upwards) growth direction. The decrease in CL corresponds with decreasing N concentrations (see below). The cross-section XS1 marks the location of equally spaced (35 μm) C-isotope spot analyses (~15 μm diameter probe), conducted near the central axis of the crystal. As shown in Figure 30, the variation in $^{13}C/^{12}C$ (relative to the downward face) is systematic and linear, with the darker (outer, or upwards) layers are ^{13}C-enriched by +0.4 ‰ compared to the inner (downwards) layer. SIMS analysis of the upwards and co-mounted downwards {001} surfaces of S0011Bu and S0011Cd surfaces, respectively, confirmed a difference of +0.4‰ (Fig. 30).

Consequently, assuming the bulk combustion $\delta^{13}C_{VPDB}$ value of -22.58‰ was equated with the average (or mid-point of the cross-section) value, the upper and downwards {001} surface compositions were calculated as -22.38‰ and -22.78‰, respectively. The uncertainty in these values, excluding those associated with the combustion measurements, is estimated at ±0.05‰. Depending on which of the two {001} surfaces was utilized in a particular SIMS session, the corresponding reference value was utilized. Consequently, some results using S0011B or C may have stated that the reference $\delta^{13}C_{VPDB}$ values as -22.58‰ prior to the recognized problem, or -22.38‰ and -22.78‰ (upper and downwards, respectively) afterwards. The {001} surface reference $\delta^{13}C$ values held only for those exposed surfaces, and subsequent re-polishing to refresh the surface has subtly changed their composition. Furthermore, subsequent inter-calibration of S0011Bd and S0011Cd surfaces with the more accurately determined S0270 diamond RM (see below) now indicates that all the aforementioned values for S0011 are slightly biased. The previously mentioned CCIM values of S0011Bd or S0011Cd faces should be corrected by +0.20‰ (estimated uncertainty ±0.1‰) to be consistent with current CCIM calibration, i.e., $\delta^{13}C_{S0011Cd/Bd,VPDB}$ = -22.58‰, which is fortuitously the same as the original bulk value.

The inadequacy of S0011 as a reference material is further evident when SIMS [N] and N-isotope measurements are considered. Although the variations in [N] were already

known at a macro-scale from UV spectral data, it is useful to describe the variations within the S0011 samples measured by SIMS. Nitrogen contents were determined across S0011A (cross-section XS1, Fig. 3), adjacent to the previous transect for C-isotopes. The N contents linearly decrease from 250 ppm to 100 ppm, corresponding to a decrease in CL intensity, and the mean [N] = 177 ppm (Fig. 31). Two other cross-sections of S0011A done closer to the edge of the crystal showed similar systematic variations, but slightly different average concentrations (214 ppm and 235 ppm), indicating some lateral (normal to the growth direction) variations in [N]. These composite [N] values determined by SIMS encompass the combustion bulk reference value of 187 ppm (Table 2) and the mean IR spectral value = 185 ppm (unpublished data).

The relative N-isotopic compositions across S0011A (XS1) also show systematic variations, increasing by ~9‰ from the downward to the upward surface (Fig. 32). The CGSMS $\delta^{15}N_{AIR}$ value of +9.5‰ for S0011 (Table 2) is effectively a N-weighted average of this profile, and therefore it would be possible to calculate the surface compositions in a similar way to the C-isotopes. Nevertheless, as much better material is now available, S0011 is declared inadequate as a N-isotope reference material at all scales.

4.2 S0203 DIAMOND (COMPARATIVE MATERIAL)

Three CGSMS C- and N-isotope determinations from fragments of S0203 (sub-sample A) are reported in Table 2. The CGSMS and SIMS C-isotope data are too heterogeneous for this sample to be useful for the purposes of calibration, and will not be considered further. The N-isotopes, however, are equivalent within assigned analytical uncertainties, with mean $\delta^{15}N_{AIR}$ = -5.51 ±0.28‰ (2σ). Compared with S0270, the calculated $\delta^{15}N^{CGSMS}_{S0203,S0270}$ = -5.11 ± 0.44 (Table 4). The three pieces analyzed by CGSMS were from unknown locations with the sub-sample S0203A, but the weights are equivalent to cubes of about 700 µm on a side, individually encompassing significant portions of the sample. The mean of the three CGSMS analyses should further suppress any original heterogeneity, and therefore it is likely to be an accurate estimate of the value of the entire sub-sample S0203A.

As shown previously (Figure 6), S0203 comprises finely CL-zoned fibrous diamond, and the SIMS N-isotopes also reveal systematic zoning. Figure 33 and 34 plot the variation in $\delta^{15}N$ relative to the innermost values and [N], respectively, against distance from the inner to outer edge of S0203B. For N-isotopes, there is a systematic and gradual decrease of -2.5‰ through 1.5 mm, then a slight increase of +1‰ towards the edge.

These trends are accompanied by a general decrease in [N] from 1400 to 700 ppm. Although S0203B is clearly heterogeneous in N-isotopes, it is useful to calculate an average relative N-isotope difference with S0270. Because the SIMS $\delta^{15}N$ analytical uncertainties scale inversely with [N], calculating an error-weighted mean of all the S0203B data gives an estimate of a nitrogen-weighted mean for the entire sub-sample, which yields $\delta\ ^{15}N^{SIMS}_{S0203,S0270}$ = -5.34 ±0.30‰ (Table 4). Such a value would be expected from a hypothetical CGSMS analysis that consumed the entire sub-sample, which in this study was not done, but it is suggested that the three separate CGSMS analyses previously mentioned are representative of the entire sample. The $\delta\ ^{15}N_{S0203,S0270}$ values for both CGSMS and SIMS are equivalent within uncertainties (Table 4).

4.3 S0270 DIAMOND (PRIMARY REFERENCE MATERIAL)

This sample is currently the primary RM for CCIM C- and N-isotope measurements.

4.3.1 C-ISOTOPES

Three CGSMS C-isotope measurements of S0270J (Figs. 9, 15) are reported in Table 2 ($\delta^{13}C_{VPDB}$ = -8.94‰, -8.87‰, and -8.74‰), with blanket analytical uncertainties given as ±0.07 ‰ (2σ). By incorporating these blanket uncertainties, a weighted mean can be calculated as $\delta^{13}C_{VPDB}$ = -8.85 ±0.04‰ (2SE) or ±0.25‰ (2σ), where the latter uncertainty is magnified by the high MSWD = 8.4. The high MSWD suggests C-isotope heterogeneity existing within S0270. As shown below, however, there is no evidence from the SIMS data of heterogeneity within S0270J, and particularly on the scale of this small piece. It is possible that the individual $\delta^{13}C$ errors for CGSMS data are underestimated for this particular analytical work. Applying a blanket uncertainty of ±0.2‰ is required to produce an ideal fit (MSWD =1), and doing so yields $\delta^{13}C_{VPDB}$ = -8.85 ±0.12‰ (Table 2), which is taken as the best estimate and uncertainty from CGSMS analysis.

The micrometer-scale C-isotope characteristics of S0270 (MC08) diamond were first investigated in the SIMS study of Howell et al. (2013a). The mean of 20 spots sampling center to outer parts of cuboid and octahedral areas gave $\delta^{13}C_{VPDB}$ = -8.96‰ ±0.05‰, (1STD = ±0.13‰), with some excess scatter beyond analytical errors. Two analyses from the outer margins gave $\delta^{13}C_{VPDB}$ = -8.62‰ and -8.65‰, and by excluding those two values yields 1STD = ±0.09‰. These data established that S0270 was remarkably homogeneous over most of the crystal, with slightly more positive values (~ +0.3‰)

towards the outer edges. Infrared spectroscopic analyses of [N] in that study gave means of 1968 ppm and 2669 ppm for cuboid and octahedral sectors, respectively.

Following laser cutting of the sub-samples described above, further SIMS characterization was carried out. In session IP13037, 11 sub-samples (S0270C though M) were co-mounted in indium (mount M0151) and analyzed for C-isotopes, with spots placed to adequately cover each sub-sample. Both octahedral and cuboid portions were targeted if present, for a total of 65 analyses. Figure 35 shows a cumulative probability curve of all 65 values of $\delta^{13}C$, calculated relative to the mean value. The ^{13}C data form a Gaussian distribution, with MSWD = 1.19 (P = 0.14), with approximately equivalent values for the standard deviation (STD = 0.067‰) and individual spot uncertainties (±0.061‰, 1σ). These results for the entire group of analyses indicate that there is no detectable C-isotope heterogeneity statistically resolvable at the scale of individual spots. Consequently, there is no evidence of isotopic heterogeneity greater than ~0.2‰ (3STD, 99% coverage) at the scale of the ion probe spots (~15 μm) for these sub-samples.

Figure 36 plots the mean $\delta^{13}C$ (±2σ, ‰) for each sub-sample for session IP13017, referenced to the mean value for the entire group. The MSWD = 2.2 for the 11 sub-samples (P = 0.011), indicating the possibility of some isotopic heterogeneity existing between sub-samples. Alternatively, this excess statistical scatter could be due to unaccounted biases from the sub-samples being located in different parts of the mount ('geometric' effects). In particular, S0270C is the furthest away from the main group (~4 mm), and it displays the largest deviation from the mean. If this sub-sample is omitted, the MSWD = 1.4 (P =0.19), indicating a good statistical fit. Under routine conditions, a minimum external uncertainty of ±0.05‰ (maximum 0.10‰) is added to the data to account for uncharacterized geometric effects, shown in Figure 36 as the slightly larger error bars. Doing so for all the 11 mean values yields MSWD = 1.3 (P =0.24), indicating that no isotopic differences between samples can be discerned. Note that the particular sub-sample analyzed by combustion (S0270J) is typical of all the sub-samples in terms of C-isotopic composition.

In another experiment (session IP14014), four sub-samples (S0270B, H, K, M) were analyzed within indium mount M0188 for a total of 65 analyses. In this case, three of the sub-samples were mounted within brass jackets (see above). Taking all data individually, the C-isotope ratios form a perfect Gaussian population (Figure 37), with MSWD =0.94. Again, data quality for the session was typical, with individual 1σ uncertainties of ±0.064‰, and standard deviation of ±0.061‰ for the group. The sub-sample mean $\delta^{13}C$

values (relative to a group mean) and ±2σ uncertainties (with and without the geometric effect) are plotted in Figure 38. The MSWD = 9.0 without error expansion for geometric effects indicates apparent isotopic differences between sub-samples. Expanding each of the errors by ±0.05‰ to account for geometric effects results in MSWD= 2.8 (P=0.04), which still indicates that small differences could exist between sub-samples. Error expansion to ±0.08‰ is required for a perfect fit to the data, which falls within the typical range of ±0.05‰ – 0.10 ‰. For this mount, all samples were mounted in brass jackets except S0270B (Fig. 21). For this dataset, it is unclear whether real isotopic differences exist between these sub-samples, although experience suggests these differences are due to geometric effects.

Carbon-isotope profiles (100 µm point spacing) were acquired across cuboid (S0270C) and octahedral (S0270B) sub-samples in IP13016, both placed adjacent to one another within indium mount M1184. The $\delta^{13}C$ values (calculated relative to the session mean C-isotope ratio) are plotted in Figure 39. It is evident from these data that there is no excess variance in $\delta^{13}C$ within and between the two sub-samples, except for the outer 200 µm in S0270C where the value steadily increases up to +0.2‰. This variation at the crystal outer edge is suspected to be real, but it could also be an analytical artifact due to edge effects caused by proximity to the beveled facets that characterized the crystal edges in this particular sample. In any case, if it exists, such C-isotopic heterogeneity is spatially located at the crystal edge and can be avoided during SIMS analysis; none of the sub-samples utilized for calibration sample this part of the crystal.

To summarize the CGSMS and SIMS C-isotope results for S0270 diamond, it is concluded that there is no clearly resolvable isotopic variation, except perhaps at the outermost growth margin of the crystal, as seen in S0270C. No C-isotope differences can be determined between the octahedral and cuboid sectors, i.e., $\delta^{13}C_{S0270oct,S0270cub} = 0.0$ (Table 3). If any heterogeneity in C-isotopes is present for the sub-samples utilized for calibration, the maximum difference between any two would be 0.1‰. There is no statistically resolvable heterogeneity at the scale of individual spots (15 µm) with typical 95% confidence uncertainties of ±0.10 − 0.15‰.

4.3.2 N-ISOTOPES

The CGSMS N-isotope data for S0270 are reported in Table 2. Three fragments derived from the entirely cuboid sub-sample (S0270J) with masses 0.17 mg, 0.39 mg, and 0.97 mg (comprising the entire sub-sample) were combusted, giving $\delta^{15}N_{AIR}$ values of -

0.52‰, -1.78‰, and -0.31‰, respectively. The errors in the table (±0.5‰, 2σ) are blanket errors assigned by IPGP based on historical performance, not calculated for each analysis. Taking means and errors as given, the weighted mean $\delta^{15}N_{S0270,AIR}$ of the 3 analyses = -0.9 ±2.0‰, with MSWD = 10.1. The high MSWD indicates that either this fragment of diamond was isotopically heterogeneous, the CGSMS analytical errors are underestimated, or one or more of the CGSMS analyses are erroneous. Detailed consideration of these possibilities follows in section 5.2.

SIMS inter-comparison of N-isotopes between the 11 sub-samples of S0270 (C through M) was conducted within indium mount M0151 in session IP13036. As before, spots were placed to representatively cover each sub-sample, with a total of 52 spots on the cuboid portions only, as these are the most abundant. The MSWD = 1.3 (P = 0.09) for all spots, indicating little evidence of heterogeneity between spots. Figure 40 plots the mean $\delta^{15}N$ (calculated relative to the mean of the data set) and 2σ uncertainties for each of the 11 sub-samples. All means are statistically consistent with one another, i.e., MSWD = 0.95 (P=0.48), with no evidence of systematic differences between the sub-samples. None of the samples show systematic internal variations in isotopic composition. Note that the value of S0270J, ultimately combusted in subsequent CGSMS analyses, is typical of the mean of the group. Figure 41 plots the mean [N] and 1STD for the sub-samples, giving a median of ~2150 ppm.

Figure 42 shows profiles of $\delta^{15}N$ (relative to the mean for S0270C) across cuboid (S0270C) and octahedral (S0270B) sub-samples, mounted adjacently in M1184 (IP13018A). For S0270C, there is a slight decrease in $\delta^{15}N$ of ~0.75‰ over the 2 mm profile. This change corresponds with a gradual decrease in [N] from 2400 ppm to 1750 ppm (Fig. 43). The slightly shorter cross-section through S0270B shows no change in N-isotopic composition, but compared with the cuboid sector, has systematically more positive values by ~+0.25 to +1.0‰, and the [N] values are also systematically higher and more uniform, dropping only slightly from 2900 ppm to 2700 ppm. The S0270C cuboid sector $\delta^{15}N$ values as a whole give MSWD =1.3 (P = 0.12), indicating that on a spot-to-spot basis, there is no statistical evidence for heterogeneity. Comparing S0270 octahedral and cuboid sectors for this session, the mean $\delta\ ^{15}N_{oct,cuboid}$ value = +0.77 ±0.15 (±2σ, MSWD = 0.70, P =0.82). The grand mean $\delta\ ^{15}N_{S0270oct,S0270cub}$ value for S0270 from a number of sessions is +0.90 ± 0.15 (2STD; Table 4).

Nitrogen isotope profiling of S0270C was repeated in session IP14019 (M0153B) to confirm the presence of subtle N-isotope zoning across the cuboid sectors. The results of

the repeat experiment are shown in Figure 44. Processed collectively (N=26), there is again no statistically significant variation across the transect, i.e., MSWD = 0.87. However, graphically from left (innermost part of crystal) to right (outer) in Figure 44, there appears to be a systematic decrease in $\delta^{15}N$ of -0.5‰, and a slight increase of ~+0.2‰ towards the very edge, similar to the previous profile (Fig. 42). It is likely that the individual SIMS uncertainties for S0270C (~±0.5‰ per spot, 2σ) are slightly overestimated, and thus potentially masking real isotopic variations. The corresponding [N] concentrations are similar to previous experiments, with an inner to outer decrease from 2370 ppm to 1600 ppm, with the majority of the transect in the range 2000 – 2200 ppm (median 2100 ppm; Fig. 45).

The SIMS N-isotope data for S0270C suggest the existence of ~0.5‰ systematic variation across the outer half of the cuboid sectors, within the planar CL-banded zone. The other cuboid sub-samples of S0270 originated predominantly from the middle part of the crystal (Fig. 9), and should not be significantly affected by this internal variability. Nevertheless, on order to suppress any possible bias, it is practice to place spots in various areas of the sub-sample during calibration. Furthermore, to account for the possibility of real isotopic differences existing between sub-sample $\delta^{15}N_{AIR}$ reference values during SIMS calibration, an additional uncertainty of ±0.15‰ is propagated to the uncertainty in the recommended $\delta^{15}N$ value of S0270, as discussed in Section 5.2.

4.4 S0280 DIAMOND (REFERENCE MATERIAL)

No CGSMS data for C- or N-isotopes currently exist for S0280 diamond.

SIMS C- and N-isotope data reveal that the sub-samples (S0280B – E), all cuboid except for a small part of S0280D, are internally homogeneous, with no measurable differences between them. It should be noted that the intact diamond plate was also studied, and that there were slight increases in C-isotope ratios towards the outer edges (N-isotopes were not studied in this zone of the crystal), similar to that observed in S0270. And similar to S0270, there are substantial sub-regions with relative isotopic homogeneity useful for the purpose of SIMS calibration, but as a whole these diamonds are not perfectly homogeneous specimens. The relative isotopic ratios of S0280 (cuboid) compared to S0270 (cuboid) were determined in several SIMS sessions and mounts, yielding mean $\delta^{13}C^{SIMS}_{S0280,S0270}$ = +0.24 ±0.06‰ (Table 3), and $\delta^{15}N^{SIMS}_{S0280,S0270}$ = +0.35 ±0.09‰ (Table 4).

As indicated by the uniform CL response, S0280 sub-samples are remarkably homogeneous in N concentration, and therefore it was selected as the preferred material for calibrating [N] abundances. SIMS N-abundance analyses (N=31) of the sub-samples, in addition to the cuboid portions of the intact original plate (data from M0152_IP13039), yield 1 standard deviation = ±2.3%. The sub-sample S0270E was analyzed by infrared absorption spectroscopy at the University of Alberta. Nine analyses over the sub-sample yield a mean = 1672 ppm and median = 1662 ppm, with 1 STD = 3.1%. The same FTIR technique carried out at Macquarie University gave a mean of 1600 ppm. A combustion analysis conducted at the Open University gave 1675 ppm (Howell et al., 2013c). The reference value for SIMS calibration purposes is set at 1670 ppm (Table 5) The uncertainty in this value when applied to SIMS calibration is estimated to be ±5%, incorporating the natural variation, as well as uncertainties arising from the scatter of the independently-determined measurements.

4.5 S0289 DIAMOND (COMPARATIVE MATERIAL)

Sample S0289 was found to be useful as a SIMS C-isotope RM, but not for N-isotopes due to its very low N concentrations (~13 ppm; Table 2). The C-isotopic composition of S0289 is particularly well-determined through existing published CGSMS data (Table 2), in which 4 replicate analyses are all statistically in agreement within the individual errors of ±0.1‰, i.e., $\delta^{13}C_{VPDB}$ = -38.58 ±0.05‰. The calculated $\delta^{13}C^{CGSMS}{}_{S0289,S0270}$ = -30.00 ±0.11 (Table 3).

An example of one of the SIMS C-isotope profiles across the exposed part of this crystal (Fig. 19) is shown in Figure 46 (M0188_IP14014B), which plots $\delta^{13}C$ relative to the section average. When these data and other spots on this crystal are considered together, a calculated MSWD = 1.7 (P = 0.012), indicating probable excess variance, and the likelihood of small amounts of internal heterogeneity, as is evident from the weak systematic CL zoning across the isotopic profile (Fig. 19). Nevertheless, the mean of the SIMS C-isotope analyses produces a precise and robust value that can be referenced to diamond S0270. Several SIMS sessions were conducted to arrive at a mean $\delta^{13}C^{SIMS}{}_{S0289,S0270}$ value = -29.94 ±0.11 (Table 3). The values of $\delta^{13}C_{S0289,S0270}$ from both methods are equivalent within uncertainties (see Section 5.1 for further discussion).

4.6 S0290 DIAMOND (COMPARATIVE MATERIAL)

The C- and N-isotopic composition of S0290 is determined from a single CGSMS analysis, giving $\delta^{13}C_{VPDB}$ = -6.01‰, $\delta^{15}N_{AIR}$ = -3.90‰ (Table 2). The resulting comparison with S0270 yields $\delta^{13}C^{CGSMS}_{S0290,S0270}$ = +2.87 ±0.11 (Table 3). In the case of N-isotopes, $\delta^{15}N^{CGSMS}_{S0290,S0270}$ = -3.50 ±0.60 (Table 4).

The SIMS C-isotope and N-isotope data for S0290 show that the interior is uniform, but that there is slight deviation at the outer 400 µm margin, coincident with brighter CL zoning (Fig. 20). For example, for session IP14014 (M0188), the C-isotope analyses collectively yield a MSWD = 1.8 (P=0.005) for 30 spots across S0290, indicating variation in excess of uncertainties, with the outer margin ~ +0.2‰ higher. Nevertheless, from several SIMS sessions, the mean $\delta^{13}C^{SIMS}_{S0290,S0270}$ = +2.83 ±0.08 (Table 3), which is a robust estimate despite slight internal heterogeneity, and statistically the same as the result generated by CGSMS (see Section 5.1).

The results of one particular set of SIMS N-isotope and [N] profiles from center to outer edge across S0290 are shown in Figures 47 and 48. The outer margin shows a weak trend in $\delta^{15}N$ towards more positive values, although all analyses are statistically within error. Combining all values for two SIMS sessions yields a mean $\delta^{15}N^{SIMS}_{S0290,S0270}$ = -3.40 ±0.20‰ (Table 4), identical to the CGSMS value (see Section 5.2)

5. VALUES FOR NEW REFERENCE MATERIALS S0270, S0280

5.1 C-ISOTOPES

The determination of a C-isotope reference value for diamond S0270, the chosen material for routine calibration, may at first seem straightforward. That is, one could simply adopt the mean of the CGSMS data, as discussed in Section 4.3.1. Although this approach is desirable in its simplicity, the robustness of the value is not evident, as there are only a small number of CGSMS analyses available (N = 3) determined together in a short period under the same conditions and protocols. There are additional constraints that can be incorporated by considering the set of SIMS- and CGSMS-determined $\delta^{13}C$ values between S0270 and secondary RMs S0289 and S0290 (Table 3). It is important to note that the $\delta^{13}C_{S0xxx,S0270}$ values determined by CGSMS depend on a fixed $\delta^{13}C_{VPDB}$ value for S0270, which in Table 3 is the best estimate (-8.85 ±0.12‰) based solely upon the CGSMS value reported here (Section 4.3.1), and the values of the other materials summarized in Table 2. In contrast, the SIMS $\delta^{13}C$ values reported in Table 3 do not rely upon any assumption of a $\delta^{13}C_{VPDB}$ value for S0270, as they were determined solely using raw $^{13}C/^{12}C$ ratios from samples that were in the same mount and analyzed in the

same session under identical analytical conditions. Extremely precise and accurate SIMS $\delta^{13}C$ values can be measured and replicated in different sessions and conditions, the means of which are reported in Table 3. In the case of CGSMS, the $\delta^{13}C$ values are potentially not as tightly controlled, as the data for the pairs of samples were collected during different periods of time, by different analysts, and no doubt with subtly different procedural and analytical conditions. Assuming that the RMs are isotopically homogeneous, and the $\delta^{13}C_{VPDB}$ values for S0270 and the other RMs are correct, the $\delta^{13}C_{S0xxx,S0270}$ values should be equivalent for both methods within uncertainties.

For the S0289 – S0270 diamond pair, the CGSMS method produced $\delta^{13}C_{S0289,S0270}$ = -30.00 ±0.11‰, and the SIMS method yielded a value of -29.94 ±0.11‰ (Table 3). For the S0290 – S0270 pair, the corresponding CGSMS and SIMS values are +2.87 ±0.11‰ and +2.83 ±0.08‰, respectively. In both cases, the two methods yield results that are in perfect agreement within error.

By slightly varying the reference $\delta^{13}C_{VPDB}$ value for S0270 used to calculate $\delta^{13}C^{CGSMS}_{S0xxx,S0270}$, a solution can be determined that minimizes the differences between the SIMS and CGSMS $\delta^{13}C_{S0xxx,.S0270}$ values. This modeling yields a best-fit value of $\delta^{13}C_{S0270,VPDB}$ = -8.88‰ with estimated 2σ uncertainty of ±0.05‰. If this result is utilized in the SIMS $\delta^{13}C$ determination of S0289 and S0290, using the $\delta^{13}C^{SIMS}_{S0xxx,S0270}$ value (Table 3) it would produce SIMS-determined C-isotopic compositions that differ from the corresponding CGSMS values by +0.03‰ and -0.06‰, respectively, both within the CGSMS analytical errors. The modelled $\delta^{13}C$ value of -8.88‰ for S0270 is well within the uncertainty of the CGSMS result (-8.85 ±0.12‰, Table 2). As this analysis in more robust in taking into account the CGSMS and SIMS determinations from three different RMs (S0270, S0289, S0290), it is recommended that the $\delta^{13}C_{VPDB}$ reference value for S0270 be set at -8.88 ±0.10‰ (2σ), as summarized in Table 5. This value applies to both cuboid and octahedral components. Consideration should be given on whether or not the ±0.10‰ uncertainty (type 4) is propagated to the uncertainties in the $\delta^{13}C_{VPDB}$ values of the unknowns, as discussed in Section 3.3.

For the determination of a reference value for diamond S0280, for which no CGSMS data are available, the SIMS-determined $\delta^{13}C_{S0280,S0270}$ value of +0.24 ±0.06‰ (Table 3) can be used to calculate $\delta^{13}C_{S0280,VPDB}$ = -8.64 ±0.12‰ (Table 5). This result applies to both cuboid and octahedral sectors, keeping in mind that, as for S0270, the crystal margins are to be avoided due to slightly more positive values. If the recommended value of S0270 should change in the future, then the value for S0280 will change accordingly.

5.2 N-ISOTOPES

The CGSMS N-isotope data for S0270J yielded a $\delta^{15}N_{AIR}$ value of -0.9 ±2.0‰, with MSWD = 10.1 (Section 4.3.2). That these data are not equivalent within stated uncertainties contradicts the SIMS evaluation which showed no heterogeneity within S0270J. The statistical uncertainty in the CGSMS mean (±2‰) is also inadequate for the purpose of a reference material. In arriving at a suitably precise and accurate reference value for S0270, it is necessary to examine the CGSMS data in more detail, and then combine this information with the CGSMS and SIMS data for other samples, in a similar approach as taken for C-isotopes (Section 5.1).

The first possibility to explain the CGSMS $\delta^{15}N$ data for S0270J is that this sub-sample, and by implication the others, was isotopically heterogeneous at the scale of the combustion analyses (i.e., >200 μm). Due to the significant masses of diamond pieces combusted, the apparent range of 1.5‰ would be a minimum estimate of any heterogeneity that might have existed at smaller scales. However, the presence of isotopic heterogeneity within S0270J of this magnitude cannot be reconciled with the SIMS analyses of S0270J, nor any of the other sub-samples measured by SIMS, with analytical uncertainties that are equivalent to the CGSMS data (±0.5‰). The only systematic heterogeneity in $\delta^{15}N$ detected by SIMS was in the outer portions of the cuboid sectors, with an apparent difference of -0.5‰ in comparison to the inner portions (Figs. 42, 44). Furthermore, the N-concentrations in any part vary by no more than 10%, so a 'nugget effect' from an unusually N-rich area with anomalous isotopic composition cannot explain the CGSMS results. The standard deviation for repeat SIMS $\delta^{15}N$ analyses, particularly on small fragments such as S0270J (the one consumed for CGSMS), is consistent with the individual uncertainties of ~ ±0.25‰ (1STD). Thus, the SIMS data indicate that isotopic heterogeneity of >1.5‰ cannot and does not exist in S0270. If large zones within S0270J differed by >1.5‰, as suggested by the range of the combustion analyses, they would have easily been detected by SIMS. Consequently, the suitability of using the mean of all the CGSMS data for the SIMS reference value is brought into question.

The second possible explanation for the CGSMS $\delta^{15}N$ data for S0270 is that the analytical uncertainties are underestimated for some analyses. There is some evidence from the two replicate analyses of the ammonium sulphate standard IAEA-N-2 that the blanket uncertainty of ±0.5‰ may be too low. The difference of 0.92‰ between the two $\delta^{15}N$ values of N-2 suggests an apparent uncertainty of about ±0.75 − 1‰, depending on

whether these two analyses represent extreme values or typical values. On the other hand, in other samples (N-1, S0203A) for which replicates were conducted, the blanket uncertainty is adequate to explain the scatter. For S0270J, however, the average individual analytical uncertainty would need to be ±1.6‰ for the S0270 analyses to be considered samples of an ideal single population (i.e., MSWD = 1.0). Allowing for error expansion by this amount yields a mean $\delta^{15}N_{AIR}$ value of -0.9 ±1.0‰, such that the errors are reduced, but we are still left with the possibility of bias in the mean value.

The more plausible explanation is that at least one of the CGSMS $\delta^{15}N_{AIR}$ values for S0270 is erroneous. The two $\delta^{15}N$ values of -0.52‰ and -0.31‰ readily agree within the blanket uncertainty of ±0.5‰, indicating that the -1.78‰ value is an outlier. The (rounded-down) mid-point of these two values, $\delta^{15}N$ = -0.4‰, is therefore our preferred estimate of the N-isotopic composition of S0270 based upon CGSMS. The uncertainty of this value is difficult to estimate given the caveats mentioned previously, but it would be slightly better than the individual analyses by √2, i.e., ~±0.35‰ (2σ). This best estimate and uncertainty is reported in Table 2.

Similar to the analysis used to arrive at the C-isotope reference value for S0270 diamond (Section 5.1), modeling of the complete CGSMS and SIMS data sets can help to validate and refine the result. It should be noted that, as for C-isotopes, all of the sub-samples utilized by SIMS are from different portions of the same crystal utilized for CGSMS analysis, such that we cannot be certain that the two data sets (CGSMS and SIMS) are from compositionally identical material. The only assumptions required for the SIMS inter-comparison of the RMs are the absence of matrix effects or other uncorrected analytical biases between samples, and that the RMs are isotopically homogeneous. Isotopic heterogeneity complicates the determination of a representative mean $\delta^{15}N^{SIMS}_{S0xxx,S0270}$ for comparison with CGSMS values.

For SIMS, special experiments were conducted for the purpose of comparing S0270 with S0203 and S0290. Pieces of all three RMs were co-mounted and analyzed repeatedly in two different SIMS sessions (IP14011 and IP14012 on mount M0187), yielding precise relative differences in N-isotopic compositions. Table 4 summarizes the $\delta^{15}N_{Sxxxx,S0270}$ values for both SIMS and CGSMS. For the CGSMS values, a mean $\delta^{15}N_{S0270,AIR}$ value of -0.4‰ was utilized, and for the SIMS values, no assumption is required, as the differences are directly measured (as above, Section 5.1). For S0203, the values were $\delta^{15}N^{CGSMS}_{S0203,S0270}$ = -5.11 ±0.44‰ and $\delta^{15}N^{SIMS}_{S0203,S0270}$ = -5.34 ±0.30‰. For S0290,

the values were $\delta^{15}N^{CGSMS}_{S0203,S0270}$ = -3.50 ±0.60‰ and $\delta^{15}N^{SIMS}_{S0203/S0270}$ = -3.40 ±0.20‰. Each pair of values is equivalent within the uncertainties.

If $\delta^{15}N_{S0270,AIR}$ = -0.4‰, as measured by CGSMS, the calculated SIMS $\delta^{15}N_{S0203,\ AIR}$ value is -5.73‰, with a misfit -0.19‰ compared with the CGSMS value. Similarly for S0290, the calculated SIMS $\delta^{15}N_{AIR}$ = -3.80‰, with a misfit of +0.10‰ with the CGSMS value. These results fall well within the CGSMS $\delta^{15}N$ analytical uncertainties for these secondary RMs of ±0.3‰ and ±0.5‰, respectively. As done for C-isotopes, we can vary the $\delta^{15}N^{CGSMS}_{S0270,AIR}$ value in order to minimize the error-weighted differences between the $\delta^{15}N^{CGSMS}_{Sxxxx,S0270}$ and $\delta^{15}N^{SIMS}_{Sxxxx,S0270}$ values. The best-fit solution yields a $\delta^{15}N_{S0270,AIR}$ value of -0.40‰ ±0.35‰ (95% confidence interval). This reference value pertains to the center, cuboid part of S0270, and is presumed to reflect the majority of the sub-samples used at CCIM for calibration. As discussed previously, there is the possibility that the chosen sub-sample of S0270 used in a particular SIMS session may differ slightly from the average, owing to the slight systematic variation in $\delta^{15}N$ towards the outer part of the crystal. It is currently uncertain to what extent, if any, this may contribute to uncertainty in the accuracy of the calibrated values. As a conservative approach, an additional ±0.15‰ uncertainty may be propagated for the purpose of SIMS calibrations, thus yielding a recommended value of $\underline{\delta^{15}N_{S0270cub,AIR} = -0.40 \pm 0.50‰}$ (Table 5). Consideration should be given on whether or not the ±0.50‰ uncertainty (type 4) is propagated to the uncertainties in the $\delta^{15}N_{AIR}$ values of the unknowns, as discussed in Section 3.3.

For the octahedral portions of S0270, based upon the determined value for $\delta^{15}N^{SIMS}_{S0270oct,S0270cub}$ = +0.90‰ (Table 4), the calculated $\delta^{15}N_{S0270oct,AIR}$ value is +0.50 ±0.65‰ (Table 5). The octahedral sectors are currently not used in calibration, but can be used if required. Similarly, for S0280 (cuboid), from the determined value of $\delta^{15}N^{SIMS}_{S0280cub,S0270cub}$ = +0.35‰ (Table 4), the value for $\delta^{15}N_{S0280cub,AIR}$ = -0.05 ±0.60‰ (Table 5). As for C-isotopes, S0280 could be used as a secondary RM for N-isotopes, although a diamond with greater contrast in isotopic composition compared to S0270 is preferable.

6. SUMMARY

Table 5 presents the recommended $\delta^{13}C_{VPDB}$ and $\delta^{15}N_{AIR}$ values and associated uncertainties of the primary diamond reference material, the cuboid sectors of sample S0270 (MC08). Diamond S0280 (MC13) is adopted as a N-abundance RM, and is also

suitable as a secondary RM for C- and N-isotopes. Further research is aimed at expanding the number and type of diamond isotope RMs, and extending N-isotope analysis to ultra-low [N] diamond.

7. ACKNOWLEDGMENTS

L. Hunt kindly provided FTIR data on S0280 diamond. D. Petts provided a critical review of the manuscript and helpful suggestions on presentation and terminology.

8. REFERENCES

Boyd, S. R., Mattey, D. P., Pillinger, C. T., Milledge, H. J., Mendelssohn, M., and Seal, M., 1987. Multiple growth events during diamond genesis: an integrated study of carbon and nitrogen isotopes and nitrogen aggregation state in coated stones. Earth Planet. Sci. Lett. 86, 341-353.

Boyd, S. R., Réjou-Michel, A., and Javoy, M., 1995. Improved techniques for the extraction, purification and quantification of nano-mole quantities of nitrogen gas: the nitrogen content of a diamond. Measurement Science and Technology. Meas. Sci. Technol. 6, 297-305.

Cartigny, P., Stachel, T., Harris, J. W., and Javoy, M., 2004. Constraining diamond metasomatic growth using C- and N-stable isotopes: examples from Namibia. Lithos 77, 359-373.

Coplen, T. B., 2011. Guidelines and recommended terms for expression of stable-isotope-ratio and gas-ratio measurement results. Rapid Commun. Mass Spectrom. 25, 2538-2560.

Coplen, T. B., Hopple, J. A., Böhlke, J. K., Peiser, H. S., Rieder, S. E., Krouse, H. R., Rosman, K. J. R., Ding, T., Vocke Jr., R. D., Révész, K. M., Lamberty, A., Taylor, P., and De Bièvre, P., 2002. Compilation of minimum and maximum isotope ratios of selected elements in naturally occurring terrestrial materials and reagents. Water-Resources Investigations Report 01-4222. United States Geological Survey. 98pp.

Howell, D., Griffin, W. L., Piazolo, S., Say, J. M., Stern, R. A., Stachel, T., Nasdala, L., Rabeau, J. R., Pearson, N. J., and O'Reilly, S. Y., 2013a. A spectroscopic and carbon-isotope study of mixed-habit diamonds: impurity characteristics and growth environment. Am. Mineral. 98, 66-77.

Howell, D., Griffin, W. L., Pearson, N. J., Powell, W., Wieland, P., and O'Reilly, S. Y., 2013b. Trace element partitioning in mixed-habit diamonds. Chem. Geol. 355, 134-143.

Howell, D., Stern, R. A., Griffin, W. L., Southworth, R., Mikhail, S., Stachel, T., Verchovsky, A. B., Jones, A. P., O'Reilly, S. Y., and Pearson, N. J., 2013c. Nitrogen isotope systematics and origins of mixed-habit diamonds. Goldschmidt 2013 Conference Abstracts, pp.1328, DOI:10.1180/minmag.2013.077.5.8.

Ickert, R. B. and Stern, R. A., 2013. Matrix corrections and error analysis in high-precision SIMS $^{18}O/^{16}O$ measurements of Ca-Mg-Fe garnet. Geostandards Geoanalytical. Res. 37, 429-448.

Rakovan, J., Gaillou, E., Post, J. E., Jaszczak, J. A., and Betts, J. H., 2014. Optically sector-zoned (star) diamonds from Zimbabwe. Rocks & Minerals, 89:2, 173-178, DOI: 10.1080/00357529.2014.842844.

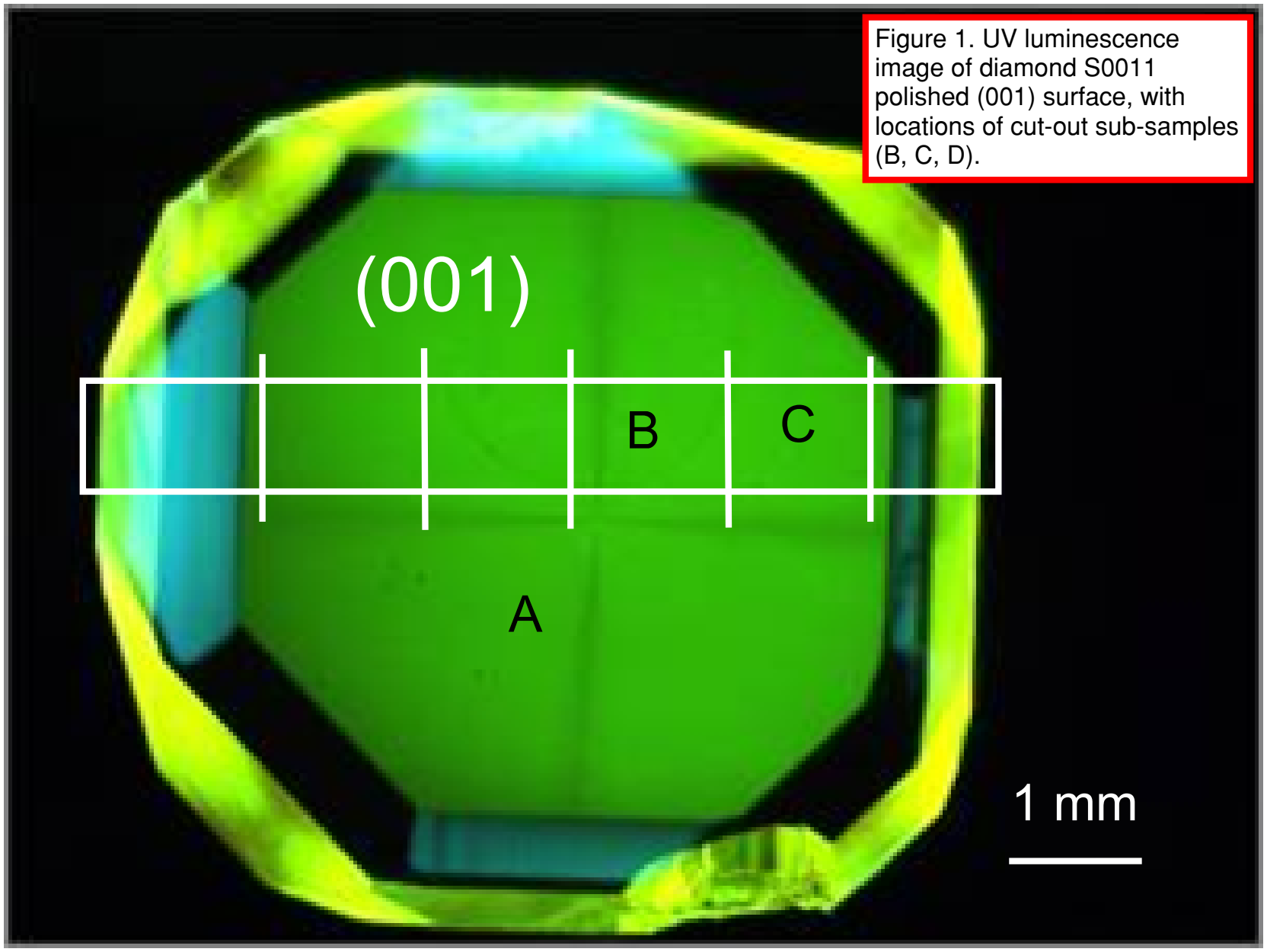

Figure 1. UV luminescence image of diamond S0011 polished (001) surface, with locations of cut-out sub-samples (B, C, D).

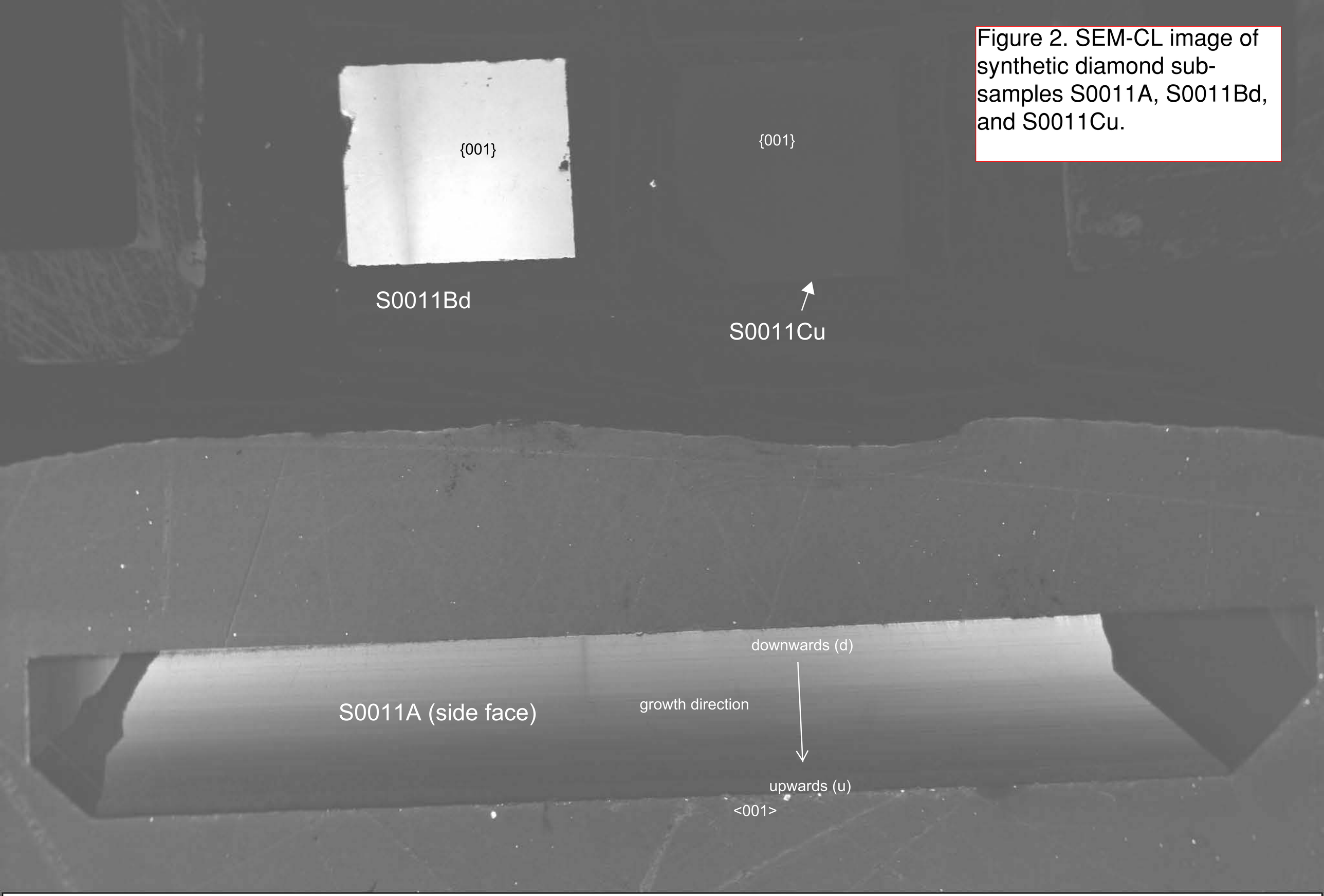

Figure 2. SEM-CL image of synthetic diamond sub-samples S0011A, S0011Bd, and S0011Cu.

Figure 3. SEM-CL image of synthetic diamond sub-sample S0011A. Location of XS1 used for isotopic profiling is shown.

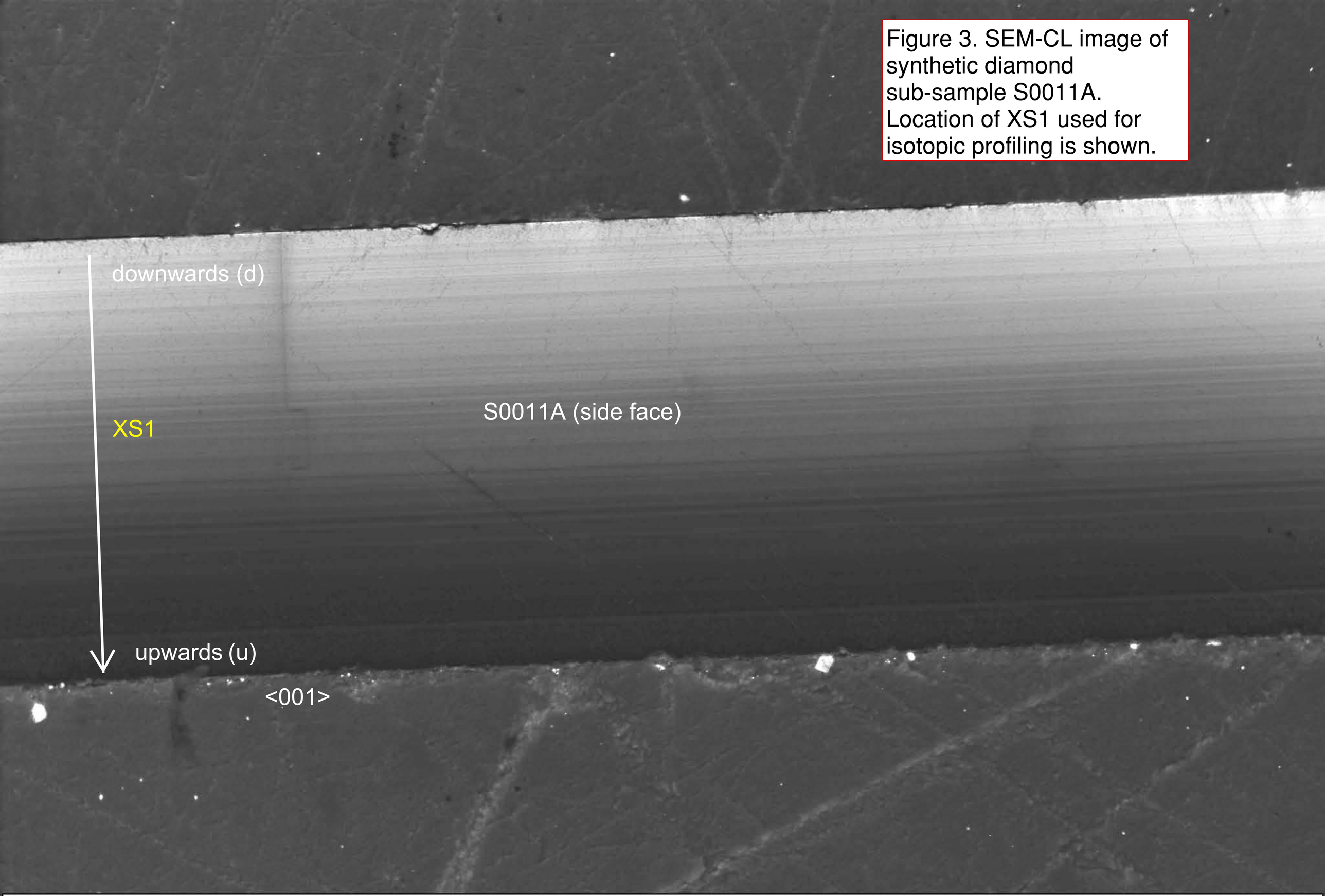

Fibrous rim

Gem interior

2 mm

Figure 4. Plane light image of diamond plate S0203(BAK).

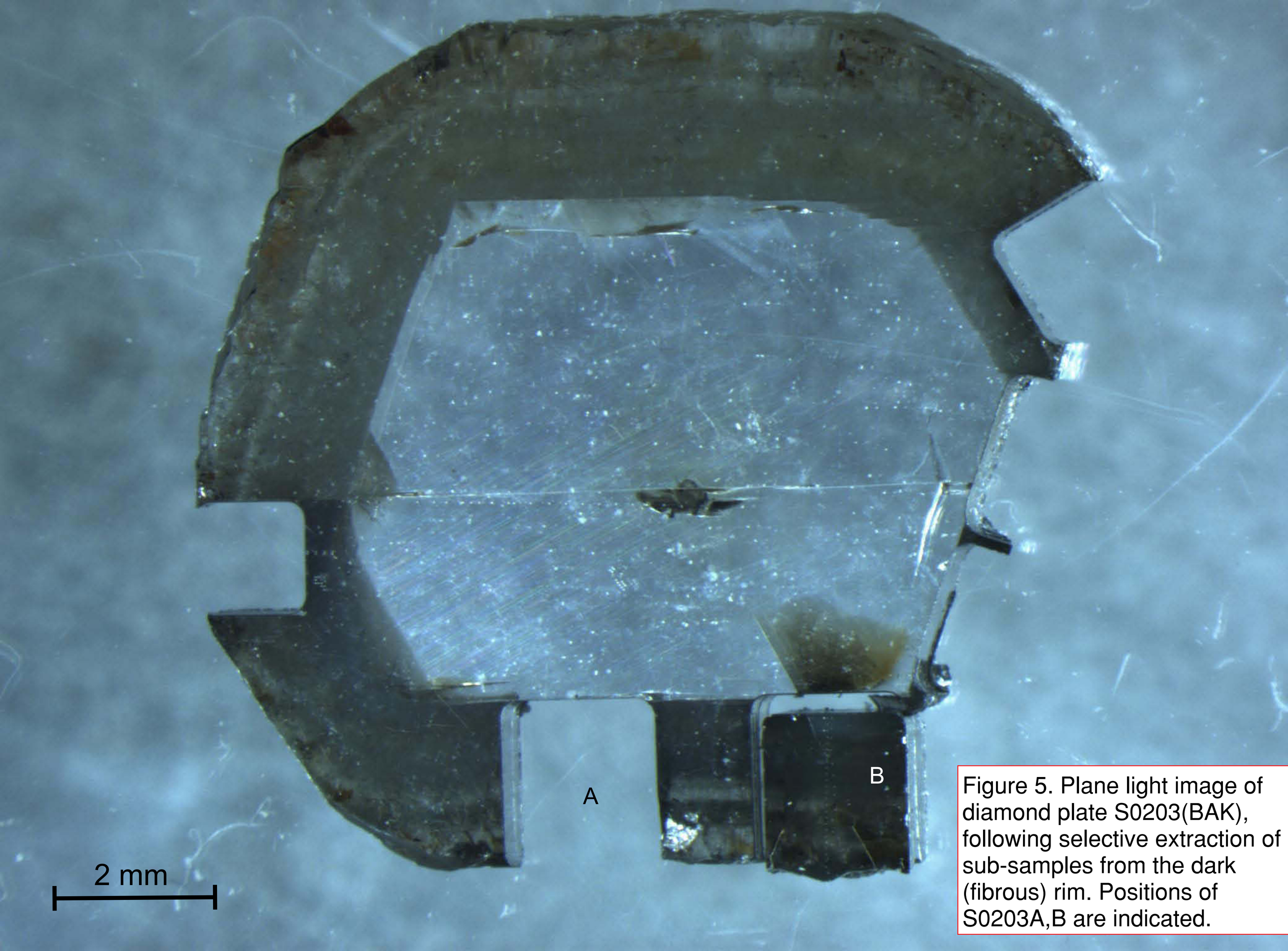

Figure 5. Plane light image of diamond plate S0203(BAK), following selective extraction of sub-samples from the dark (fibrous) rim. Positions of S0203A,B are indicated.

(m) S0203B diamond

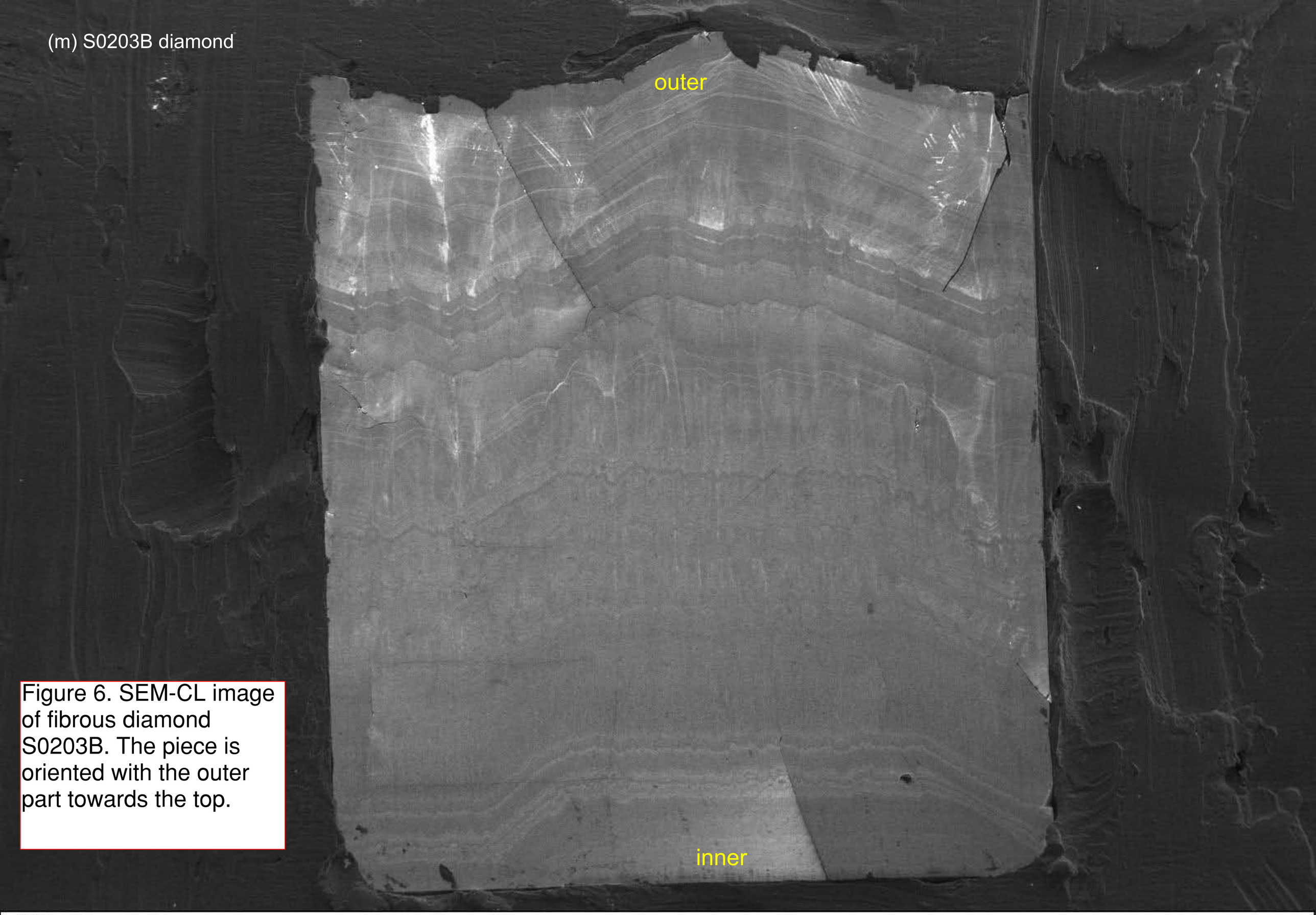

Figure 6. SEM-CL image of fibrous diamond S0203B. The piece is oriented with the outer part towards the top.

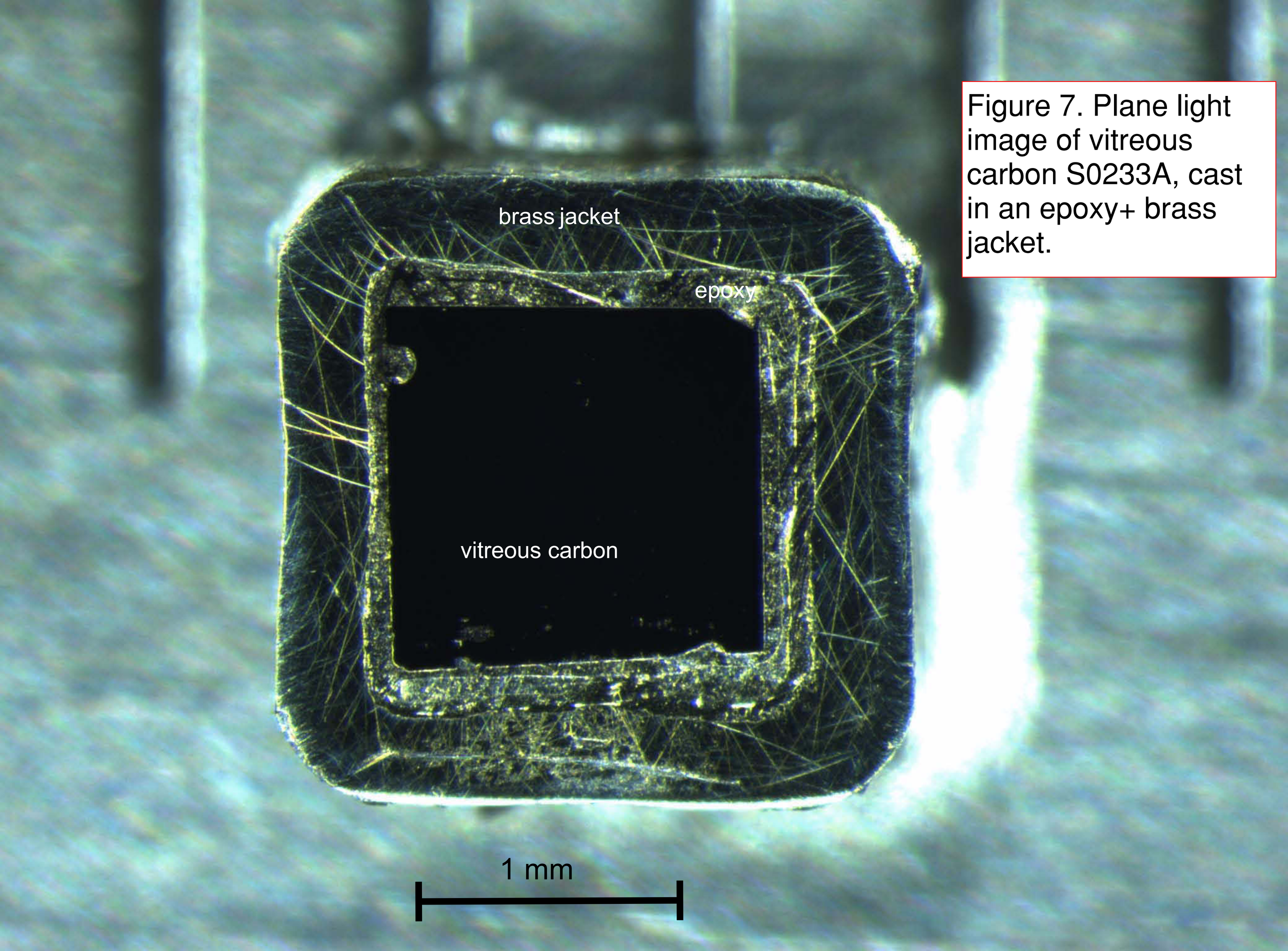

Figure 7. Plane light image of vitreous carbon S0233A, cast in an epoxy+ brass jacket.

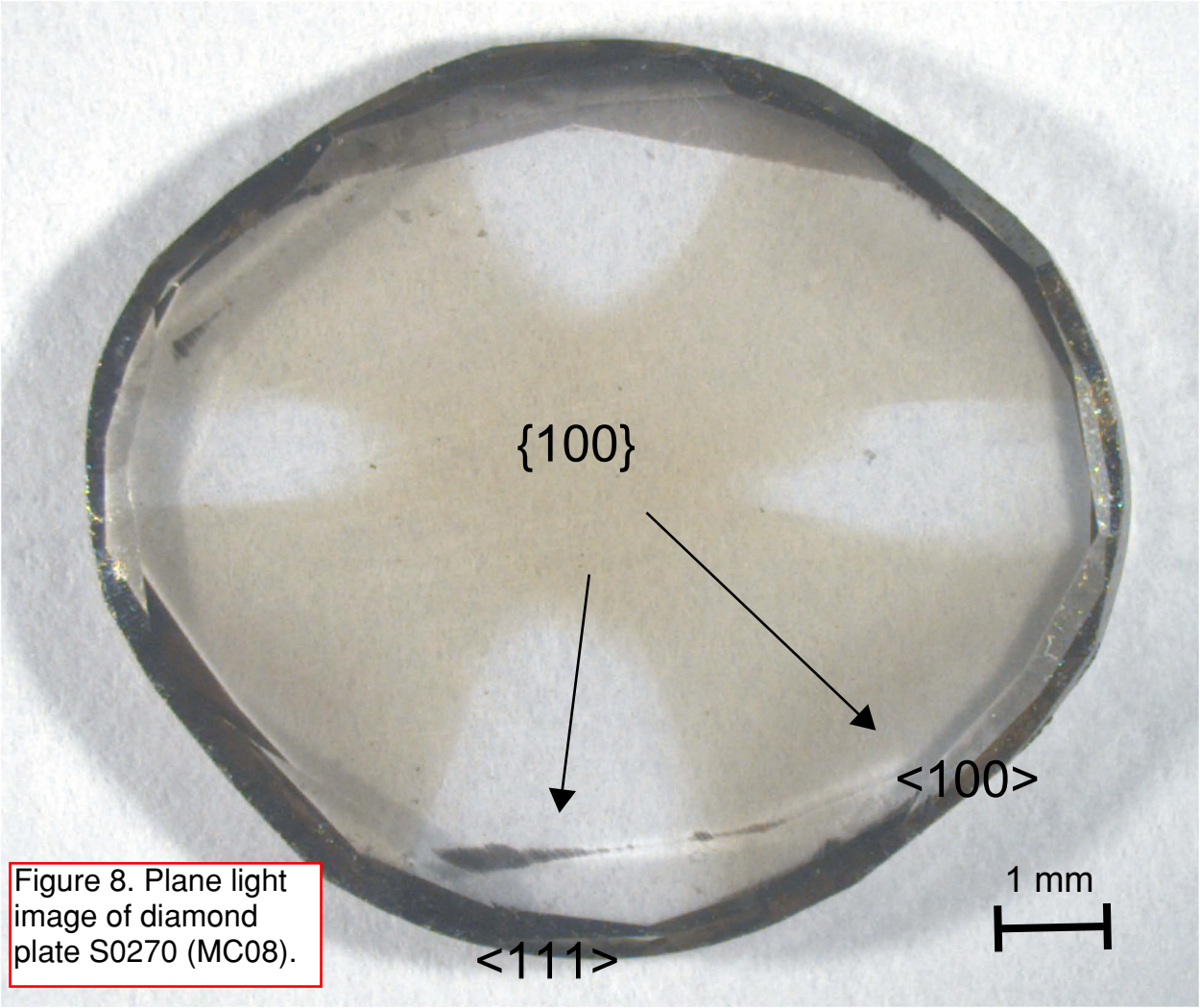

Figure 8. Plane light image of diamond plate S0270 (MC08).

Figure 9. SEM-CL image of diamond plate S0270 (MC08, S1163). Locations of laser cut sub-samples are outlined (yellow).

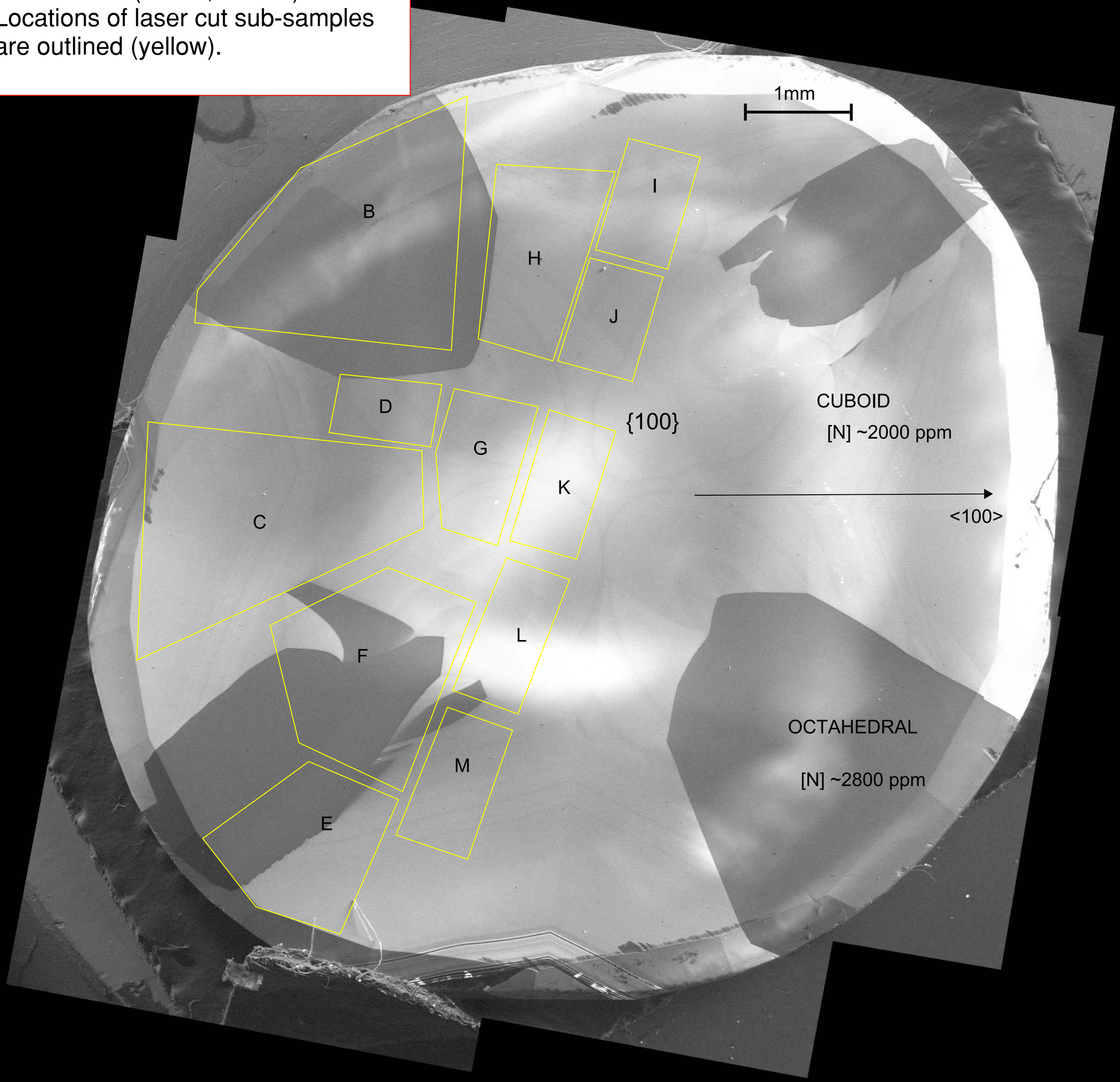

Figure 10. SEM-CL image of diamond plate S0270 (MC08, S1163), the underside of plate shown in Fig. 9.

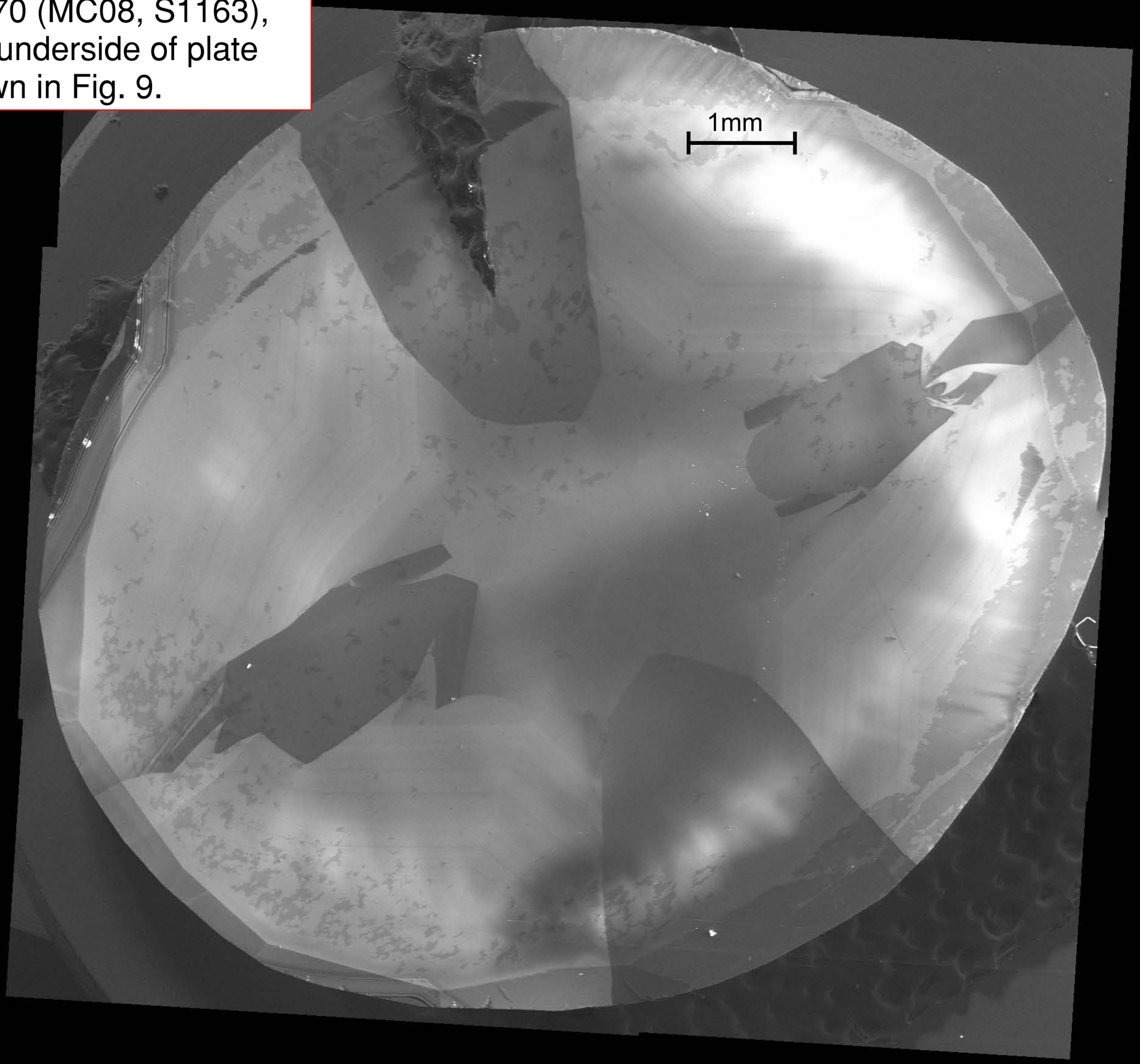

Figure 11. SEM-CL image of diamond sub-sample S0270E, which contains both cuboid and octahedral portions. Note subtle zoning continuous through sectors.

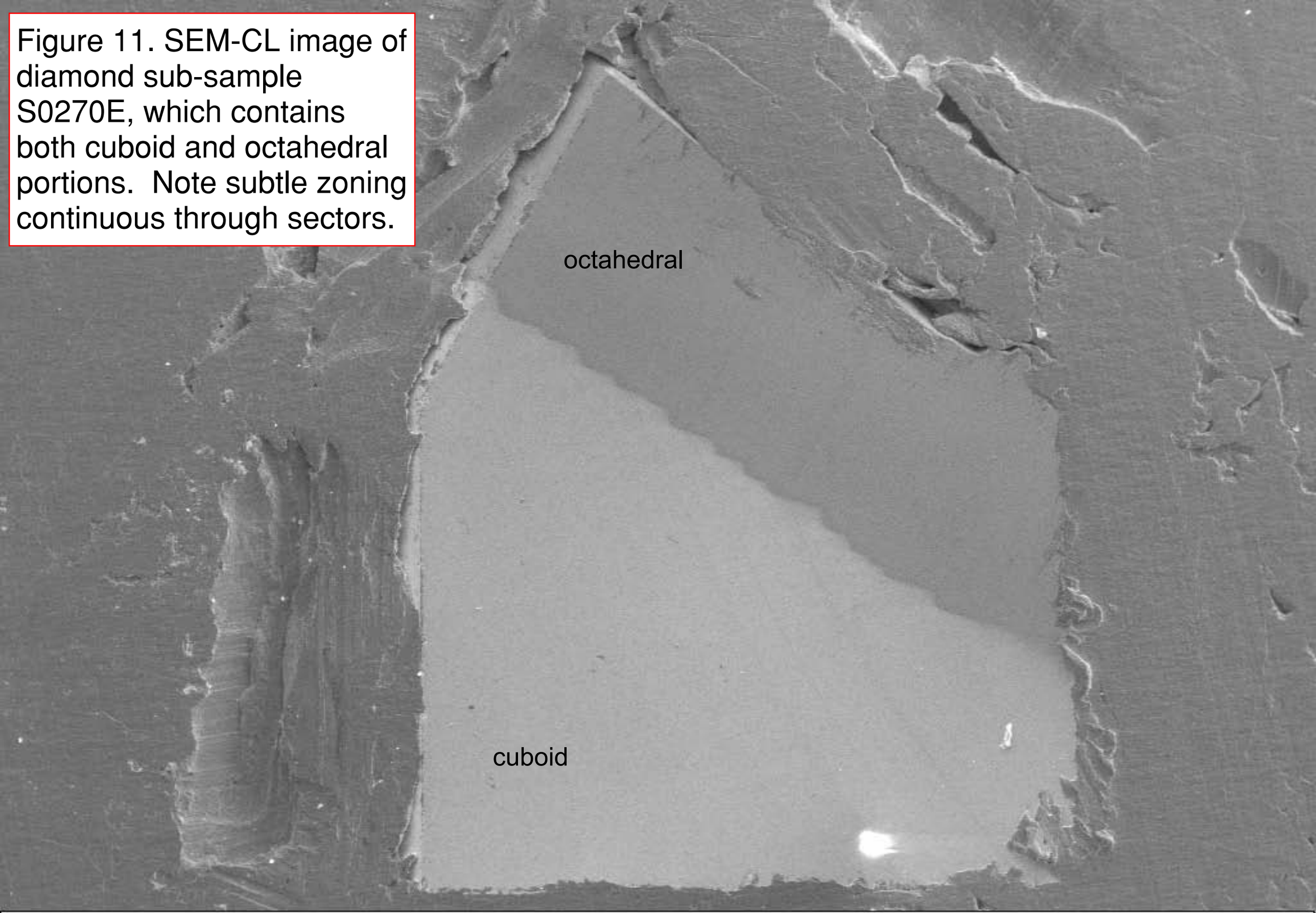

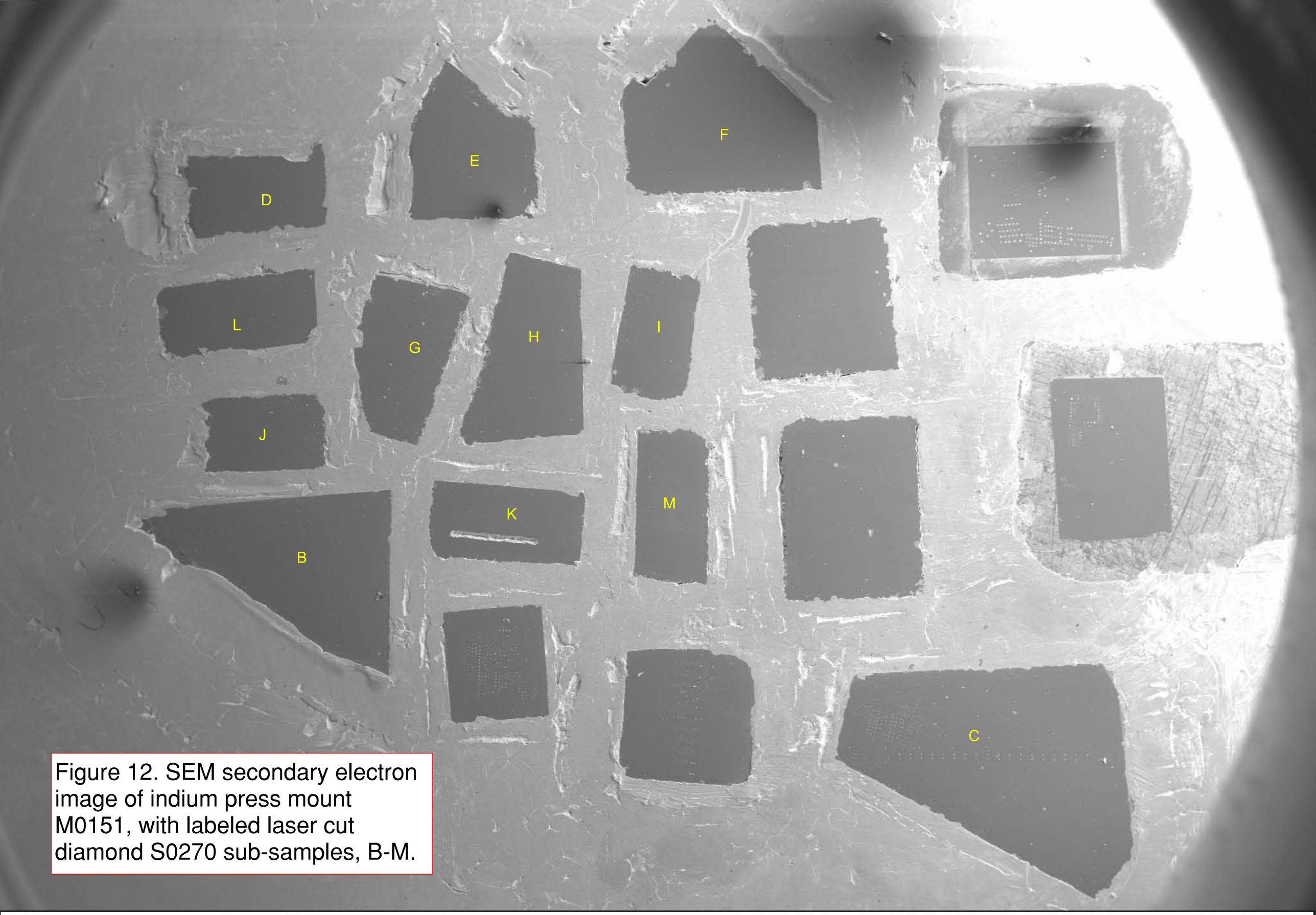

Figure 12. SEM secondary electron image of indium press mount M0151, with labeled laser cut diamond S0270 sub-samples, B-M.

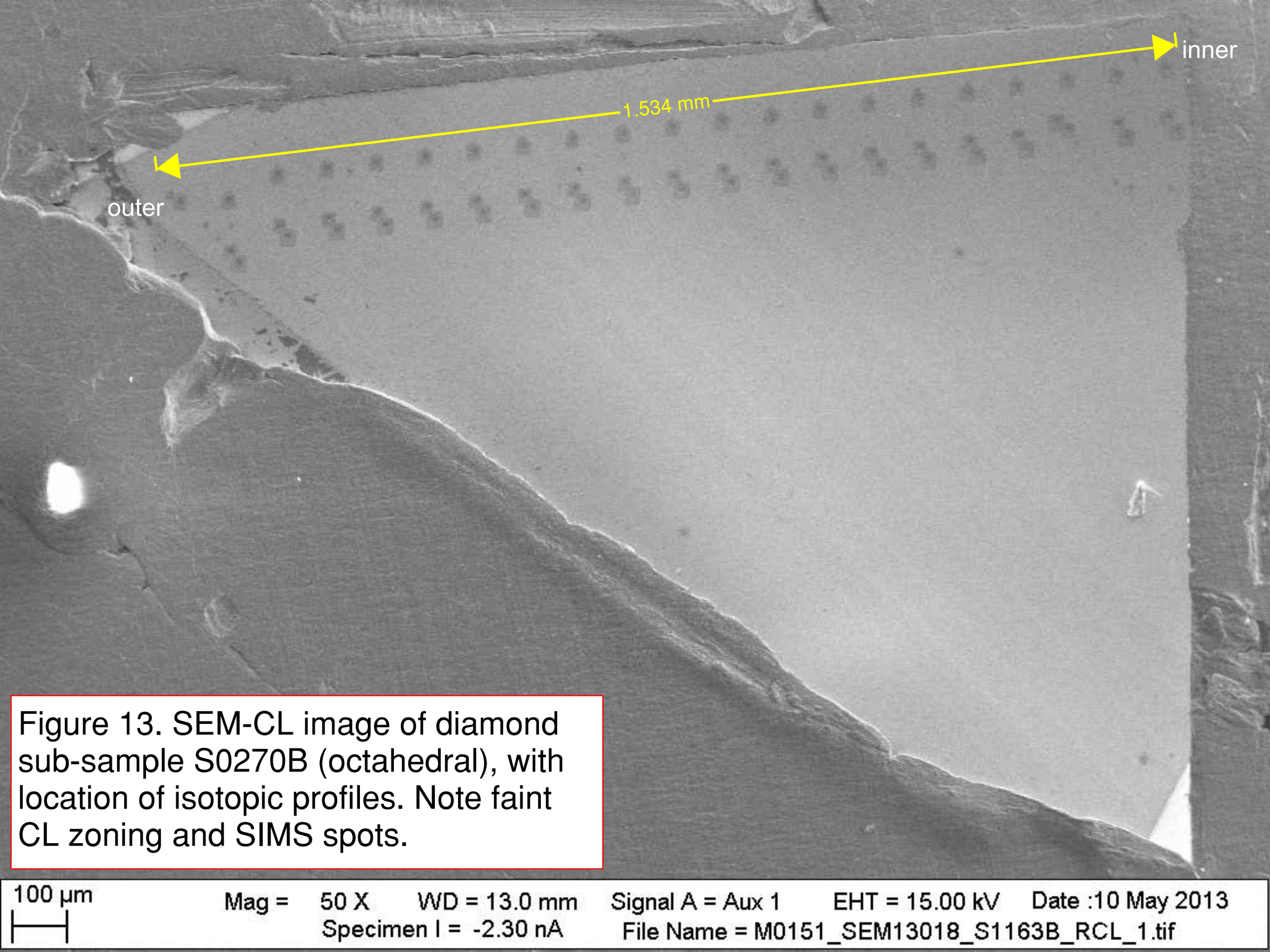

Figure 13. SEM-CL image of diamond sub-sample S0270B (octahedral), with location of isotopic profiles. Note faint CL zoning and SIMS spots.

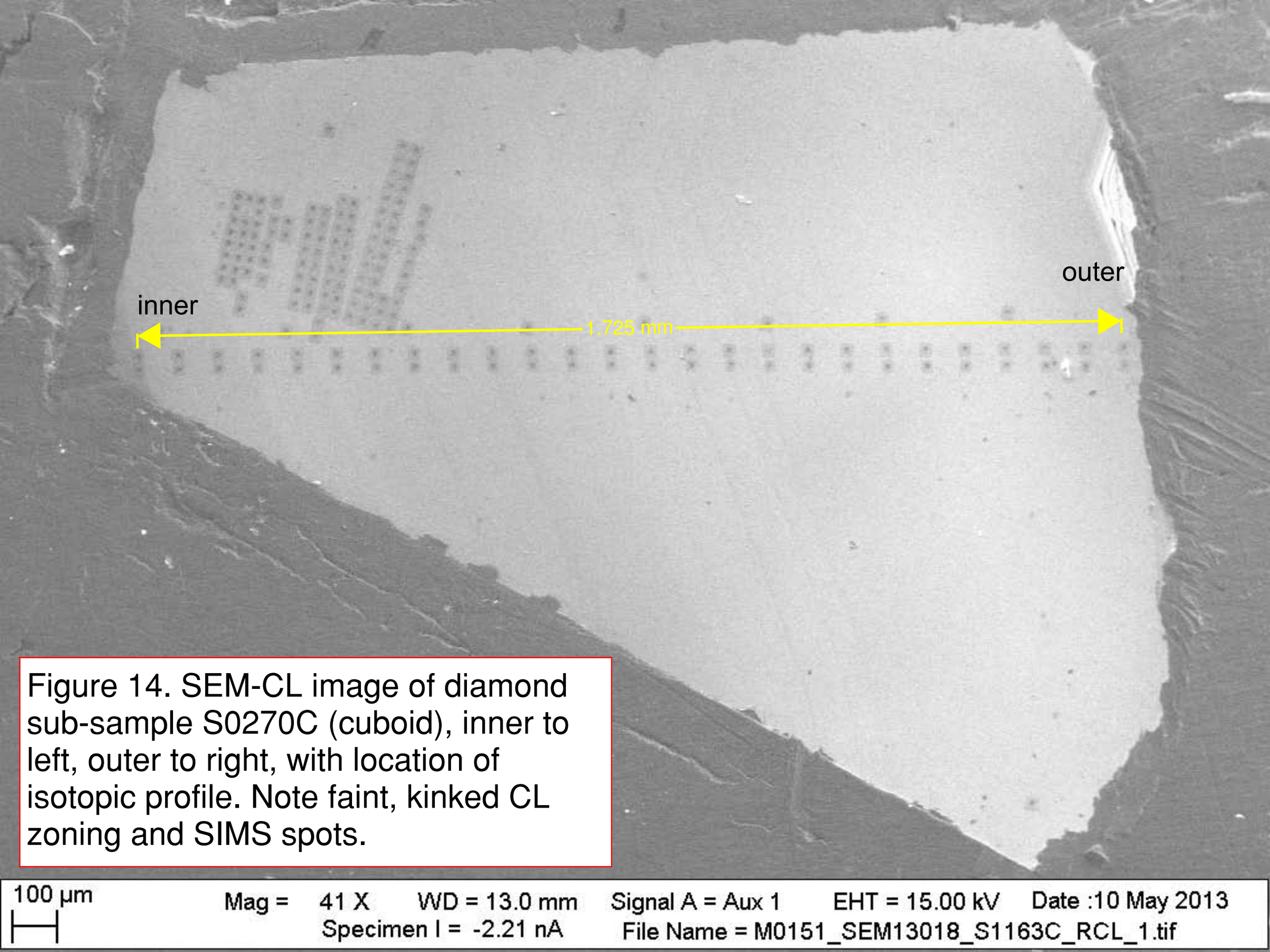

Figure 14. SEM-CL image of diamond sub-sample S0270C (cuboid), inner to left, outer to right, with location of isotopic profile. Note faint, kinked CL zoning and SIMS spots.

Figure 15. SEM-CL image of diamond sub-sample S0270J.

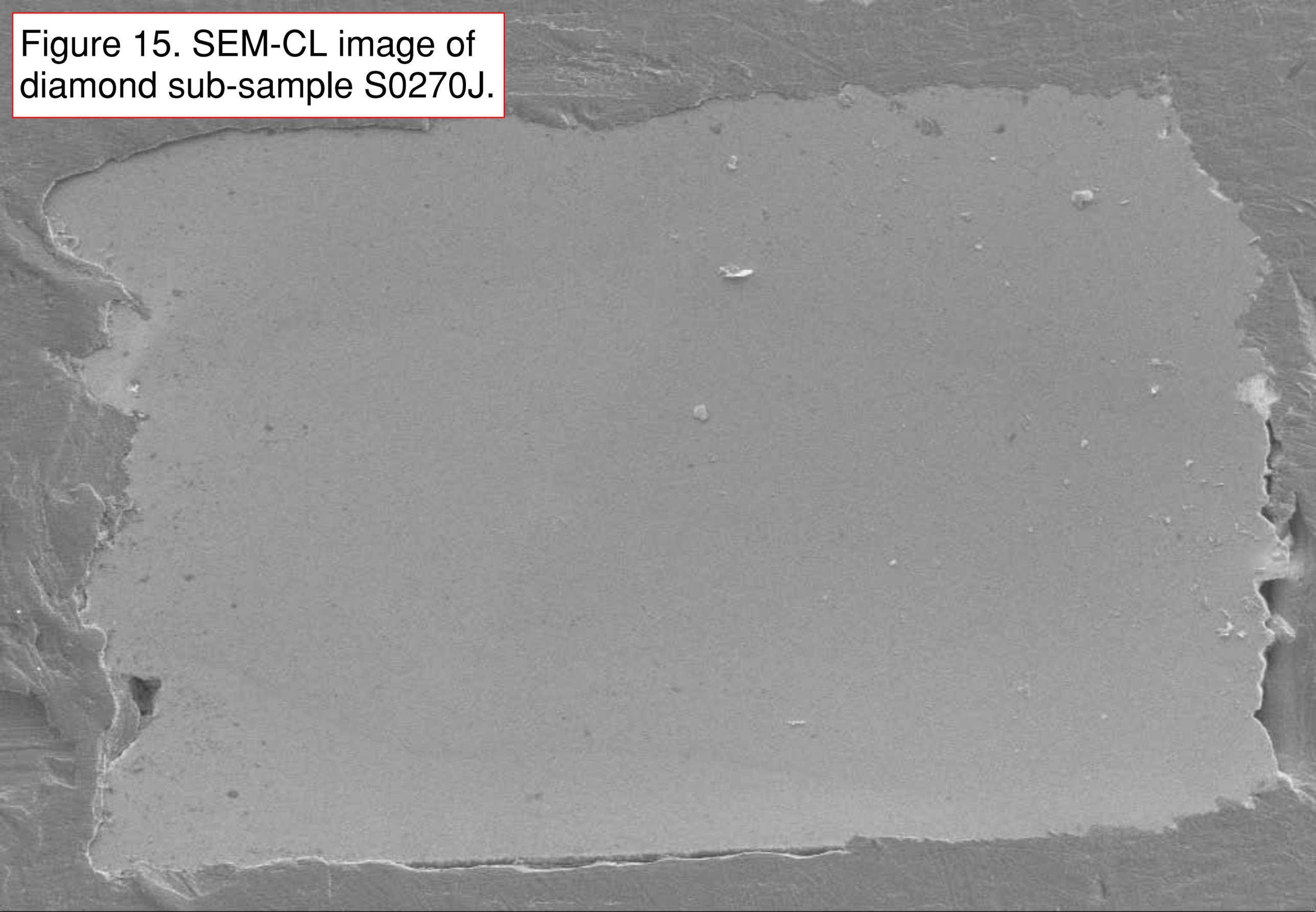

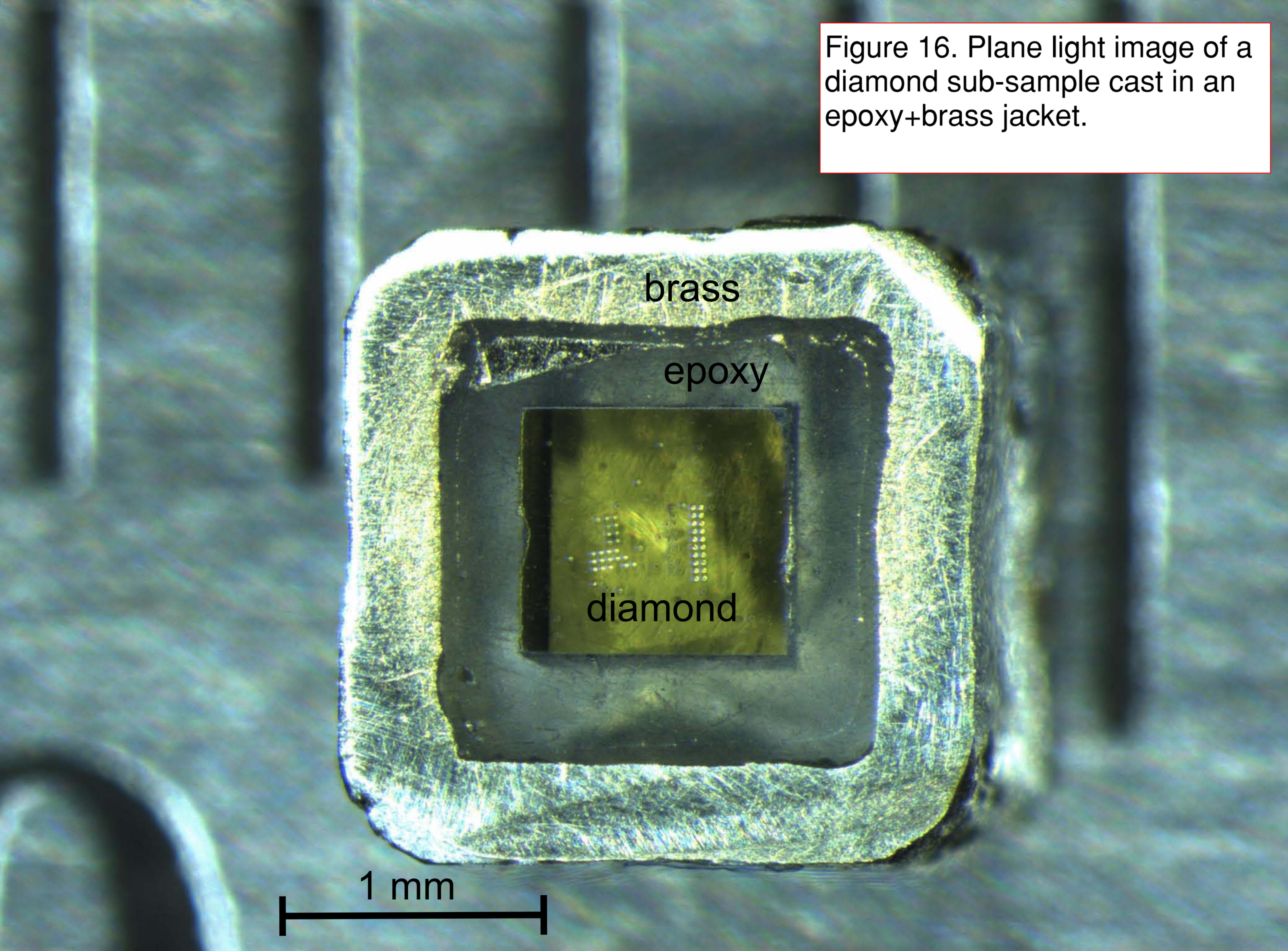

Figure 16. Plane light image of a diamond sub-sample cast in an epoxy+brass jacket.

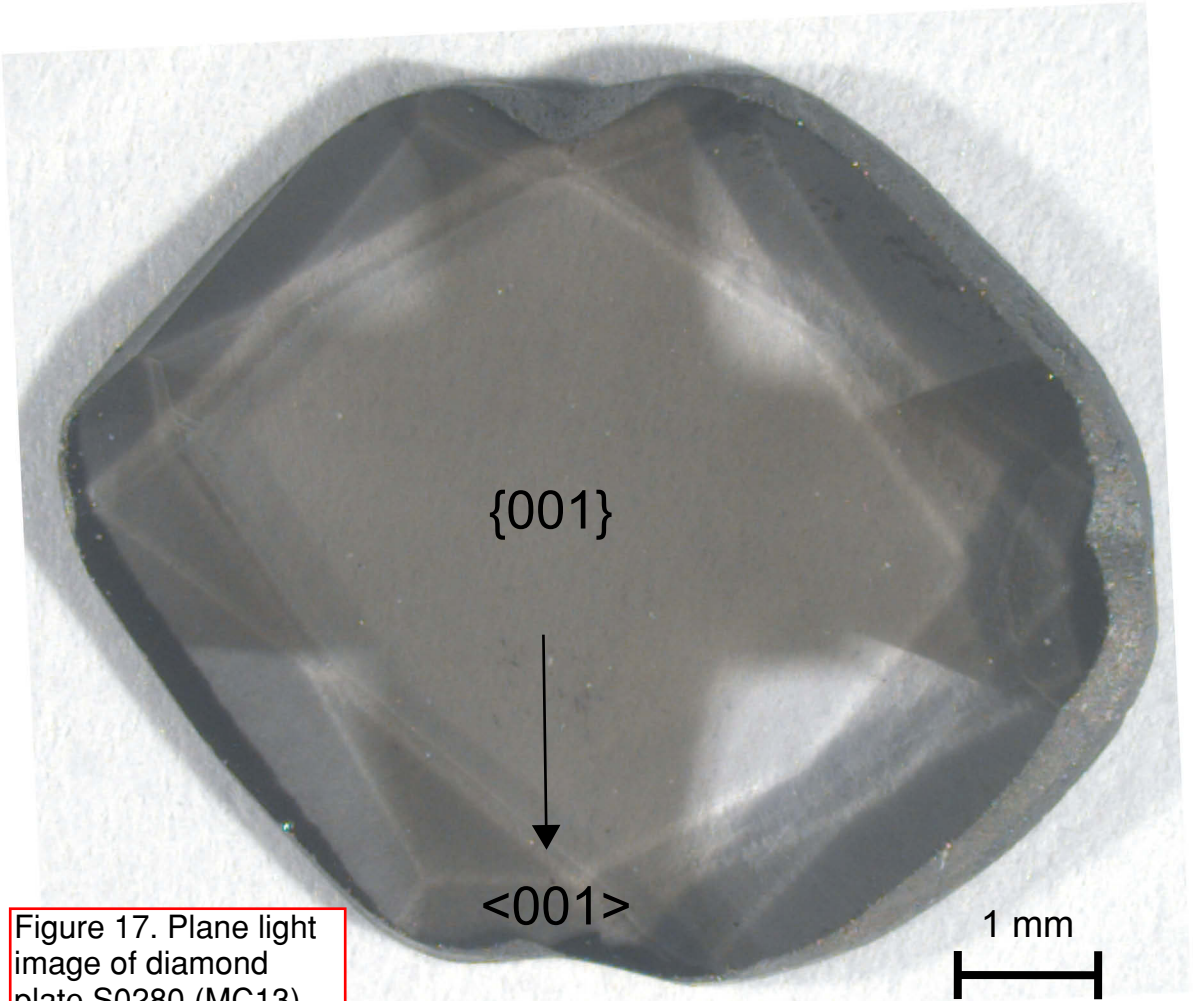

Figure 17. Plane light image of diamond plate S0280 (MC13).

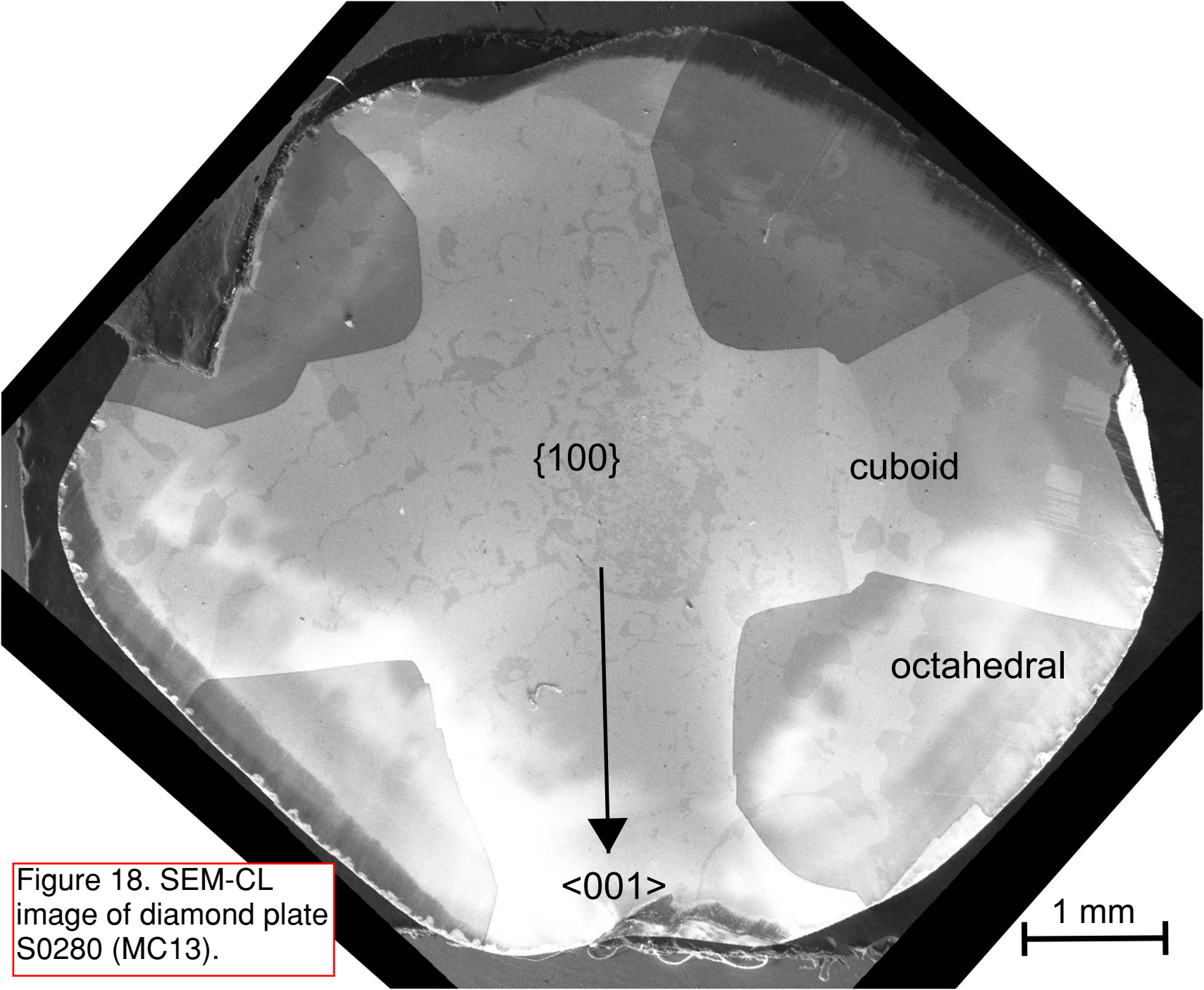

Figure 18. SEM-CL image of diamond plate S0280 (MC13).

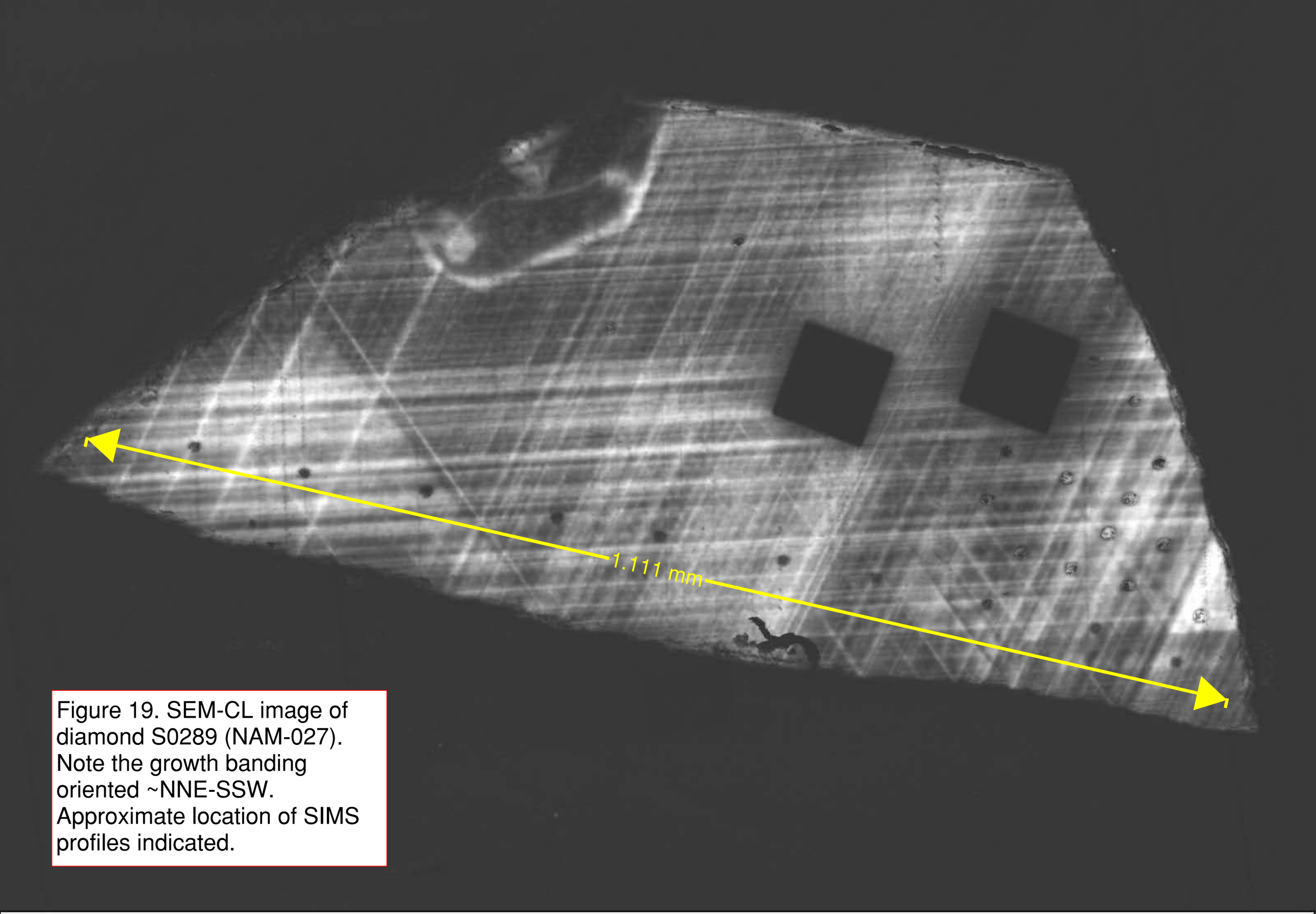

Figure 19. SEM-CL image of diamond S0289 (NAM-027). Note the growth banding oriented ~NNE-SSW. Approximate location of SIMS profiles indicated.

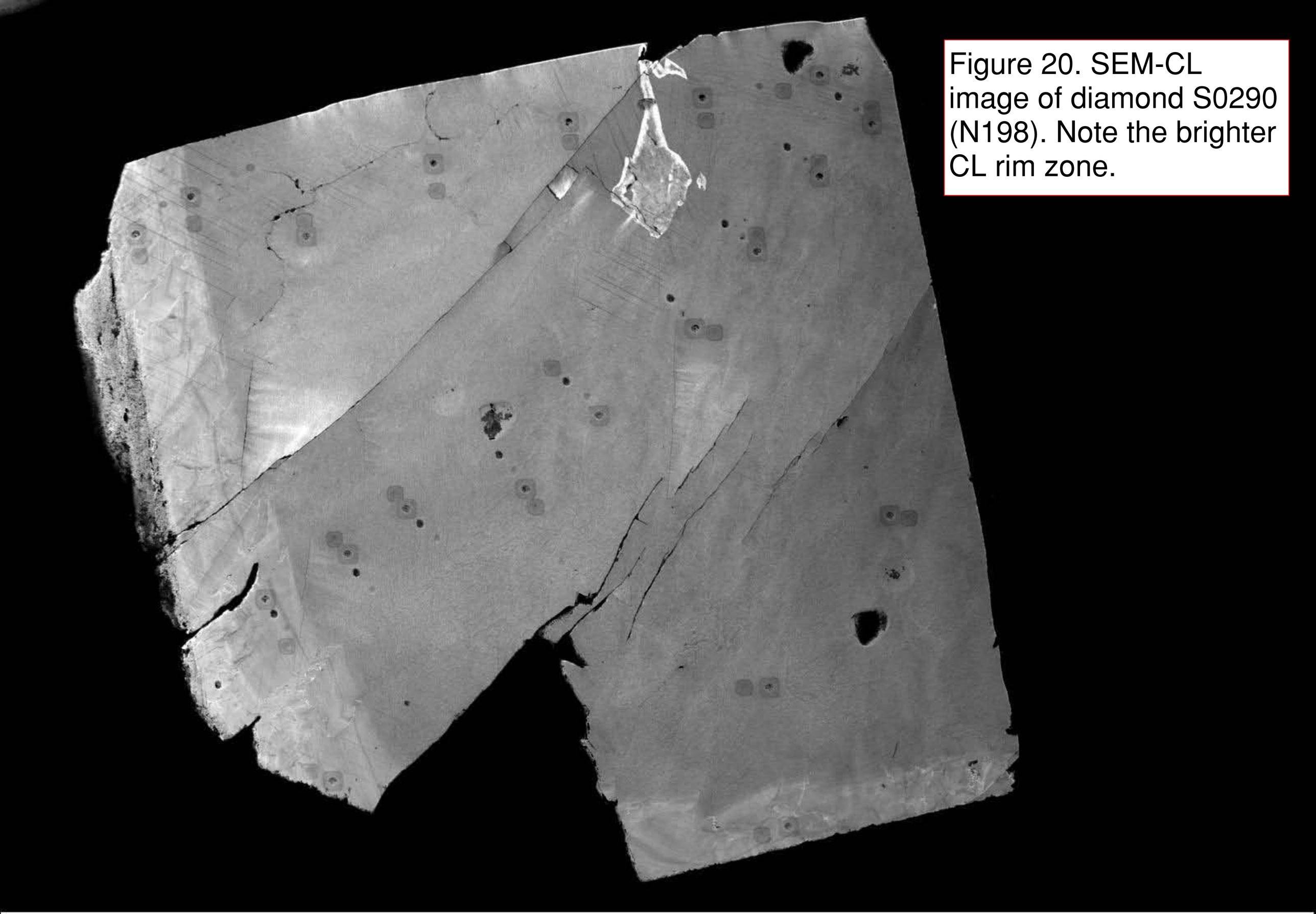

Figure 20. SEM-CL image of diamond S0290 (N198). Note the brighter CL rim zone.

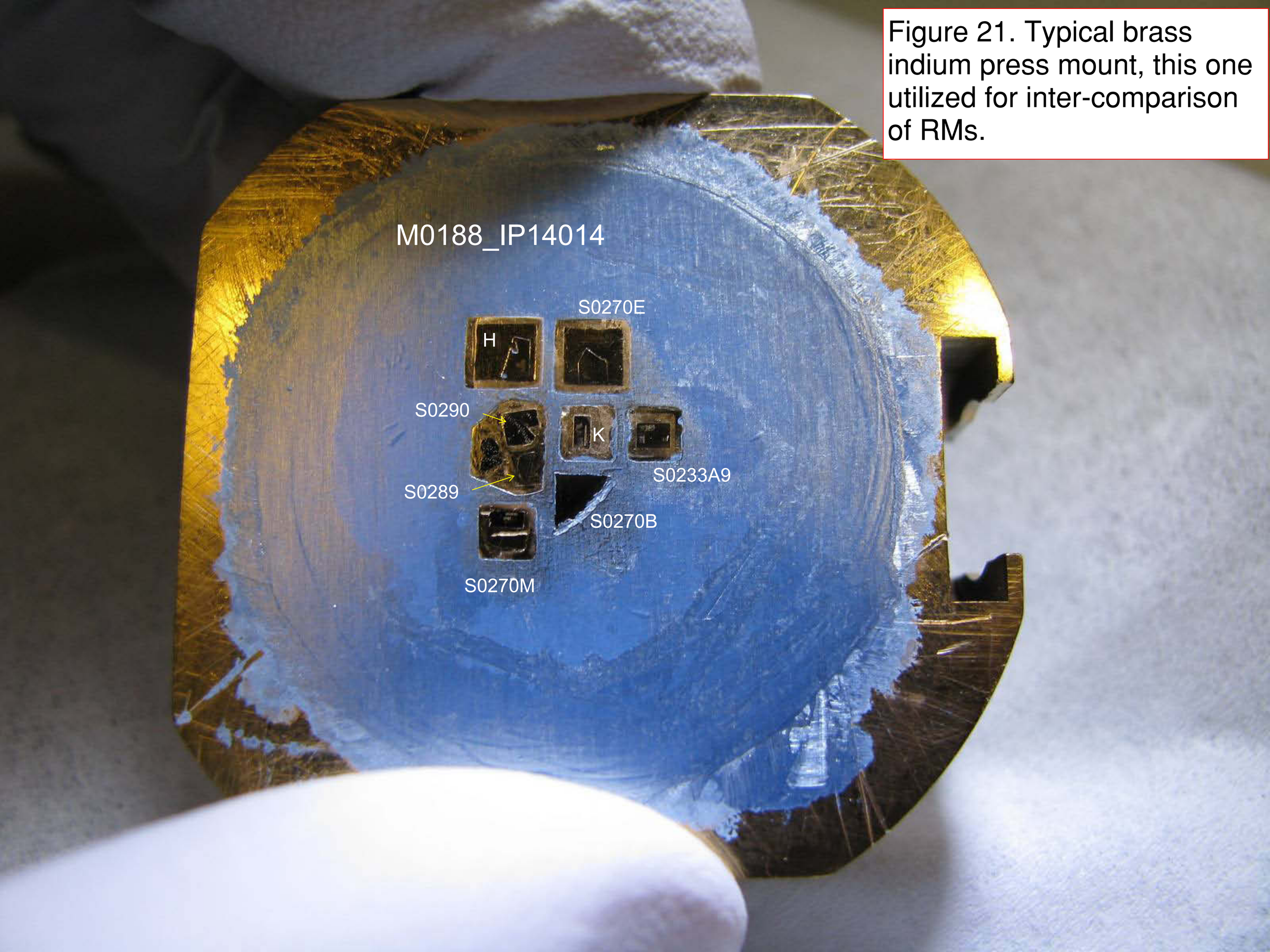

Figure 21. Typical brass indium press mount, this one utilized for inter-comparison of RMs.

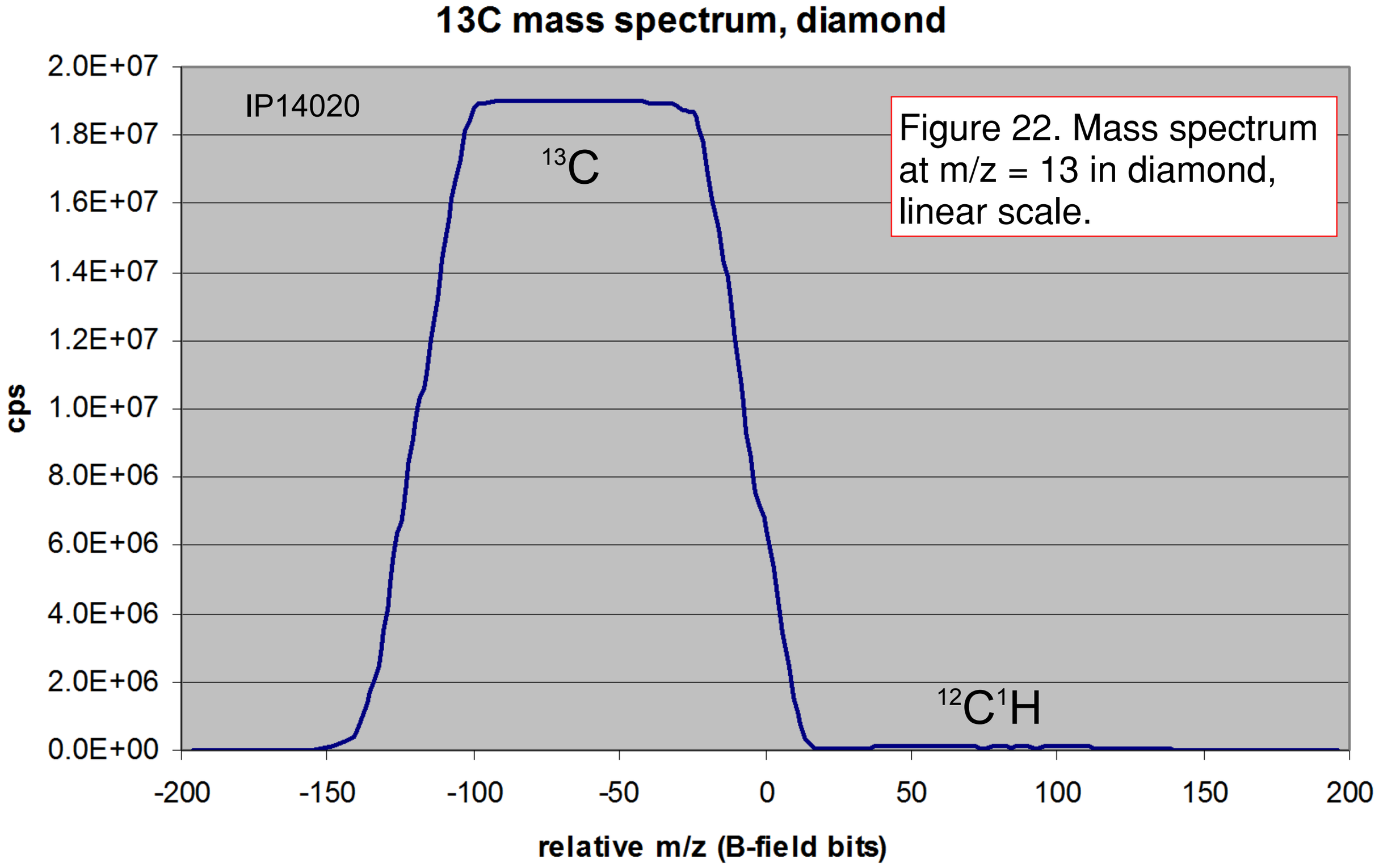

Figure 22. Mass spectrum at m/z = 13 in diamond, linear scale.

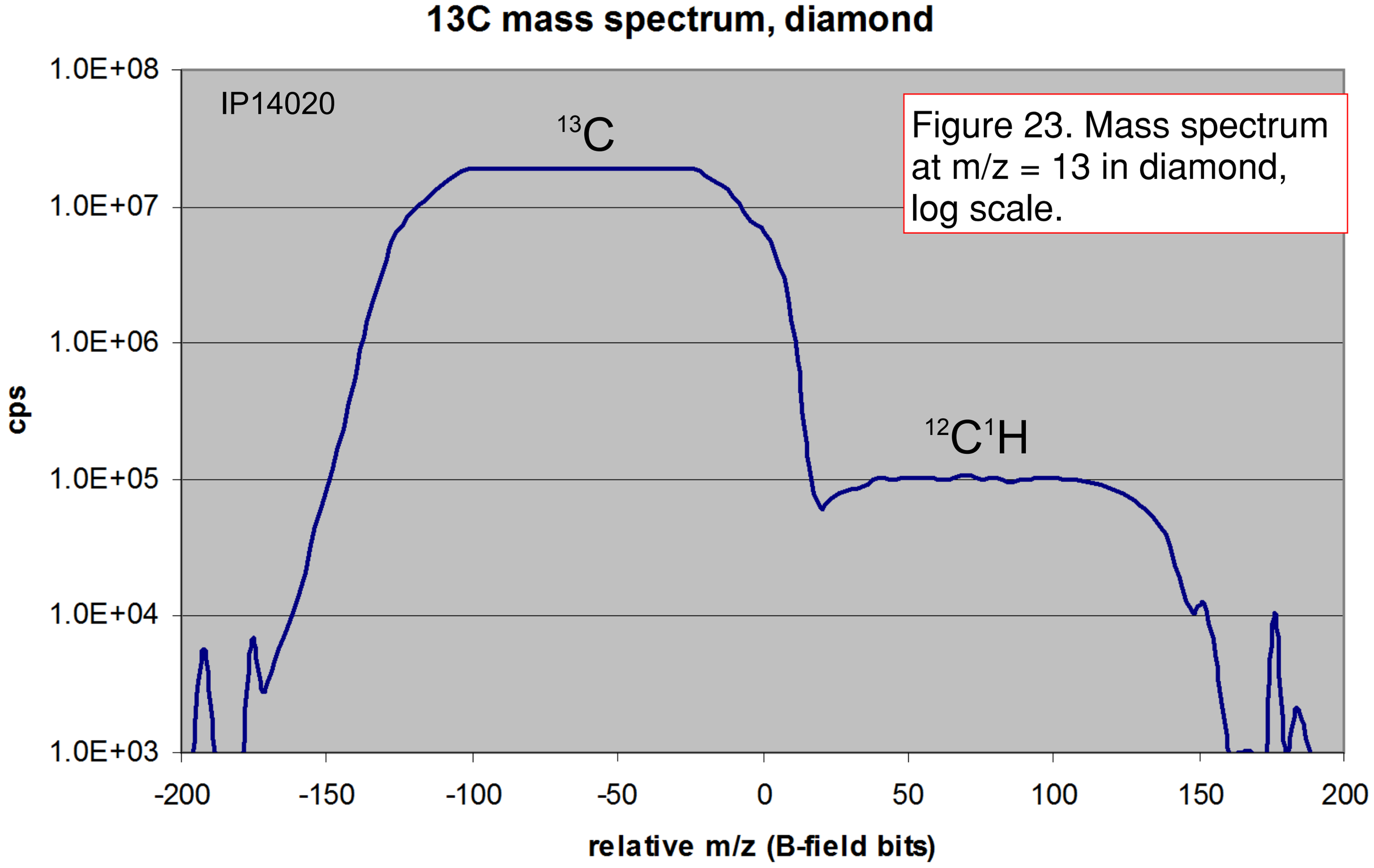

Figure 23. Mass spectrum at m/z = 13 in diamond, log scale.

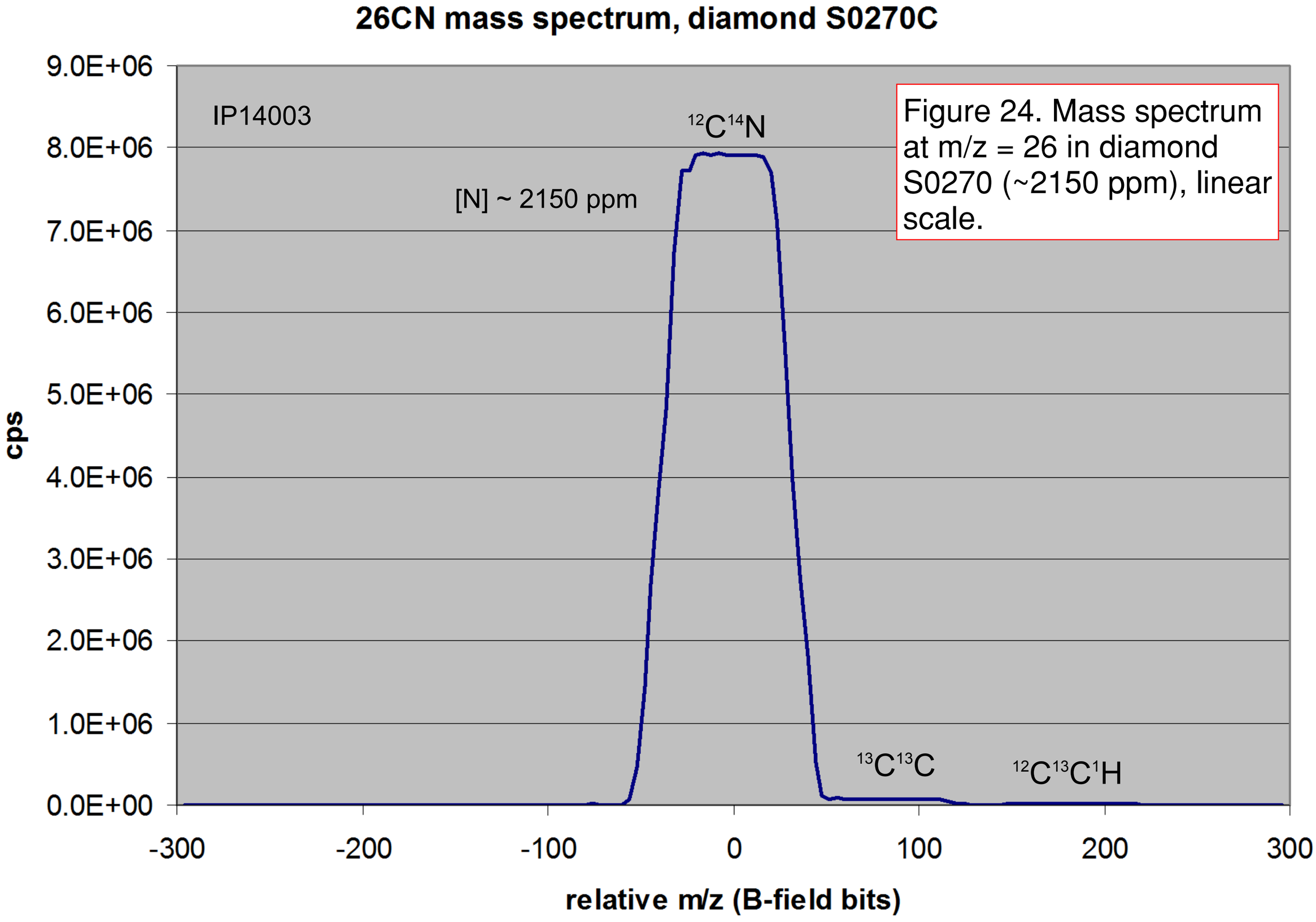

Figure 24. Mass spectrum at m/z = 26 in diamond S0270 (~2150 ppm), linear scale.

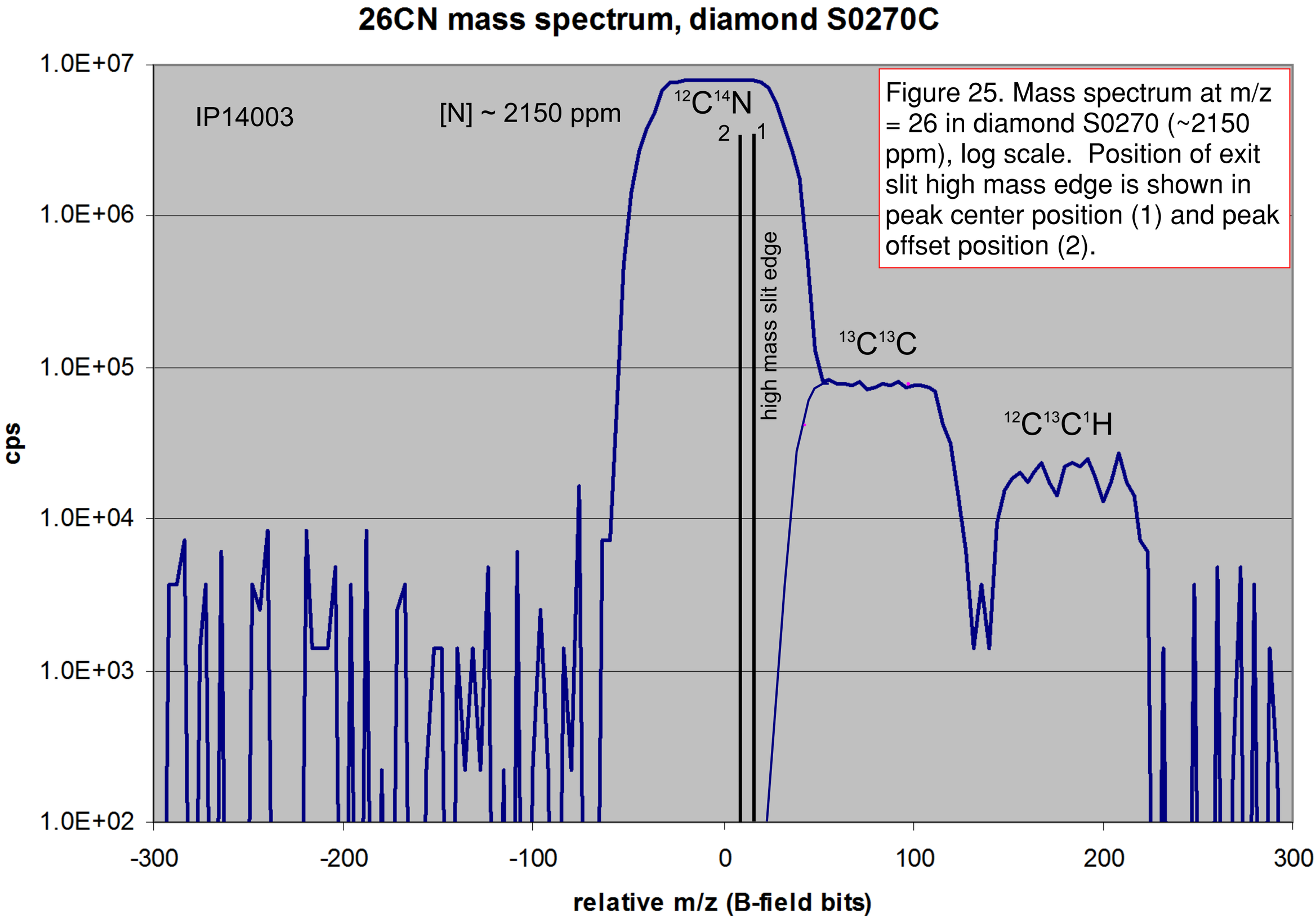

Figure 25. Mass spectrum at m/z = 26 in diamond S0270 (~2150 ppm), log scale. Position of exit slit high mass edge is shown in peak center position (1) and peak offset position (2).

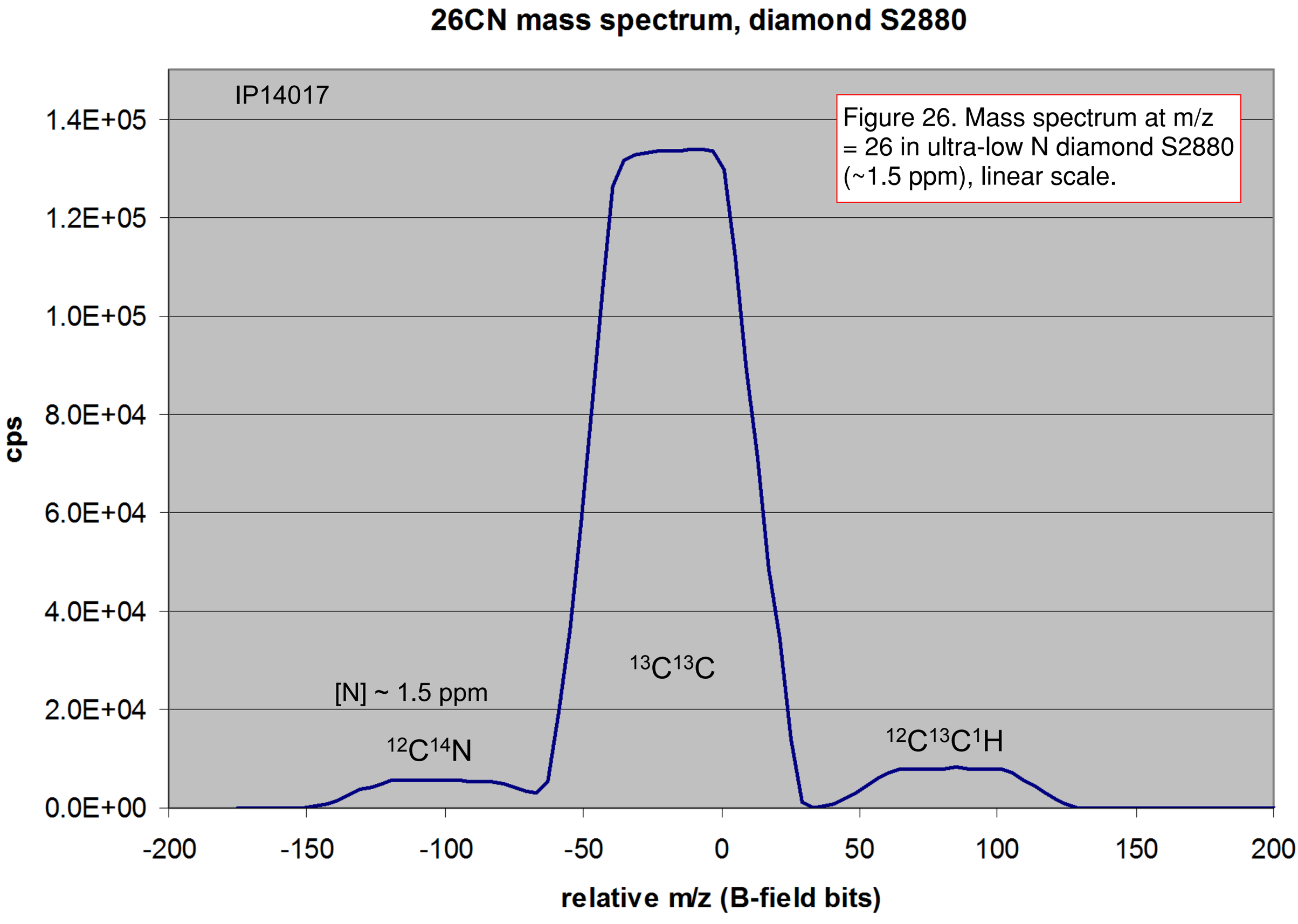
26CN mass spectrum, diamond S2880
IP14017
Figure 26. Mass spectrum at m/z = 26 in ultra-low N diamond S2880 (~1.5 ppm), linear scale.
cps
1.4E+05
1.2E+05
1.0E+05
8.0E+04
6.0E+04
4.0E+04
2.0E+04
0.0E+00
[N] ~ 1.5 ppm
12C14N
13C13C
12C13C1H
-200
-150
-100
-50
0
50
100
150
200
relative m/z (B-field bits)

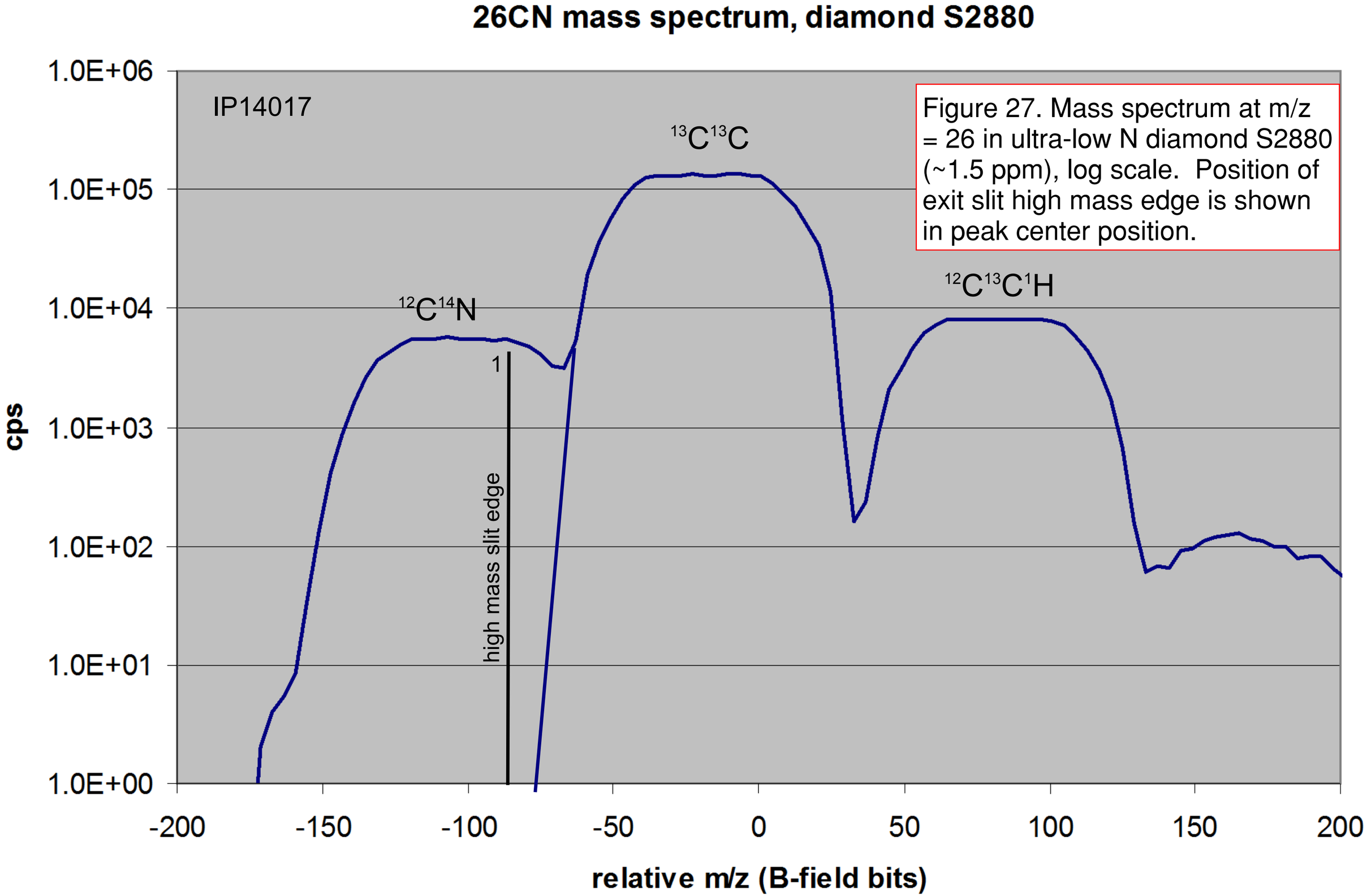
26CN mass spectrum, diamond S2880
IP14017
Figure 27. Mass spectrum at m/z = 26 in ultra-low N diamond S2880 (~1.5 ppm), log scale. Position of exit slit high mass edge is shown in peak center position.
$^{13}C^{13}C$
$^{12}C^{14}N$
$^{12}C^{13}C^{1}H$
1
high mass slit edge
cps
1.0E+06
1.0E+05
1.0E+04
1.0E+03
1.0E+02
1.0E+01
1.0E+00
-200
-150
-100
-50
0
50
100
150
200
relative m/z (B-field bits)

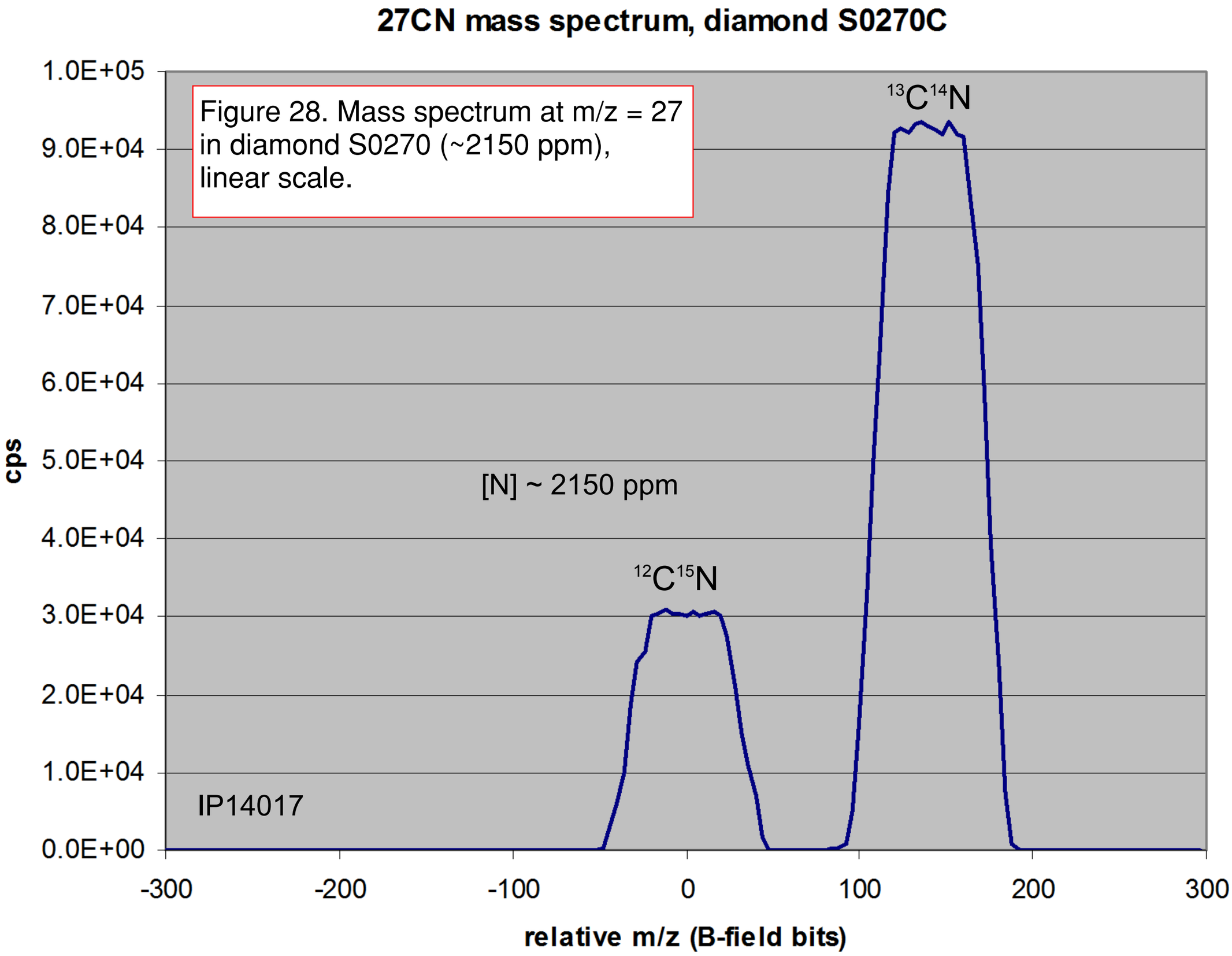
27CN mass spectrum, diamond S0270C
Figure 28. Mass spectrum at m/z = 27 in diamond S0270 (~2150 ppm), linear scale.
$^{13}C^{14}N$
[N] ~ 2150 ppm
$^{12}C^{15}N$
IP14017
cps
1.0E+05
9.0E+04
8.0E+04
7.0E+04
6.0E+04
5.0E+04
4.0E+04
3.0E+04
2.0E+04
1.0E+04
0.0E+00
-300
-200
-100
0
100
200
300
relative m/z (B-field bits)

Figure 29. Mass spectrum at m/z = 27 in ultra-low N diamond S2880 (~1.5 ppm), linear scale.

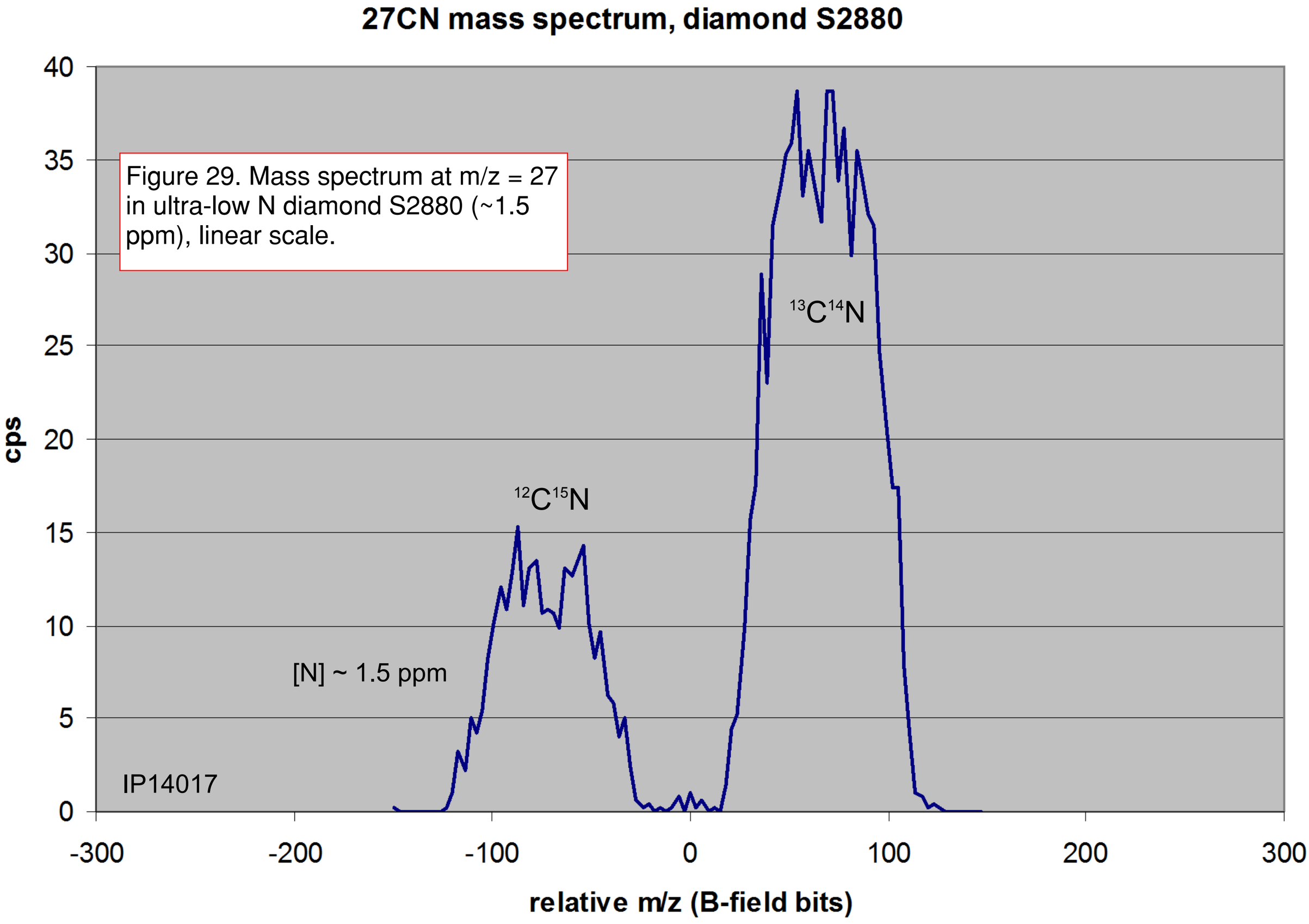

S0011A cross section, $\delta^{13}C$

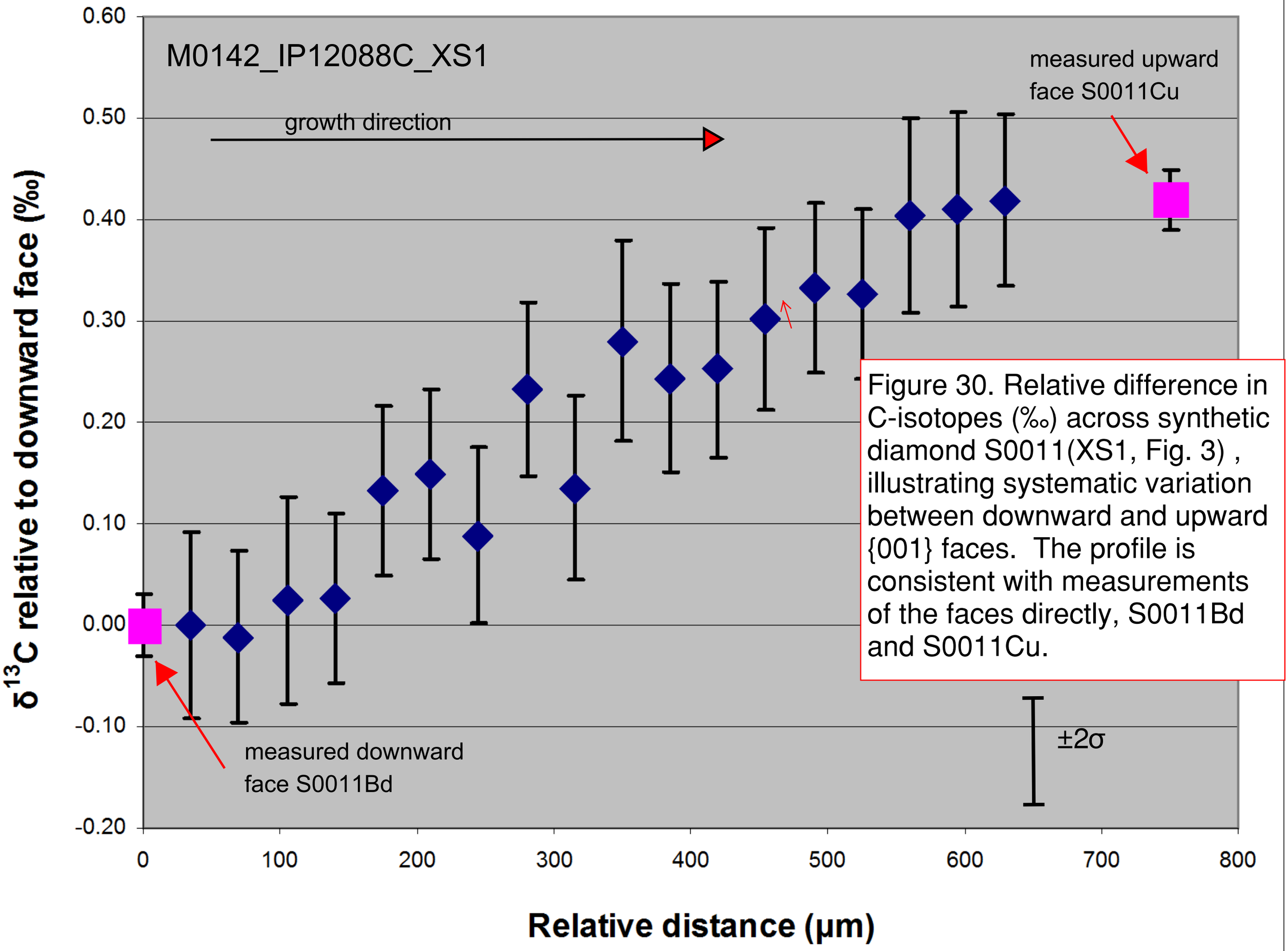

Figure 30. Relative difference in C-isotopes (‰) across synthetic diamond S0011(XS1, Fig. 3) , illustrating systematic variation between downward and upward {001} faces. The profile is consistent with measurements of the faces directly, S0011Bd and S0011Cu.

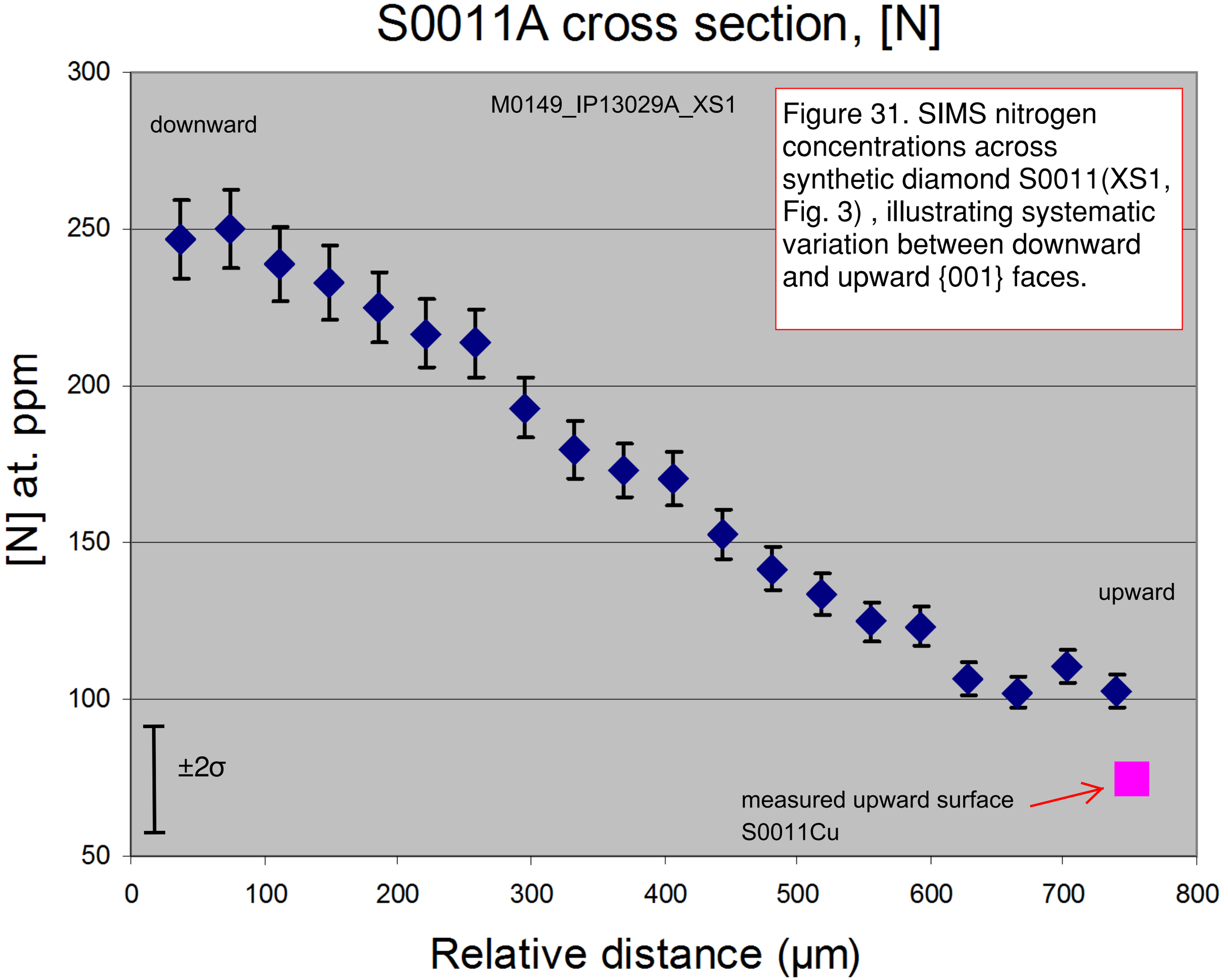

Figure 31. SIMS nitrogen concentrations across synthetic diamond S0011(XS1, Fig. 3) , illustrating systematic variation between downward and upward {001} faces.

S0011A cross section, δ15N

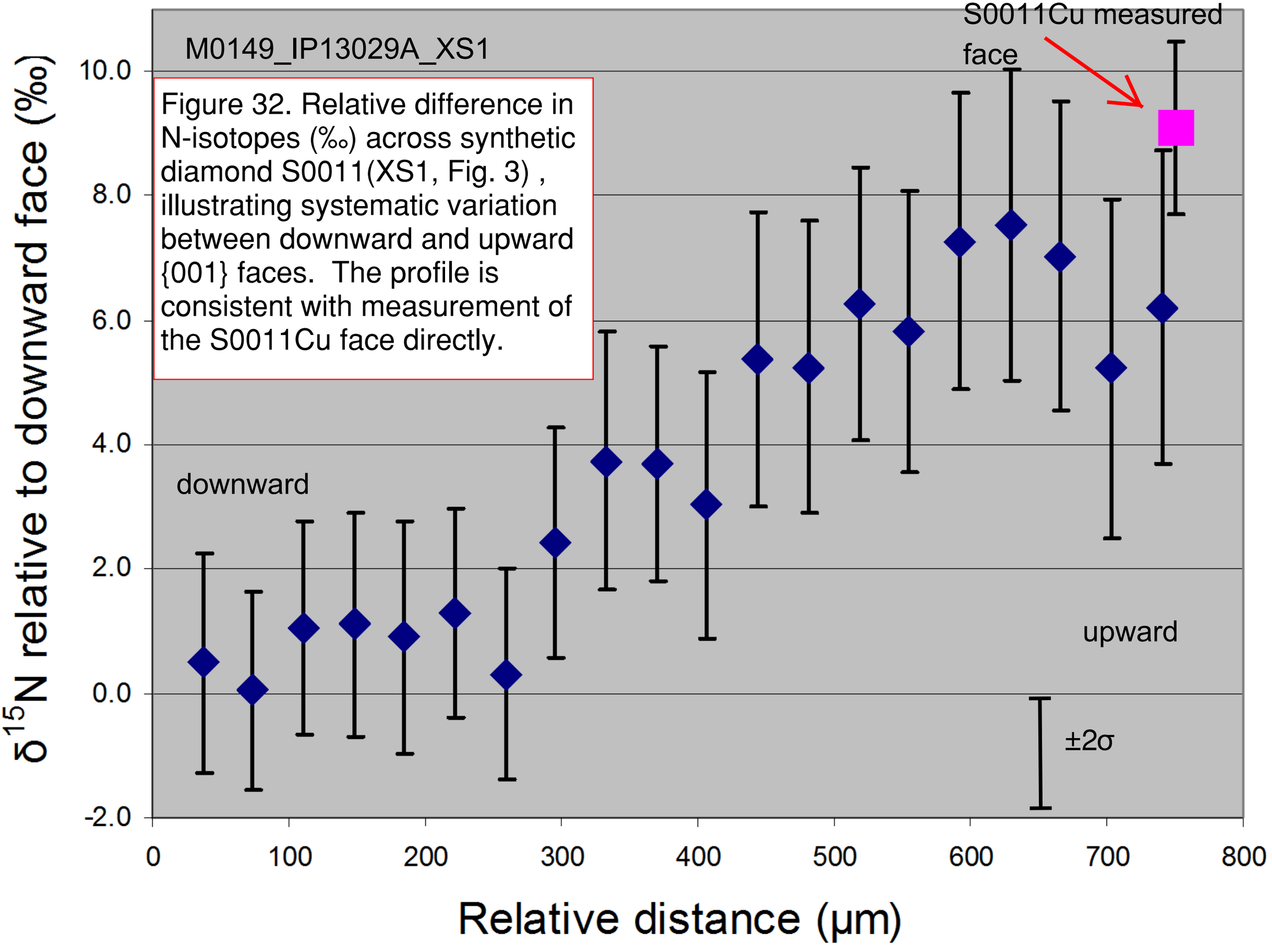

Figure 32. Relative difference in N-isotopes (‰) across synthetic diamond S0011(XS1, Fig. 3) , illustrating systematic variation between downward and upward {001} faces. The profile is consistent with measurement of the S0011Cu face directly.

S0203B cross section, $\delta^{15}N$

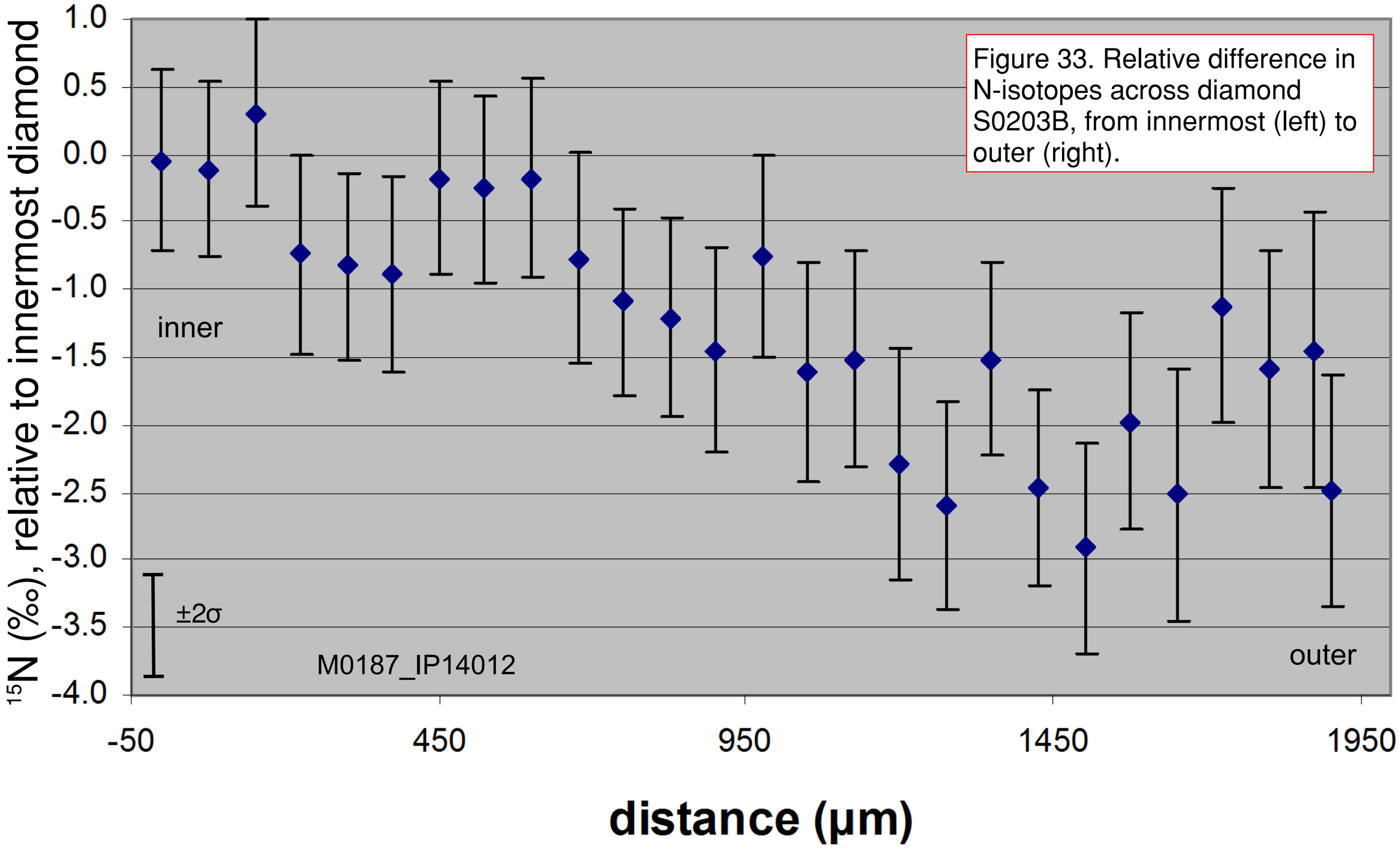

Figure 33. Relative difference in N-isotopes across diamond S0203B, from innermost (left) to outer (right).

S0203B cross section, [N]

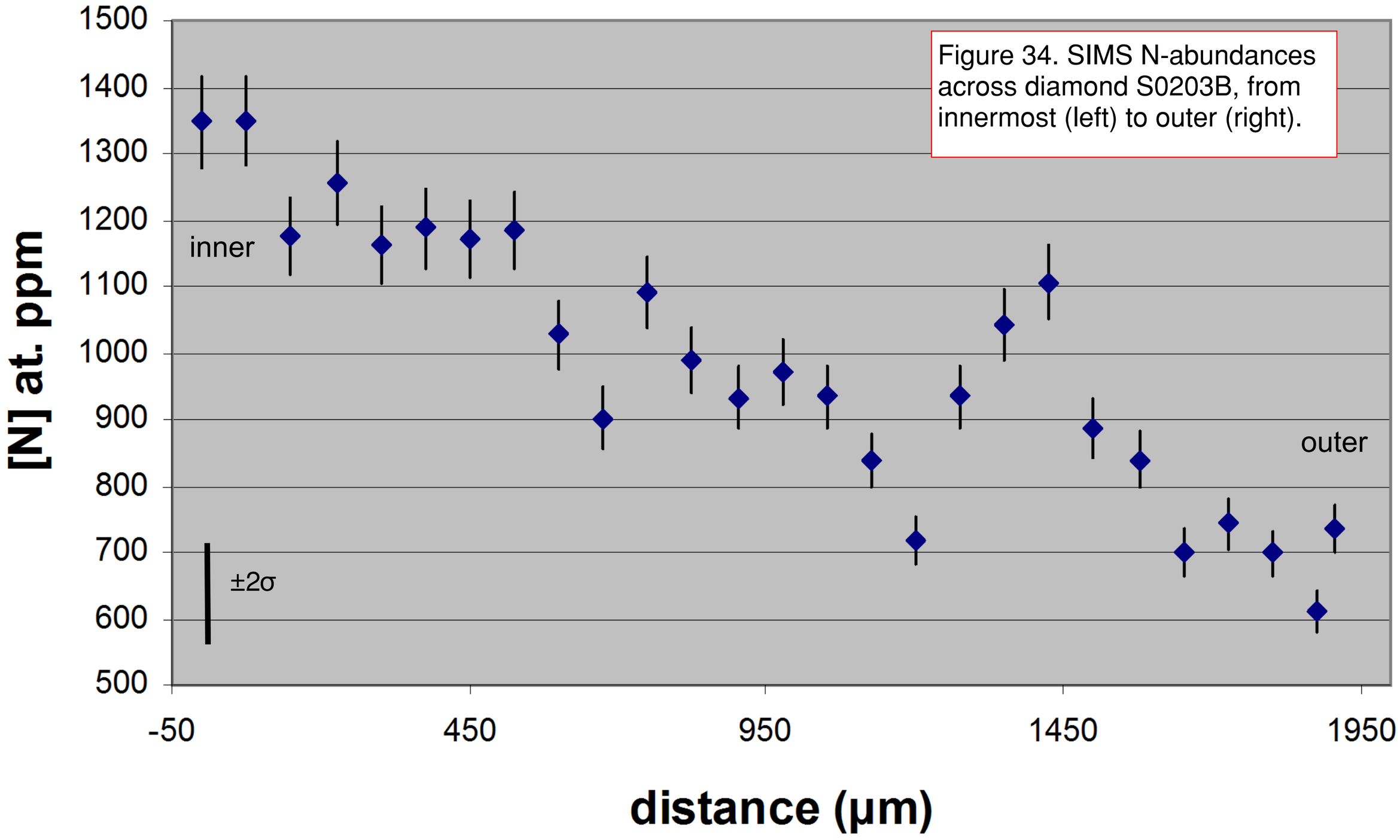

Figure 34. SIMS N-abundances across diamond S0203B, from innermost (left) to outer (right).

Figure 35. Cumulative probability of $\delta^{13}C$ (relative to mean)from 65 SIMS analyses from 11 diamond S0270 sub-samples.

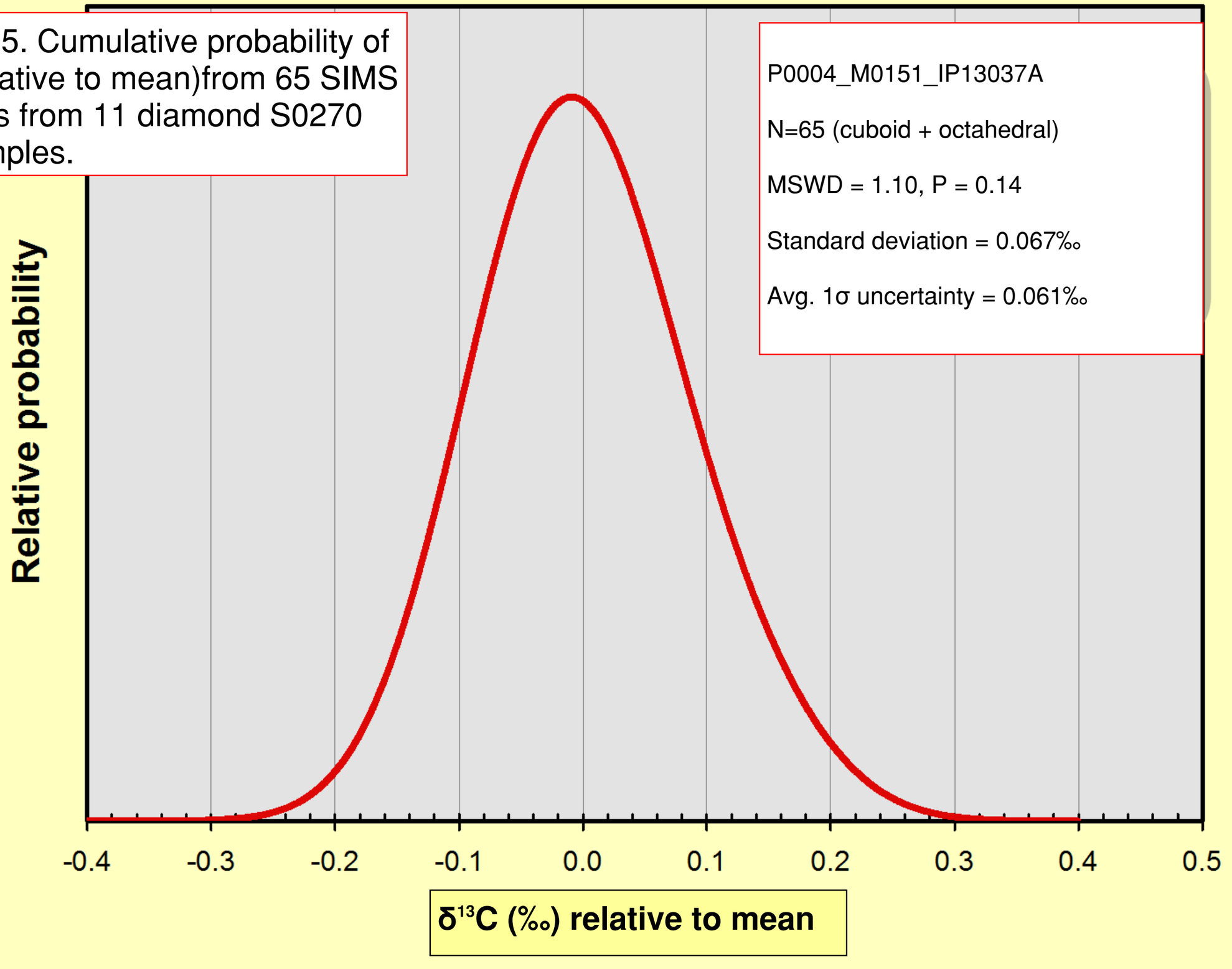

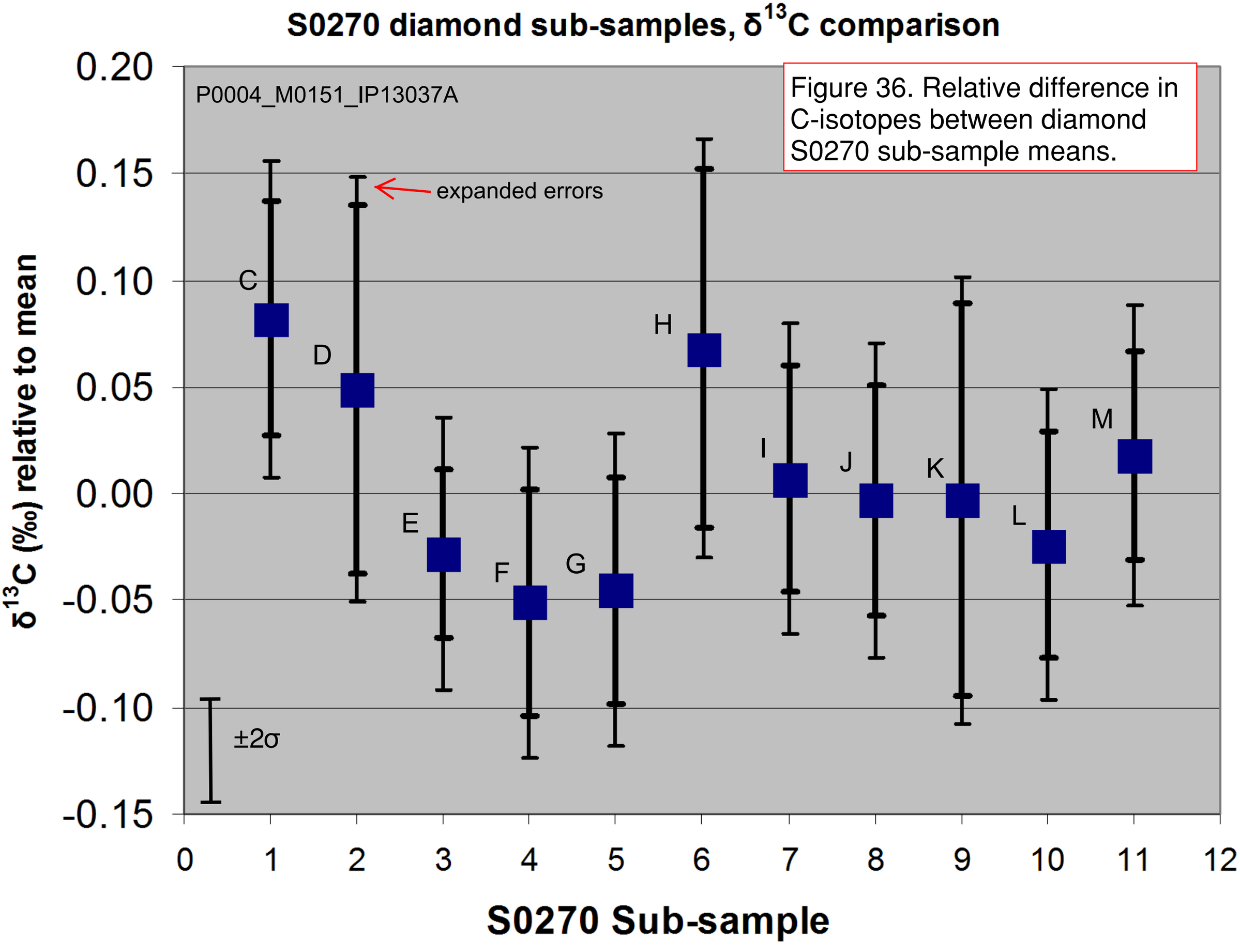

Figure 36. Relative difference in C-isotopes between diamond S0270 sub-sample means.

Figure 37. Cumulative probability of $\delta^{13}C$ (relative to mean) for 65 SIMS analyses from 4 diamond S0270 sub-samples.

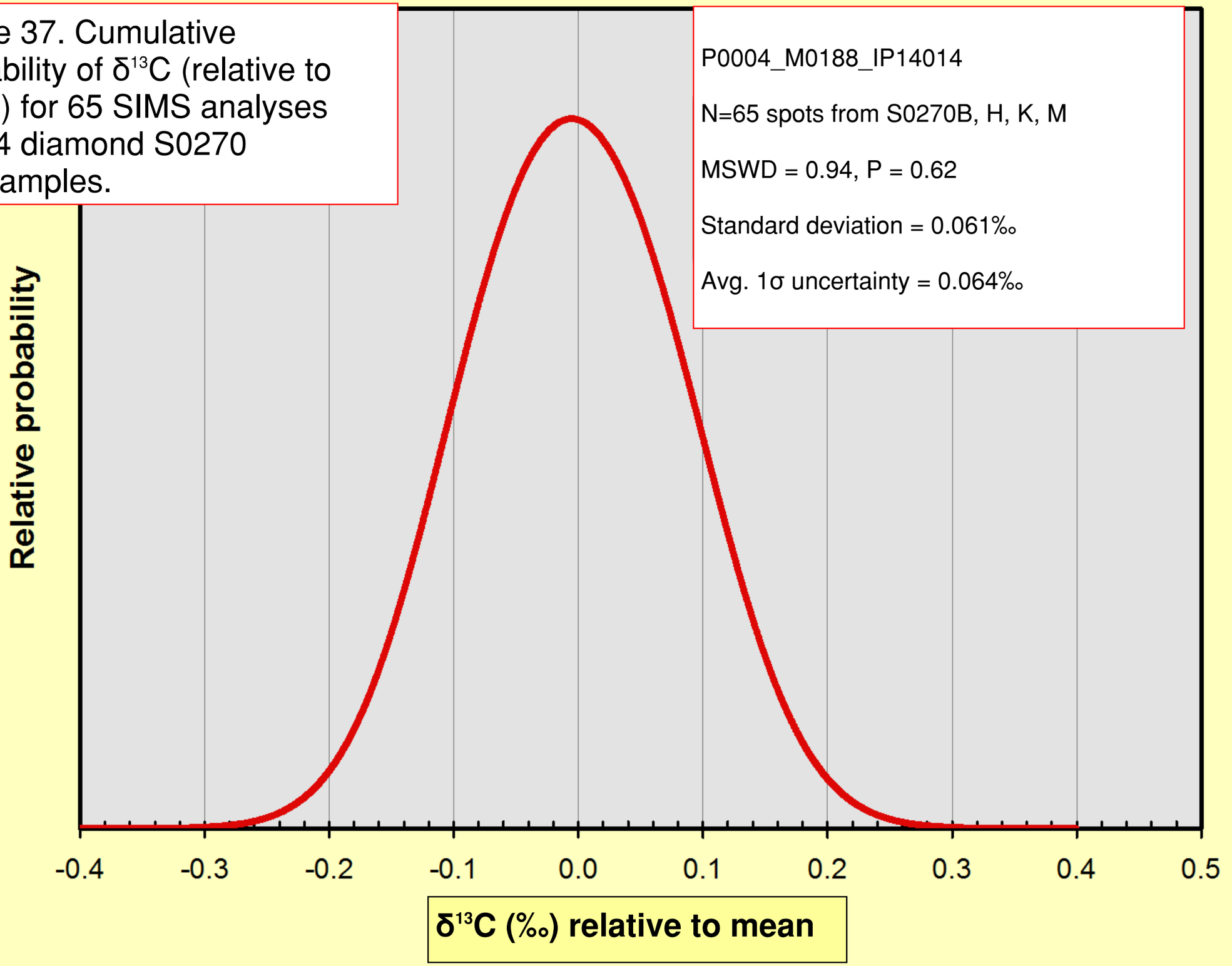

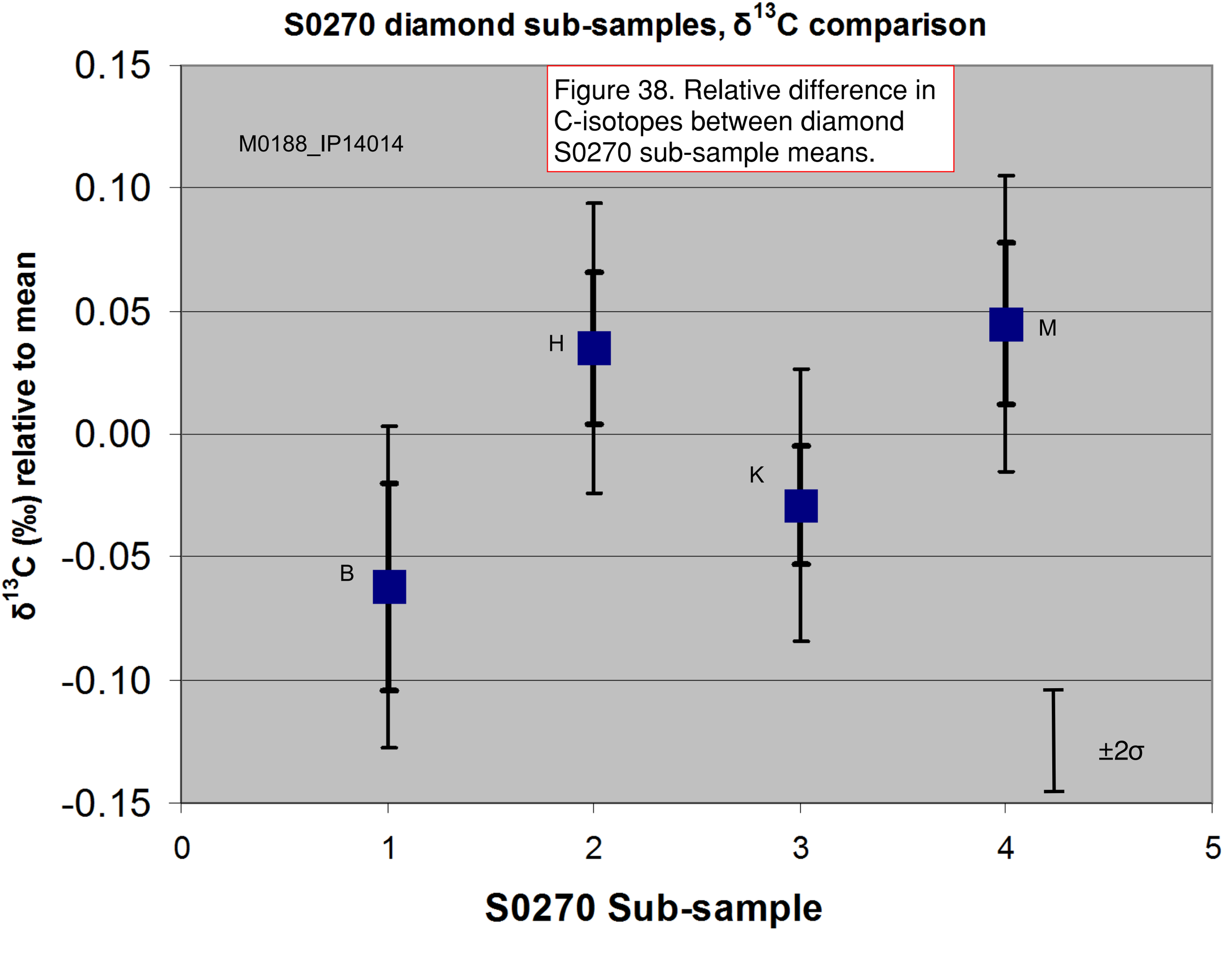
S0270 diamond sub-samples, δ13C comparison
M0188_IP14014
Figure 38. Relative difference in C-isotopes between diamond S0270 sub-sample means.
δ13C (‰) relative to mean
0.15
0.10
0.05
0.00
-0.05
-0.10
-0.15
B
H
K
M
±2σ
0
1
2
3
4
5
S0270 Sub-sample

Figure 39. $\delta^{13}C$ (relative to mean) profiles of diamond S0270 cuboid (C) and octahedral (B) sub-samples.

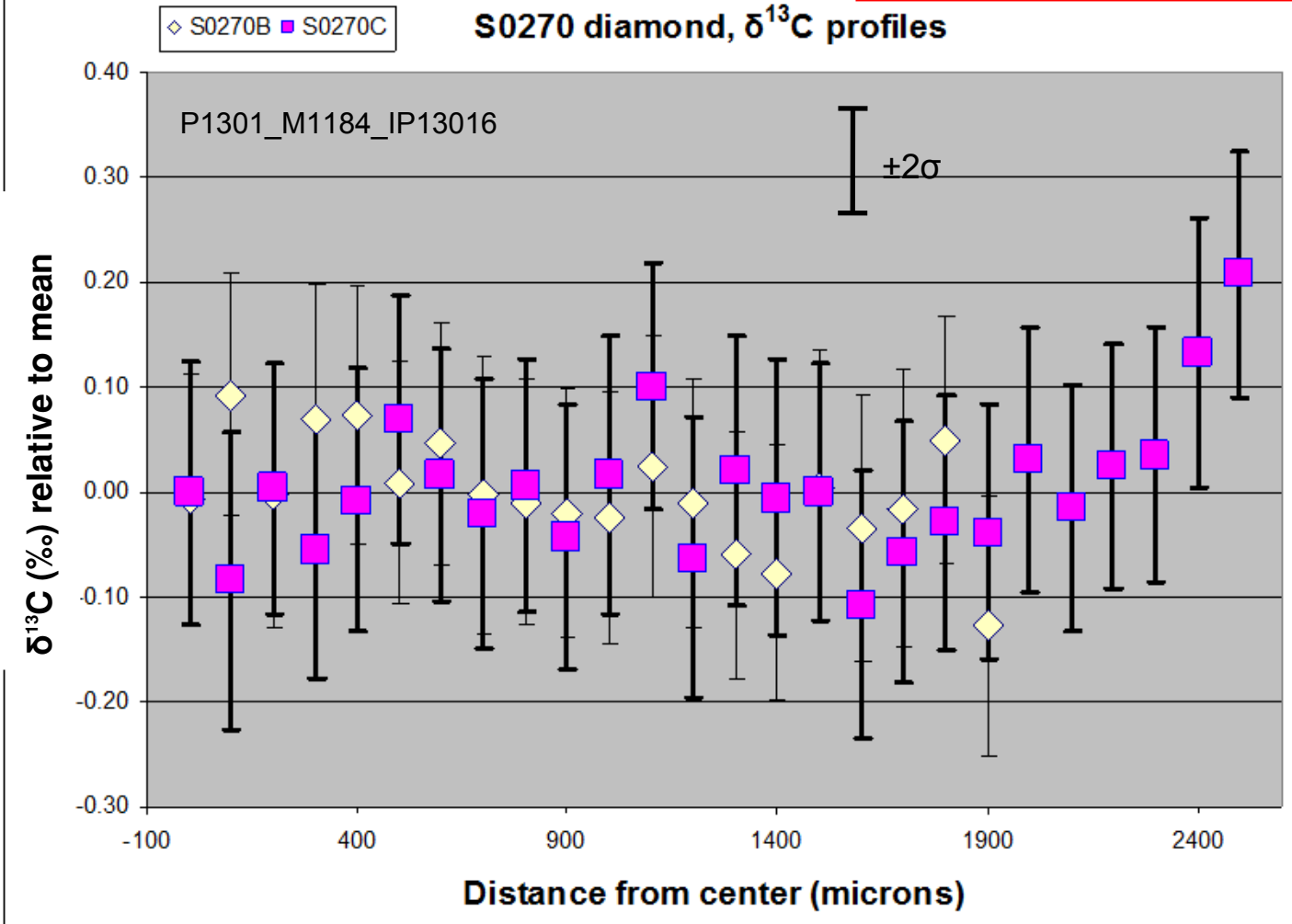

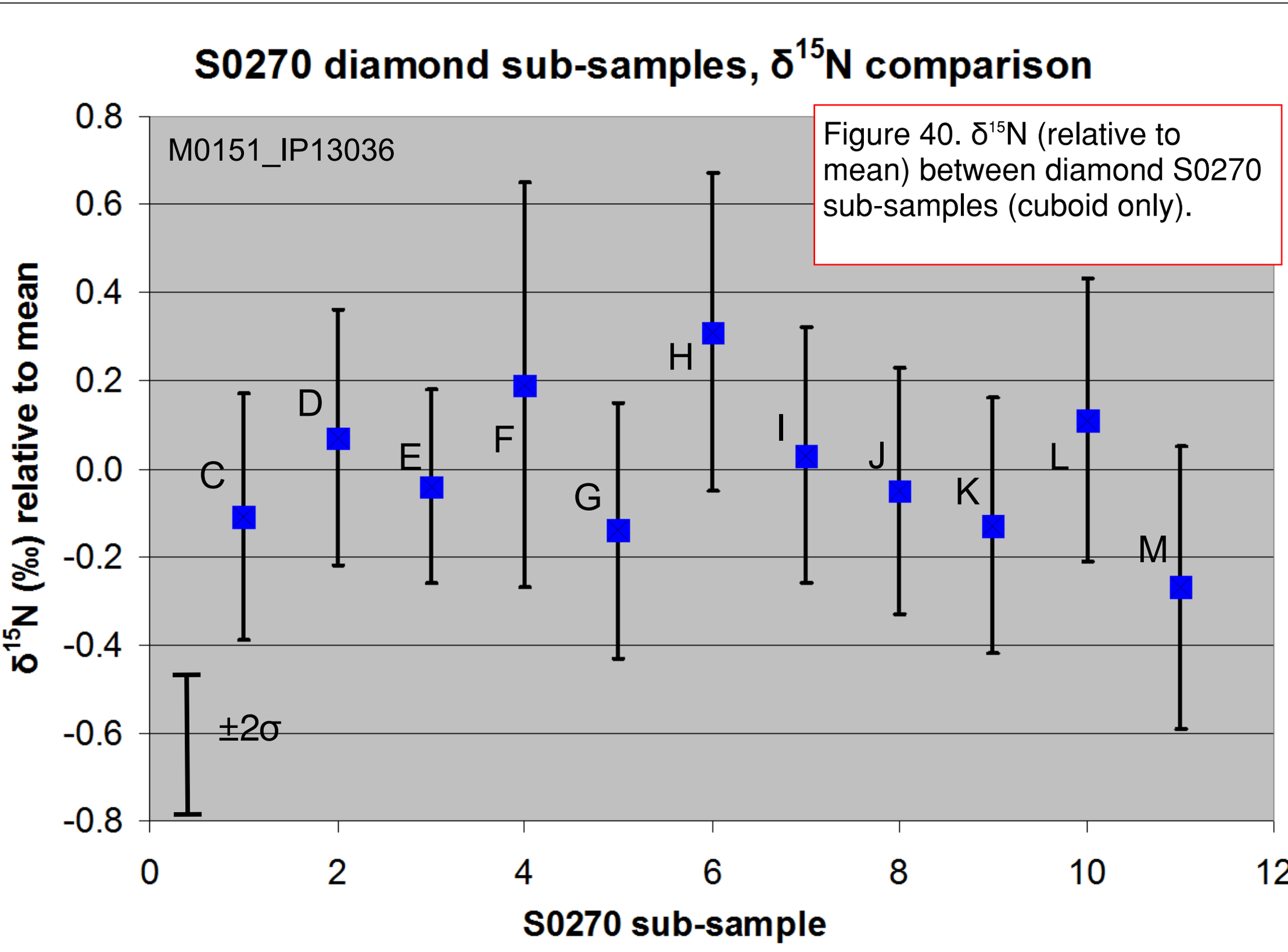
S0270 diamond sub-samples, δ15N comparison
M0151_IP13036
Figure 40. δ15N (relative to mean) between diamond S0270 sub-samples (cuboid only).
δ15N (‰) relative to mean
S0270 sub-sample
0.8
0.6
0.4
0.2
0.0
-0.2
-0.4
-0.6
-0.8
0
2
4
6
8
10
12
C
D
E
F
G
H
I
J
K
L
M
±2σ

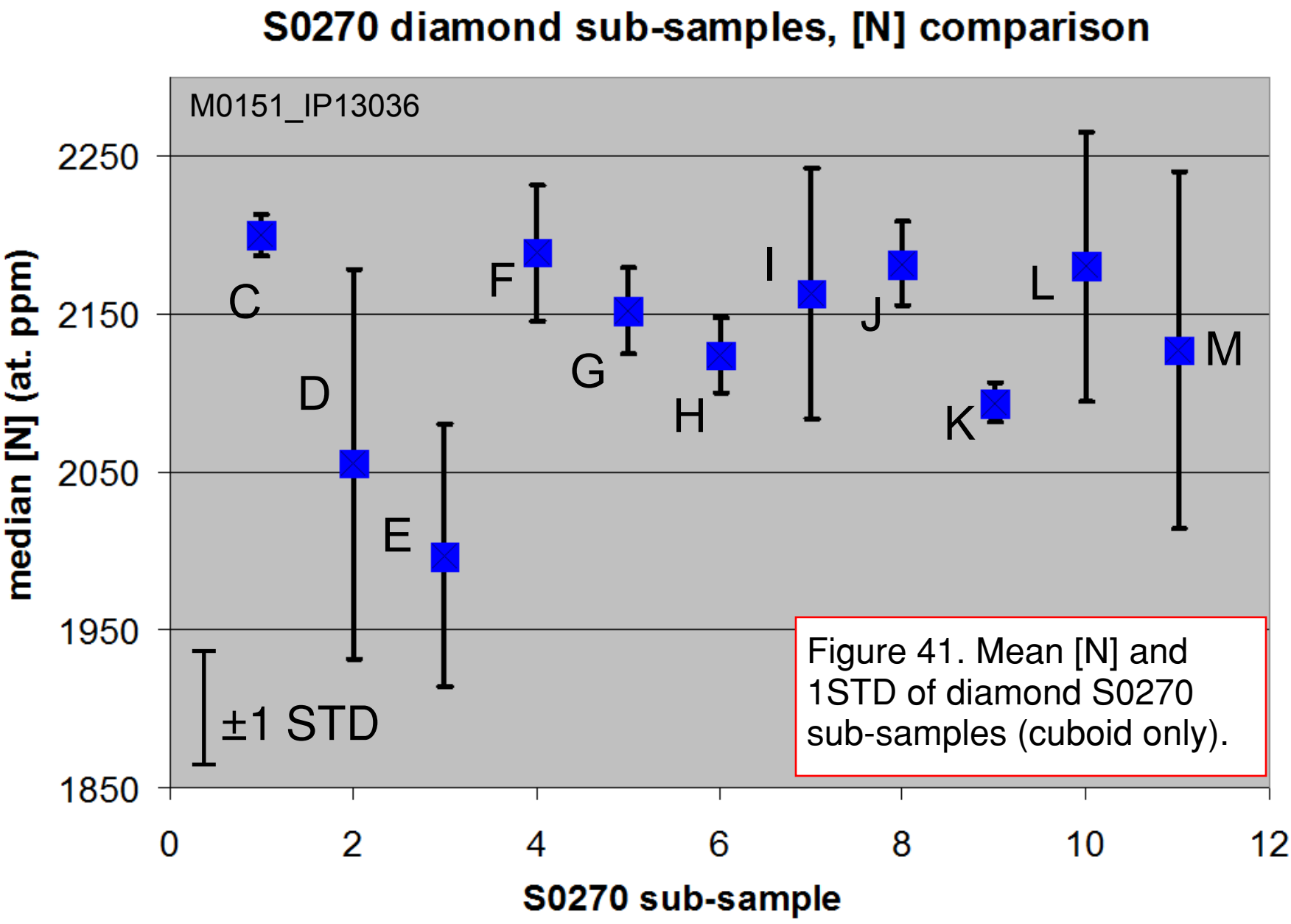

Figure 41. Mean [N] and 1STD of diamond S0270 sub-samples (cuboid only).

Figure 42. $\delta^{15}N$ (relative to mean) profiles of diamond S0270 cuboid (C) and octahedral (B) sub-samples.

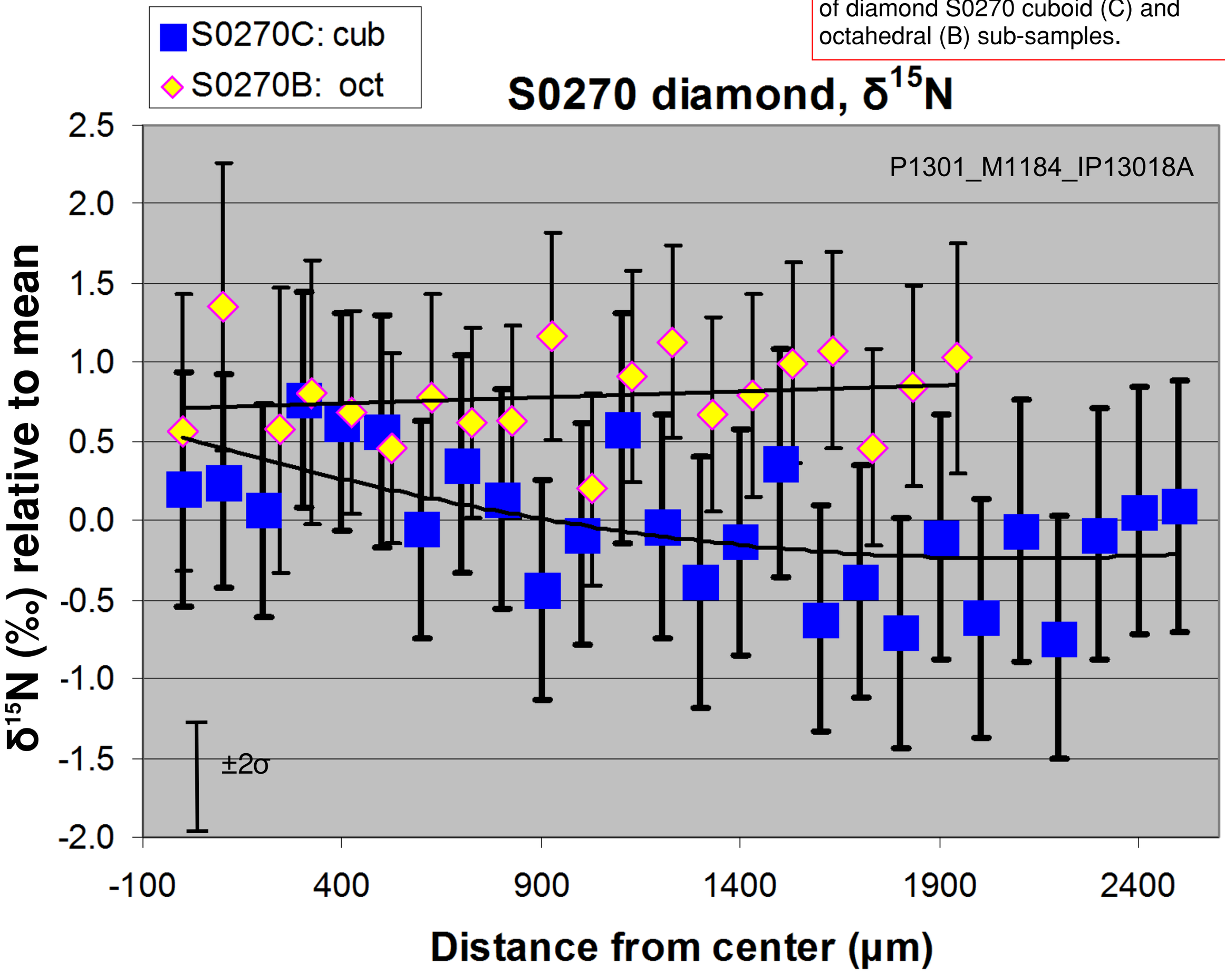

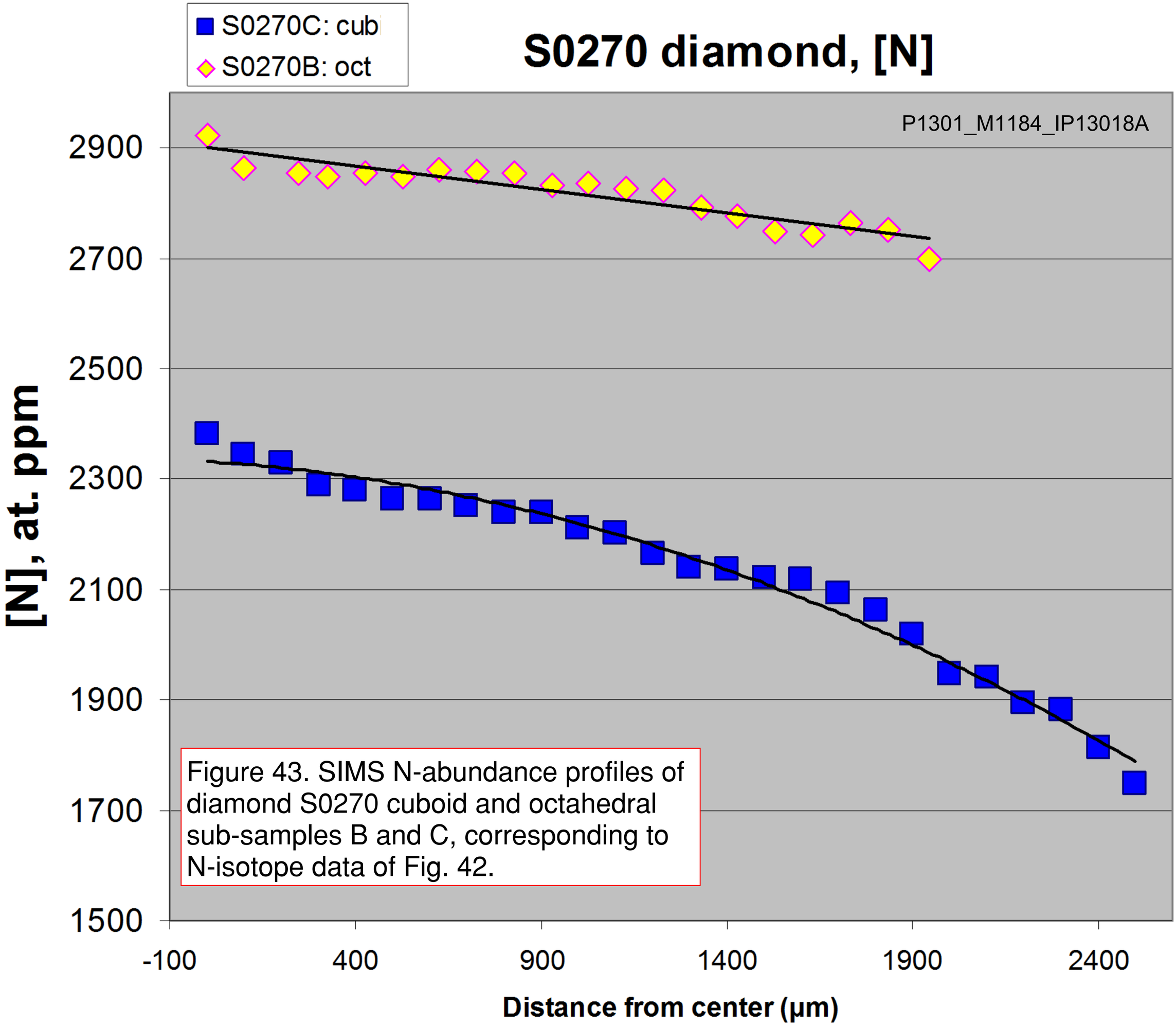

Figure 43. SIMS N-abundance profiles of diamond S0270 cuboid and octahedral sub-samples B and C, corresponding to N-isotope data of Fig. 42.

S0270C diamond cross section, $\delta^{15}N$

Figure 44. $\delta^{15}N$ (relative to mean) profile of diamond S0270C (cuboid).

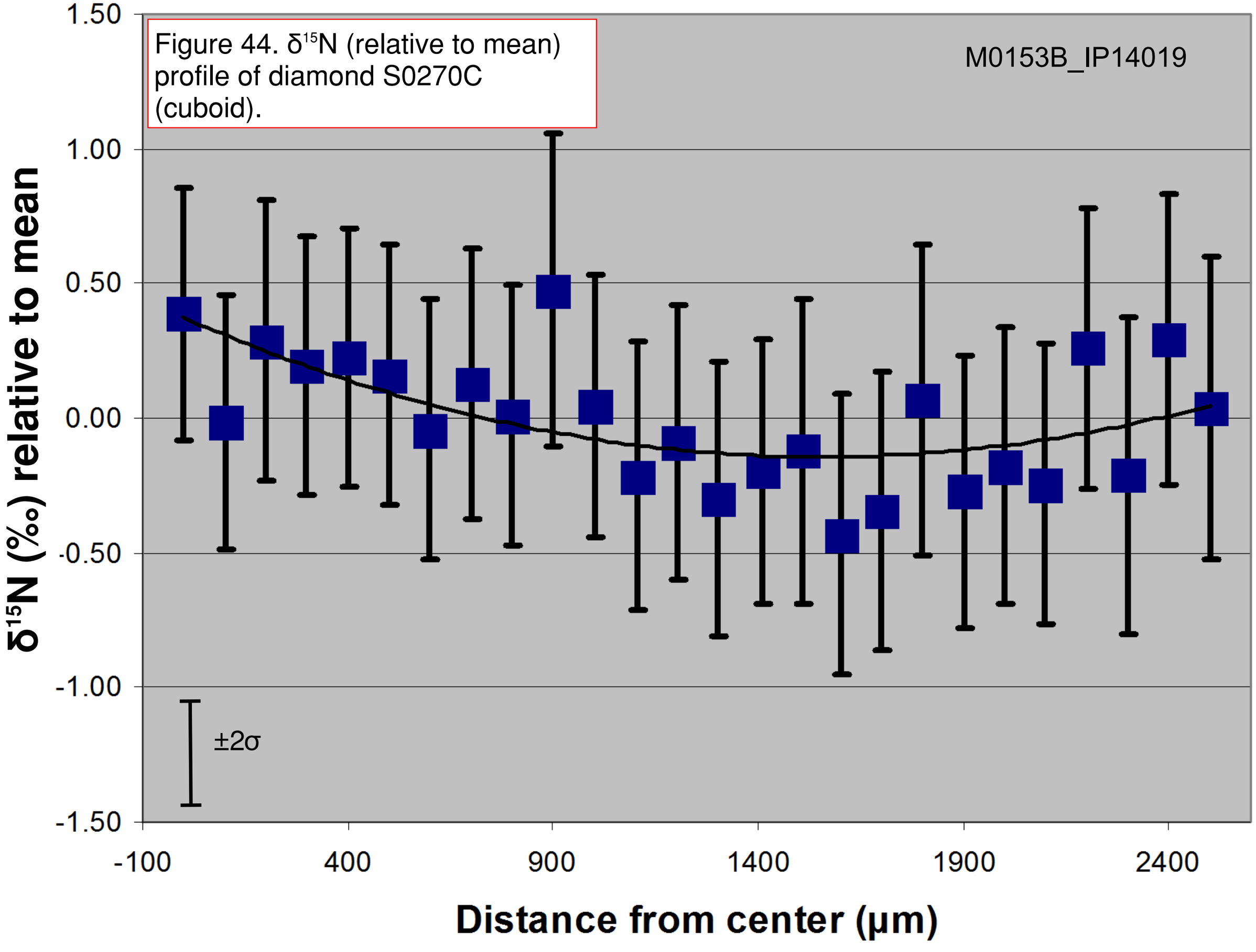

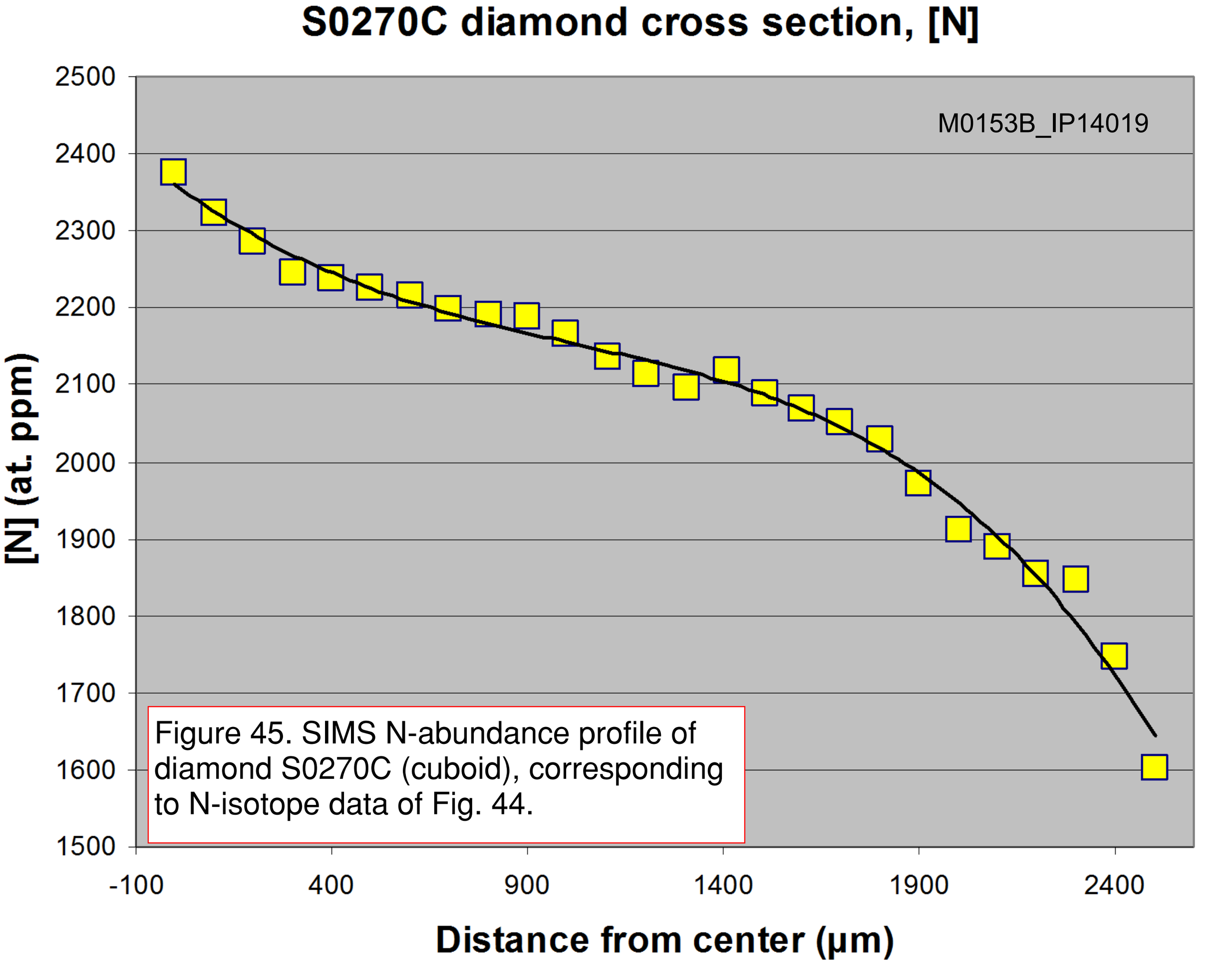

Figure 45. SIMS N-abundance profile of diamond S0270C (cuboid), corresponding to N-isotope data of Fig. 44.

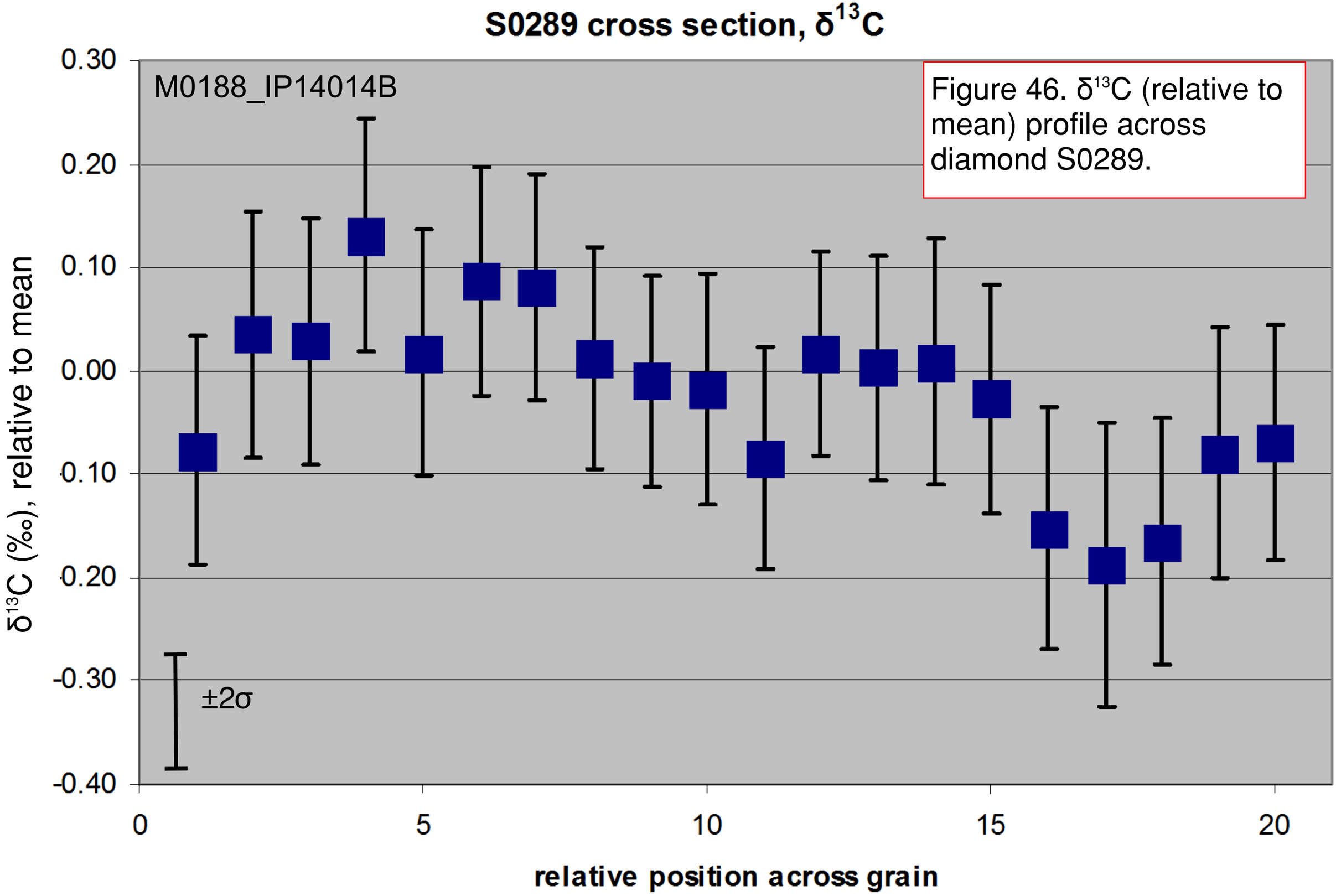
S0289 cross section, δ13C
M0188_IP14014B
Figure 46. δ13C (relative to mean) profile across diamond S0289.
δ13C (‰), relative to mean
0.30
0.20
0.10
0.00
-0.10
-0.20
-0.30
-0.40
±2σ
0
5
10
15
20
relative position across grain

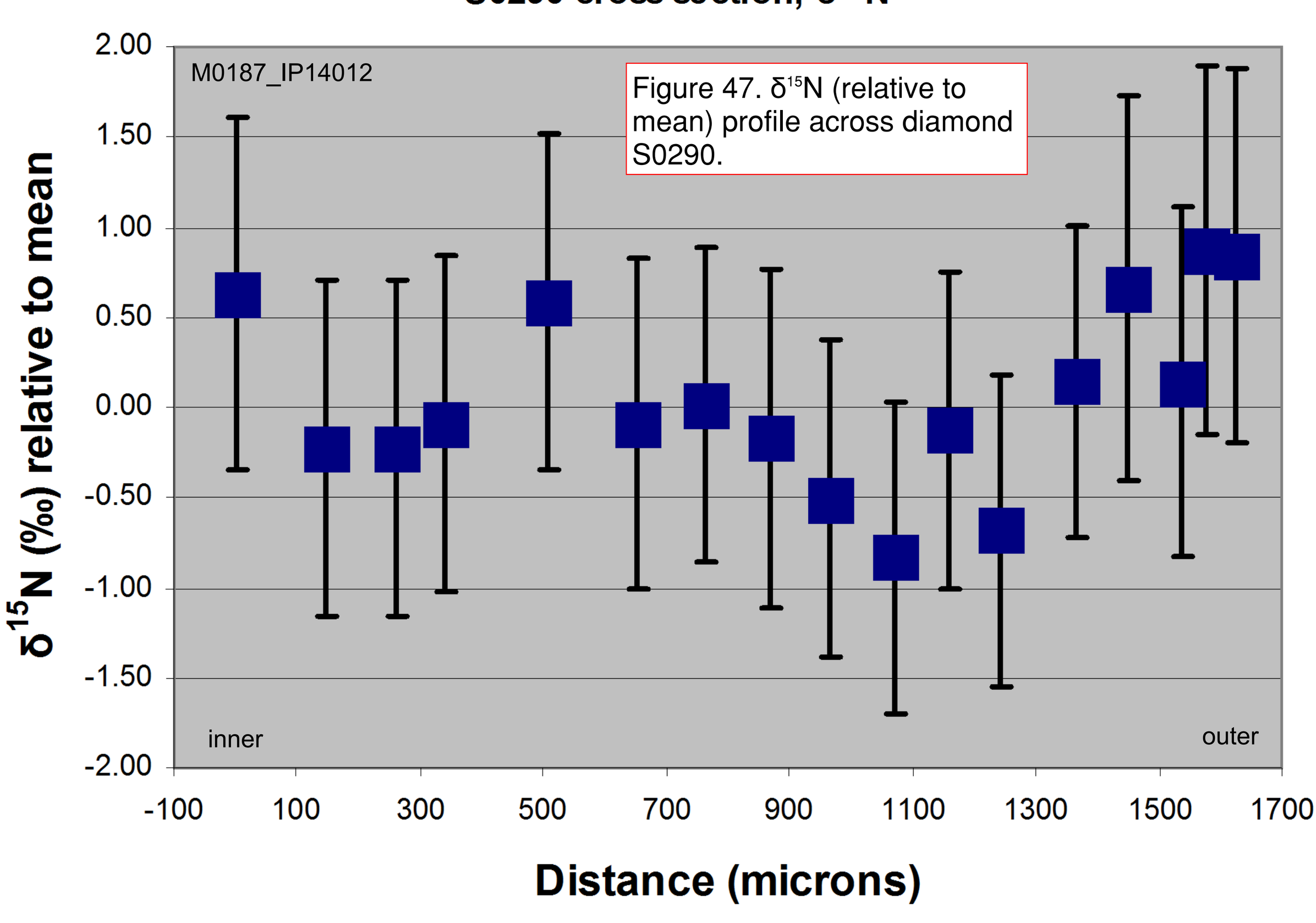
S0290 cross section, δ15N
M0187_IP14012
Figure 47. δ15N (relative to mean) profile across diamond S0290.
δ15N (‰) relative to mean
2.00
1.50
1.00
0.50
0.00
-0.50
-1.00
-1.50
-2.00
inner
outer
-100
100
300
500
700
900
1100
1300
1500
1700
Distance (microns)

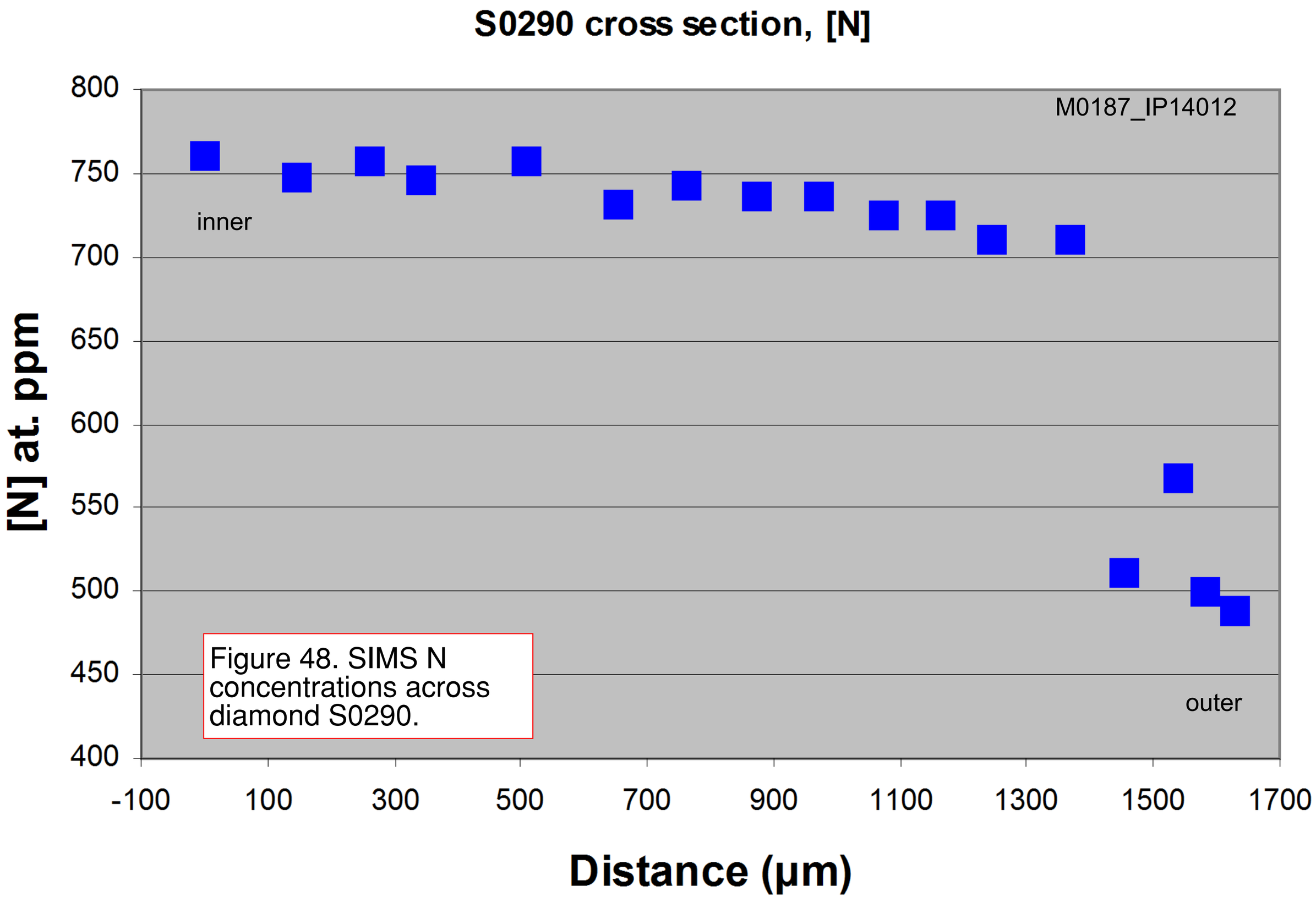

Figure 48. SIMS N concentrations across diamond S0290.

Table 1. Summary of IMS1280 instrument parameters for C-isotopes, N-isotopes, [N]

Parameter	units	$\delta^{13}C$	[N]	$\delta^{15}N$
Primary ions, 10 kV		Cs^+	Cs^+	Cs^+
Sample HV	kV	-10	-10	-10
Transfer mag		100	100	100
Entrance slit	µm	110	45	45
Contrast aperture	µm	400	400	400
Field aperture	mm	5	3	3
Energy window	eV	150	40	40
Detector low mass		L'2	L'2	L'2
Detector high mass		FC2	FC2 or EM	EM
Low mass exit slit	µm	500	500	150
High mass exit slit	µm	360	145	150
Low mas nuclide		$^{12}C^-$	$^{24}[^{12}C^{12}C]^-$	$^{26}[^{12}C^{14}N]^-$
High mass nuclide		$^{13}C^-$	$^{26}[^{12}C^{14}N]^-$	$^{27}[^{12}C^{15}N]^-$
Low mass, resolution (10%)		2000	2100	6700
High mass, resolution (10%)		2900	7000	7000
Low mass, typical count rate	cps	$1.5 - 2.5 \times 10^9$	1×10^9	$0.025 - 1 \times 10^7$
High mass, typical count rate	cps	$1.5 - 2.5 \times 10^7$	$0.0005 - 1 \times 10^7$	$0.01 - 1 \times 10^5$
Peak counting time	s	75-100	50	250-375
Total analysis time	min	4	3.5	10

Table 2. Combustion gas source mass spectrometric C- and N-isotopic analyses of diamond and other materials

Sample #	Alias sample #	Description	wt. (mg)	N (at.ppm)	$\delta^{15}N_{AIR}$ ‰	± 2σ ‰	$\delta^{13}C_{VPDB}$ ‰	± 2σ ‰	Reference values	Reference	Comments
S0011		HPHT diamond		186.6	+9.5	0.5	-22.58	0.02		data from Cartigny, P. (pers. comm.)	
S0270J	MC08/S1163	natural diamond: cubic	0.39	2072	(-1.78)	0.5	-8.87	0.07			N-isotope value considered erroneous; see text
S0270J	MC08/S1163	natural diamond: cubic	0.17	1191	-0.52	0.5	-8.94	0.07			
S0270J	MC08/S1163	natural diamond: cubic	0.97	2291	-0.31	0.5	-8.74	0.07			
S0270 best estimate		natural diamond: cubic			-0.40	~0.35	-8.85	~0.12			see text
S0203A	BAK	natural diamond: fibrous	1.04	660	-5.66	0.5	-5.15	0.07			
S0203A	BAK	natural diamond: fibrous	1.45	874	-5.67	0.5	-5.58	0.07			
S0203A	BAK	natural diamond: fibrous	1.237	849	-5.19	0.5	-6.06	0.07			
S0203A best estimate		natural diamond: fibrous			-5.51	0.28					see text
S0233A		vitreous carbon	1.25	10419	+6.15	0.5	-20.12	0.07			
S0289	INAM/ NAM-027	natural diamond		~13	~-3	1	-38.58	0.05		data from Cartigny et al. (2004)	C-isotopes wt. mean and 2SE (N = 4); N-isotopes avg. of 2
S0290	N198	natural diamond	2.7888	612	-3.90	0.5	-6.01	0.02		data from Cartigny, P. (pers. comm.)	
IAEA-N-1		amonium sulfate	0.1729		+0.23				0.43 ±0.07	reference values from Coplen et al. (2002)	
IAEA-N-1		amonium sulfate			+0.45				0.43 ±0.07	reference values from Coplen et al. (2002)	
IAEA-N-2		amonium sulfate	0.2384		+19.86				20.32 ±0.09	reference values from Coplen et al. (2002)	
IAEA-N-2		amonium sulfate	0.2799		+20.78				20.32 ±0.09	reference values from Coplen et al. (2002)	
Renne II		calcite					-3.66		-3.60	reference values from Cartigny, P. (pers. comm.)	
Renne II		calcite					-3.66		-3.60	reference values from Cartigny, P. (pers. comm.)	

References:

Cartigny et al. (2004) Constraining diamond metasomatic growth using C- and N-stable isotopes: examples from Namibia. Lithos, v 77, p. 359-373.

Coplen et al. (2002) Compilation of minimum and maximum isotope ratios of selected elements in naturally occurring terrestrial materials and reagents. USGS Water Resources Investigations Report 01-4222, 98 pp.

Table 3. Relative difference in C-isotope ratios (δ) between diamond RMs and cuboid sample S0270 by CGSMS and SIMS

Sample-S0270$_{cuboid}$	CGSMS data*		SIMS Data	
	(‰)	±2σ	(‰)	±2σ
S0270 octahedral ($\delta^{13}C_{S0270oct,S0270cub}$)			0.0	
S0289 ($\delta^{13}C_{S0289,S0270cub}$)	-30.00	0.11	-29.94	0.11
S0290 ($\delta^{13}C_{(S0290,S0270cub)}$	+2.87	0.11	+2.83	0.08
S0280$_{cub}$ ($\delta^{13}C_{S0280cub,S0270cub}$)			+0.24	0.06

*CGSMS $\delta^{13}C_{VPDB}$ value used for S0270 = -8.85‰

Table 4. Relative difference in N-isotope ratios (δ) between diamond RMs and cuboid sample S0270 by CGSMS and SIMS

Sample-S0270$_{cuboid}$	**CGSMS data***		**SIMS Data**	
	‰	±2σ‰	‰	±2σ‰
S0270$_{octahedral}$ ($\delta^{15}N_{S0270oct,S0270cub}$)			+0.90	0.15
S0203 ($\delta^{15}N_{S0203,S0270cub}$)	-5.11	0.44	-5.34	0.30
S0290 ($\delta^{15}N_{(S0290,S0270cub)}$	-3.50	0.60	-3.40	0.20
S0280$_{cub}$ ($\delta^{15}N_{S0280cub,S0270cub}$)			+0.35	0.09

*assumed CGSMS $\delta^{15}N_{AIR}$ value for S0270 (‰) = -0.4

Table 5. Recommended values for diamond isotope RMs used at CCIM (2014)

Sample Number	Alias	$\delta^{13}C_{VPDB}$ (‰)	±2σ (‰)	$\delta^{15}N_{AIR}$ (‰)	±2σ (‰)	[N] at.ppm	±2σ (%)	Purpose	Comments
S0270 (cuboid)	MC08/S1163	-8.88	0.10	-0.40	0.50	~2150		primary RM for $\delta^{13}C$ and $\delta^{15}N$	± includes possible systematic variations between SIMS calibration sub-samples; [N] variable and not recommended for calibration
S0270 (octahedral)	MC08/S1163	-8.88	0.10	+0.50	0.65	~2800		not currently used	[N] variable
S0280 (cuboid)	MC13/S1166	-8.64	0.12	-0.05	0.60	1670	5	primary [N] RM; secondary RM for $\delta^{13}C$ and $\delta^{15}N$	